Some meteorological parameters affecting the image quality of the William Herschel telescope on La Palma

Azzaro, Marco

MSc Thesis

Some meteorological parameters affecting the image quality of the William Herschel Telescope on La Palma

MARCO AZZARO DECEMBER 1996

Abstract

Understanding of the factors which limit the image quality of a ground based telescope is still an interesting challenge despite the effort devoted to the problem since the early days of optical astronomy. At the Roque de los Muchachos observatory, on the island of La Palma (Canary Islands) this problem has been studied as part of a programme aimed to improve the optical performance of the biggest instrument at the observatory, the anglo-dutch William Herschel Telescope. The programme comprises a range of studies to investigate the possible factors deteriorating the image quality at the telescope.

This thesis forms part of the meteorological studies of this programme and it is based on the data collected by a meteorological station recently installed at the observatory. In particular, phenomena such as wind direction, wind speed, pointing direction of the telescope dome relative to the wind direction, air and soil temperatures, relative internal/external temperatures, barometric pressure and humidity have been investigated and the relationship between these and the image quality at the telescope has been analyzed. The image quality is found to be particularly sensitive to the wind direction and the internal differences in temperatures. The season of the year also seems to have an influence on the image quality.

In the conclusions, suggested further avenues of investigation are given.

UNIVERSITY OF DURHAM

DEPARTMENT OF PHYSICS

MSc THESIS

Some meteorological parameters affecting the image quality of the William Herschel Telescope on La Palma

AUTHOR

MARCO AZZARO

December 1996

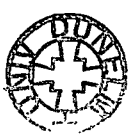

Contents

Declaration

I presently state that the work presented in this thesis has not been previously submitted for any degrees or other qualifications at this or other University. All of it is original except where reference to the work of other persons is made, and of my own with the following exception:
the seeing data used through the analysis have been provided by N. O'Mahony; the schematic layouts of the Casella meteorological station in Chapter 1 have been provided by A. Osborne and the Casella Co.; the geographic maps of La Palma and the Observatory site of the Introduction and Chapter 1 have been provided by the Instituto de Astrofisica de Canarias.

Marco Azzaro

Acknowledgments

It is a pleasure to thank J.M. Breare and J.A. Smith for their support during these two years of work and N. O'Mahony for providing part of the data used and good hints and information. Many thanks to A. Osborne and K. Kolle for their advice about the meteorological station. Many thanks to C. Moreno for his software support and to M.W. Asif and N. Walton for cleaning up my english. Many thanks to M. Bontempo, L. Morrison, all the CAMC personnel, C. Benn and all the NOT personnel, who made me available very valuable meteorological data. Many thanks to my colleagues and all the Observatory staff for the friendly atmosphere which helped me so much for this research work.

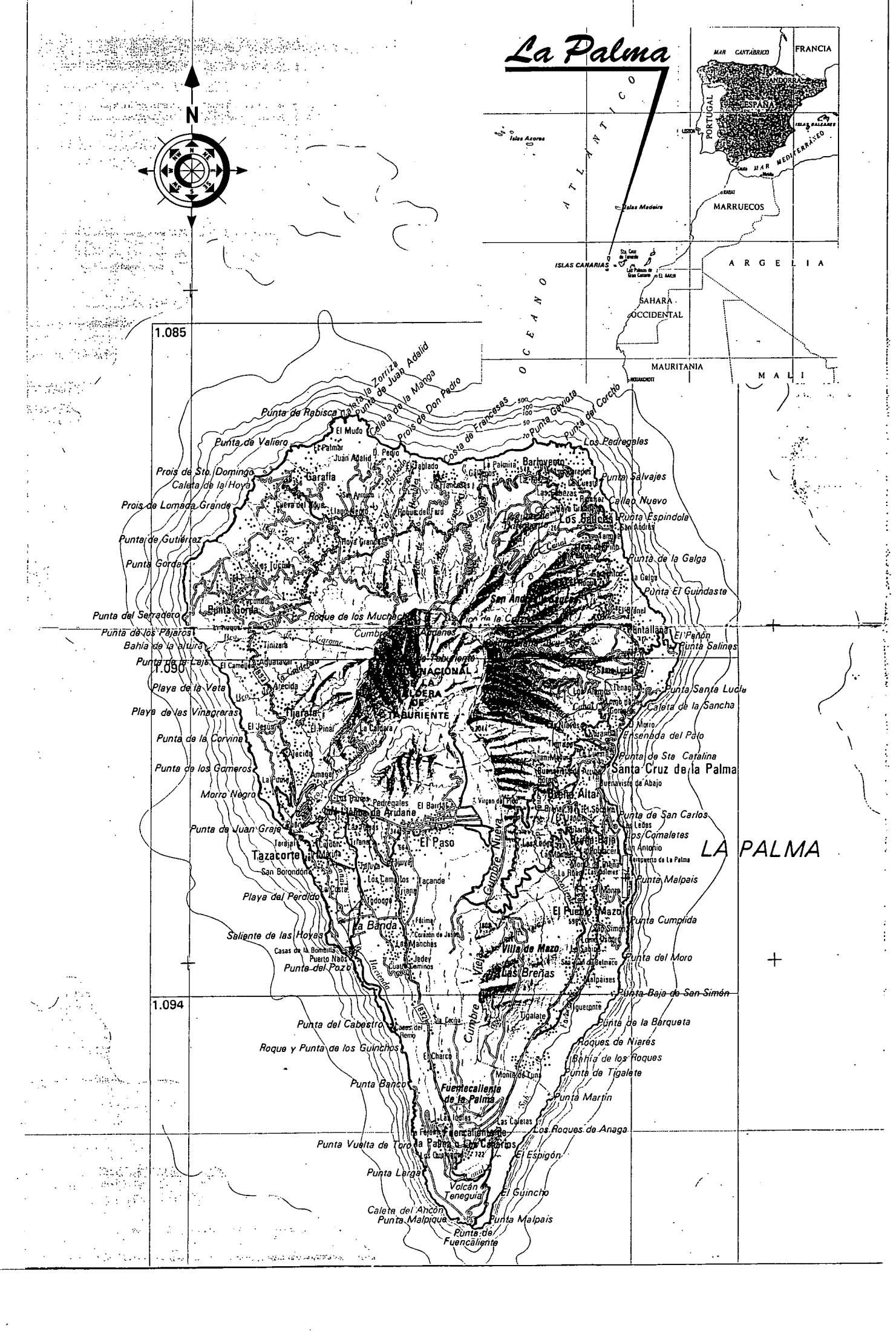
La Palma
N
MAR CANTÁBRICO
FRANCIA
ANDORRA
ESPAÑA
PORTUGAL
ISLAS BALEARES
MAR MEDITERRÁNEO
Islas Azores
Islas Madeira
MARRUECOS
ISLAS CANARIAS
ARGELIA
SAHARA OCCIDENTAL
MAURITANIA
MALI
OCEANO ATLÁNTICO
1.085
1.090
1.094
Punta de Rabisca
Punta de Valiero
Prois de Sto. Domingo
Prois de Lomada Grande
Punta de Gutiérrez
Punta Gorda
Punta del Serradero
Punta de los Pájaros
Bahía de la Alura
Punta de la Laja
Playa de la Veta
Playa de las Vinagreras
Punta de la Corvina
Punta de los Gomeros
Morro Negro
Punta de Juan Graje
Playa del Perdido
Saliente de las Hoyas
Punta del Pozo
Punta del Cabestro
Roque y Punta de los Guinchos
Punta Banco
Punta Vuelta de Toro
Punta Larga
Caleta del Ancón
Punta Malpique
Punta de Fuencaliente
Punta Malpais
Punta del Corcho
Los Pedregales
Punta Salvajes
Callao Nuevo
Punta Espindola
Punta de la Galga
Punta El Guindaste
El Penón
Punta Salinas
Punta Santa Lucía
Caleta de la Sancha
Ensenada del Palo
Punta de Sta. Catalina
Punta de San Carlos
Los Comaletes
Punta Malpais
Punta Cumplida
Punta del Moro
Punta Baja de San Simón
Punta de la Barqueta
Roques de Nierés
Bahía de los Roques
Punta de Tigalate
Punta Martín
Los Roques de Anaga
El Espigón
El Guincho
Costa de Francesas
Barlovento
Los Sauces
Garafía
Tijarafe
Tazacorte
El Paso
Los Llanos de Aridane
La Banda
Villa de Mazo
Las Breñas
El Pueblo Mazo
Santa Cruz de la Palma
Breña Alta
Breña Baja
Fuencaliente de la Palma
Parque Nacional de la Caldera de Taburiente
LA PALMA

INTRODUCTION

1 The seeing problem

The present work has been carried out as a part of the project, called the Half-arcsecond Programme, to improve the imaging quality of the three anglo-dutch telescopes of the Isaac Newton Group (referred to as ING in this thesis) on La Palma, in particular the largest of these, the 4.2 m William Herschel Telescope (WHT). The project involves many other things apart from meteorology, such as a study of differential temperature of structures, ventilation of buildings and cooling of the mirrors (see § 3). A very considerable effort is being devoted to the atmospheric influence on the image quality of the WHT and the present work accounts for some of the work done at the Observatory on this subject.

1.1 Light distortion

We know that electro-magnetic radiation can be considered either as a flow of particles (photons) or as an (electro-magnetic) wave motion, depending on the property of the radiation we are looking at. In this case we are concerned with the propagation of light through the atmosphere, so it is convenient to adopt the wave motion type description. A wavefront of radiation is a surface passing through all the points with the same phase and its direction of motion is usually perpendicular to the wavefront.
Radiation coming from distant stars, although having spherical wavefronts when still close to the emitting star, has plane and parallel wavefronts when reaching the Earth's atmosphere, because of the great distance of the source from the Earth. After hitting the upper atmosphere, the radiation has to pass through different layers, each of which has an effect on the shape of its wavefront. We can divide the path of the radiation from the upper atmosphere to the primary mirror of a telescope into 4 main parts:

1) The upper atmosphere layer. This is that part of the atmosphere high enough not to be affected by the Earth's surface. The movement of this air is therefore independent of the orography underneath. Its lower limit is typically one kilometre above the Earth's surface.

2) The air close to the Earth's surface. In this zone the movement and turbulence of the air strongly depend on the surface corrugation underneath and the effect is bigger at low levels. This will be referred to as the "surface layer".

3) The air in the proximity of the dome. This includes the air *inside* the dome as well as the occasional outflow through the dome slit in the case of a higher internal temperature.

4) The air in the proximity of the mirror.

The upper atmosphere is never steady and often airmasses collide forming fronts where winds are not constant in force or direction, so that viscous friction creates turbulence in the front's surroundings. Turbulence changes the density of the air and therefore its refractive index; air with a different temperature also has a different refractive index, so that the radiation wavefront coming from the star is distorted in some irregular way, and this distortion changes with place and time.
Down in the surface layer the situation is even worse: even light winds hitting the irregular surface of the Earth cause pressure differences. High ground temperature creates bubbles of air with different temperatures, usually rising up and therefore producing buoyancy forces which in turn alter the local pressure of an air cell.
The dome is doubtless another obstacle to air flow and more eddies and turbulence are to be expected around the dome slit. The air inside the dome is usually warmer than the open environment, so that there is an air flow rising from the dome through the dome slit creating turbulence and temperature differences.
Finally, just above the mirror there may be some turbulence due to the temperature of the reflecting surface, usually higher than that of the tube of the telescope or the dome. This is common during the first part of a night, because the mirror has a large mass and the time required for it to cool down is longer than that of other elements around it.

1.2 Diffraction limit

Even an optically perfect instrument receiving a plane wavefront has a limit, beyond which another phenomenon deteriorates the image produced at the focal plane of the instrument. The fact that only a part of the wavefront is selected by the objective of the instrument (depending on its size) causes interference and the image of a point source is not a point, but the well known Airy disc surrounded by diffraction rings.
Two closeby point-sources will then be seen as a single one if their angular distance does not allow the instrument to resolve them. A plot of the intensity of an Airy disc image shows a central main peak with symmetric smaller peaks on the sides, decreasing in intensity away from the centre. The Rayleigh criterion says that two sources will be resolved if the first minimum of one of the peaks falls on the central maximum of the other, or if the distance between the centres of the two discs is equal to the diameter of the discs (the two discs have the same diameter depending on the aperture of the instrument).
These distances are measured in the focal plane of the instrument, so they could be measured in millimetres, but they refer to objects on the celestial sphere, so that the angular measure equivalent to the image they project on the focal plane is usually preferred. The unit is then the second of arc, or arcsecond. Following this criterion we can define the diffraction limit of an instrument (Dawes limit) L as $L = 1.22\frac{\lambda}{D}$, where

λ is the wavelength of the radiation and D the aperture of the instrument.
The theoretical Dawes limit of the William Herschel Telescope is 0.018 $\widehat{''}$ (arcseconds) in the ultra violet band ($\lambda = 0.3\mu$), 0.03 $\widehat{''}$ in the optical ($\lambda = 0.5\mu$), and 0.12 $\widehat{''}$ in the infra red band ($\lambda = 2\mu$).

1.3 The definition and terminology of seeing

From what we have seen so far it is clear that the "history" of the radiation which reaches the mirror of a telescope affects image quality, as well as the intrinsic limits of the instrument, such as optical quality, misalignment, incorrect focus, vibrations, tracking errors etc.
The total distortion of the wavefront of radiation reaching the focal plane of an instrument is what we call "Seeing", and, using the profile of the diffraction disc of an instrument, we can define a measure of the seeing as the Full Width Half Maximum of the central peak in arcseconds.
Typical seeing values for the WHT are 0.6 $\widehat{''}$ on a very good night and 2 $\widehat{''}$ or more during a poor night.
It is clear that these values are far bigger than the theoretical values of the diffraction limit stated above. We can then define r_0 (coherence or Fried length) as the aperture size at which the image spread introduced by the atmosphere is equal to the diffraction limit of the aperture.
In practice r_0 is a measure of the size of a "seeing cell", a region of the atmosphere in which the phase of the radiation does not change significantly. A good value of r_0 (for $\lambda = 0.55\mu$m) is 20 cm at the best sites.
Seeing varies with time, so it is useful to define τ_0 (characteristic seeing timescale), which is the typical replacement time of a seeing cell. A good value of τ_0 (for $\lambda = 0.55\mu$m) is about 6 msec.
Another important factor in seeing measurements is the area of the sky for which wavefront deformation remains approximately constant. As we did before for the diffraction disc and seeing, we measure it as an angle and therefore in arcseconds. This angle is denoted by θ_0 and typical values (for $\lambda = 0.55\mu$m) are around 4 $\widehat{''}$.

1.4 The importance of image quality

Having a better image quality gives both *better* Astronomy and *more* Astronomy. Some astronomical programmes of high scientific merit require high count rates or spatial resolutions which are not available now. Others, which require higher photon collecting efficiency and higher signal to noise ratio, would be possible now, but they require an unaffordable amount of observing time. All this is contained in the following equations:

$$s/n = \frac{S}{\sqrt{S + D\,(B + T + C + R)}}$$

and

$$S = \eta \Delta_e A_e t N_\gamma 10^{0.4 m_*}$$

where:
S is the source signal, D the image size in pixels, B the sky background per pixel, T the thermal background per pixel, C the detector dark current per pixel and R the detector read-noise per pixel. The signal S is the product of the detector quantum efficiency η, the photon flux N_γ at the bottom of the atmosphere from a star of magnitude $m = 0$, the (point) source magnitude of the target m_*, the effective width of the detector sensitivity function Δ_e and the telescope effective collecting area A_e. Thus the detector quantum efficiency, the image size at the detector and the telescope collecting area are equally important in getting a good signal to noise ratio. Research is therefore oriented towards better detectors, bigger telescopes and reduced image size at the focal plane.
We can clarify all this even better with a numerical example: a spectroscopic observation carried out with a 1 $\widehat{''}$ $\times 2$ $\widehat{''}$ slit would collect only 26% of the flux with a 2 $\widehat{''}$ FWHM image of a point source, but 55% of the flux with a 1 $\widehat{''}$ image and 94% of the flux with a 0.5 $\widehat{''}$ image. An image size reduction by a factor of 2 allows a throughput gain of a factor of 2, which means that the same result of a telescope with doubled diameter can be achieved.
One may achieve significant decrease in image size with the aid of Active or Adaptive Optics (see next section), but these techniques need a good knowledge of atmospheric characteristics if they are to be effective.
A few examples of investigations which would greatly benefit from seeing improvements are given below.
Photodissociation regions have been modeled in quite some detail to determine their spatial structure and the dependence of line emissions on physical conditions in the cloud they are associated with; so far observations have been unable to quantify detailed physical distribution models and in the case of the IRCAM (Infra Red Camera used on WHT) observation of M17 this limit was set by the quality of the seeing. The same experiment for the Orion Nebula or our Galaxy's centre would require resolution down to 0.2 $\widehat{''}$
The atmospheres of our solar system planets have not suffered modifications from biological processes, so they can give much information on primordial abundances and help to produce realistic models of the evolution of the Earth's atmosphere; a great variety of observations of the Solar System planets requires sub-arcsecond image sizes, such as measurements of the thickness of Saturn's rings, resolution of the Pluto-Charon system or the search for comets or faint Solar System objects.
The possible detection of planets around other stars needs much higher angular resolution and greater sensitivity than is usually available. Reduced image size provides both. 0.2 $\widehat{''}$ is a critical value for detecting disks in Taurus, or jets around young stars at a distance of 20 AU, or binary systems at 200pc with a separation of 40 AU from the central object to the companion.
Astrometry can be much more accurate with reduced image sizes, provided that the appropriate detector to match small images is used.

The measures of stellar rotation and velocity dispersion profiles over the central few parsecs of a galactic centre would allow the central mass to be determined and therefore blackhole candidates could be recognized as such.
Finally, multiple images of quasars produced by gravitational lenses have a typical separation of 1 $\widehat{''}$, but many other systems consisting of multiple objects would need 0.5 $\widehat{''}$ resolution to be resolved.

2 Means of reducing the image size

We have seen, since the beginning of this thesis, how the image produced by an optical instrument is deteriorated by the atmosphere. To minimize this deterioration has always been a challenge for astronomers and several methods are nowadays available:

1) Observe from outside the atmosphere (Hubble Space Telescope).

2) Careful selection of astronomically good sites.

3) Improve dome design, ventilation and general control of local seeing.

4) Enhancement of images after observations, shift and add, optical aperture synthesis, etc.

5) Active optics

6) Adaptive optics

The main advantages or limits of each of these methods are discussed below.

2.1 Observe from outside the atmosphere

This first method is obviously the most effective, but nevertheless it is practically limited by several aspects: its *cost* is the highest among the methods listed above, then the *range of instruments* which can be mounted on the telescope is severely reduced with respect to a ground based observatory and finally any *technical problem* on the space ship is very difficult to handle from the Earth.

2.2 Site selection

Careful and detailed site tests are today a usual practice before the construction of any new telescope; the best sites are now well known and it could be said that it is difficult to find sites with significantly better seeing than the known ones, so this field is fully exploited already.

2.3 Control of local seeing

To improve local seeing through building design and ventilation or thermal control is possibly the cheapest contribution to the seeing problem. This is the aim of the Half-arc-second programme, which is illustrated in the next section. The astronomical community is presently devoting a lot of effort to this field and current results look very promising, but once local seeing is at its best, there still remains the upper atmosphere effect. So far the technology of optics hasn't been fully exploited to reduce the effect of the upper atmosphere.

2.4 Postprocessing of images

Postprocessing of images, such as removing the wavefront-tilt induced motion by shifting short exposure images before adding them, or by using instantaneous interference patterns from several apertures, is not applicable to all existing instruments as a fast time resolution is required. Moreover, it is not usable for conventional spectroscopy and many detectors are limited in postprocessing applications. Finally, the phase information of the image is only partly recovered with such techniques.

2.5 Active optics

An optical system whose elements have a fixed shape and position is called *passive*; this means that no real time control is possible of any of its parts and their positions and shapes are fixed or just temporarily modified by disturbing forces. A system which is not *passive* in the sense that it is able to improve the signal performance through some control on the shape and position of its elements, is then *active*. "Active optics" is therefore a broad term indicating all the techniques which enable an optical system to compensate for environmental deteriorations of the optical signal, and, as it will be seen later, "Adaptive optics" is a subset of it. In practice, the term "Active optics" is most commonly used for those systems which can correct the image distortion caused by long timescale changes, such as flexure of the primary mirror or of the telescope tube, due to gravity force, which has different effects according to the telescope position (see Tyson 1991). These systems make a continuous automatic adjustment of the shape and tilt of the primary mirror and (or) a continuous re-alignment of the secondary mirror axis and can cope with corrections with frequencies up to about 10 Hz. The controllers of the shape of the mirror are sensitive to mechanical changes of the structures and physical variations in the parabolic mirror shape, therefore the actual information about the quality of the optical signal is not involved.
In the early days the only solution to flexure problems was to make quite thick primary mirrors and stiff telescope structures; *active optics* allows much thinner (and lighter) primary mirrors and structures, because the system has the ability to keep them in shape.

2.6 Adaptive optics

Atmospheric distortion of a star image is mainly due to air pockets, with different refractive indices, which move around and combine with each other along the light path. Most of this distortion is in the phase corrugation and tilt of the wavefront, more than in its amplitude. The wavefront's phase corrugation and tilt both contribute to the image quality: corrugation broadens the image while tilt moves it around. We can describe the situation as follows.
We saw in section 1 of this introduction that, at a good seeing site during a good night, a (say) 20 cm aperture telescope would give diffraction limited images. If we consider the WHT, we can divide its mirror into parts of diameter 20 cm and accept that each part receives a plane wavefront. Now, the wave phases on these parts will differ from each other and the difference will increase as the distance between the parts increase. The timescale of the pattern's variations induced by such a mechanism can be as short as 1 ms. As explained in the previous section, the so called *active optics* systems can't cope with correction frequencies above 10 Hz, therefore something else must be used to compensate for the effect of the atmosphere. We can solve the problem if we divide the mirror into parts of 20 cm of diameter, which can be moved by means of hydraulic pistons, and drive them according to the phase difference measured using part of the light in a closed loop scheme. An *adaptive optics* system usually includes a deformable mirror and a tilt mirror, which are driven by pistons controlled by the phase reconstructor. The deformable mirror can either be the primary mirror or another deformable plane mirror set further down in the optical train of the telescope. The tilt mirror is usually a flat mirror placed right before the deformable mirror. The information to feed the phase reconstructor can be taken from the main beam, with a partly reflecting surface which splits the light, or from an artificial laser guide star. The latter method is the most efficient, as no light is lost from the main beam; it requires a powerful laser focussed at a point up in the high atmosphere above the turbulence region. The resulting backscattered radiation can be used to detect the phase variations occurring lower down in the atmosphere. This technique allows accurate phase measurements, limited only by dissimilarities in range between the artificial star and the object to be observed. This error, called *focal anisoplanatism*, decreases when the altitude of the artificial star increases, but above about 20 Km the backscatter of the molecules starts to be too small to be useful. This problem is solved either with multiple laser stars or using the resonance backscatter from a stable sodium layer sited in the mesosphere at an altitude of about 90 Km (see Lincoln lab. j. 1992).

3 The Half-arcsecond programme

3.1 General aim and plans

The project started in 1993 with the primary aim of reducing the seeing at the William Herschel Telescope and, possibly, at the other two anglo-dutch telescopes as well. The name comes from the ideal value of 0.5 $\widehat{''}$ seeing (at a wavelength of 1 μm), being considered a reasonable goal for a site of this class, but it doesn't mean that this value

has to be achieved exactly. Some of the actions to improve seeing started immediately, while others were expected to require some investigations first, of which this research on meteorological characteristics of the observatory is an example.

Seeing tests

Seeing tests have been carried out with a Differential Image Motion Monitor (DIMM) mounted on a 5 meter tower located 50 meters North of the WHT. Data from the DIMM complement the seeing data collected at the telescope by the telescope operators during their night work and, after May 1995, those automatically logged by the autoguider (See Chapter 1 § 6).

Temperature monitoring

About 80 temperature sensors have been fitted on the structure and dome of the WHT to monitor differential temperature variations along the instrument and difference in temperature of various elements close to the light path.

Oil cooling

The azimuth and elevation movements of the telescope are supported by hydraulic bearings with high pressure oil to reduce friction and get smooth and precise pointing of the telescope. This oil keeps the lower part of the telescope some 10 degrees hotter than the rest and this temperature difference causes rising air currents which are to be minimized. For this reason a new plant to cool the oil of the bearings has been considered and presently is nearly complete on the southern side of the WHT building.

Mirror cooling

The mirror of the INT is cooled during the day so that at the beginning of the night the mirror quickly stabilizes with the night air temperature and small turbulent currents on the surface of the mirror can be avoided; although the success of this experiment is not yet finally confirmed, a similar and more powerful system is under construction for the WHT.

Instrumentation cooling

All the devices at the different focal stations generate heat and should be cooled. This is planned for the near future.

Dome temperature

The dome absorbs heat from the Sun during the day and takes several hours to cool down. The cooling time should be minimized by isolating the dome during the day and ventilating it as soon as the Sun sets.

Staff training

Warm air coming from the building through open doors, lights left on when not necessary and similar sources may increase the heat given to the dome during the day. The staff must be aware of this and understand the importance of minimizing the effect.

Telescope focus

The focussing of the telescope has recently turned out to be much more important than expected. It is necessary to setup a standard procedure of focussing and also to improve the automatic temperature correction to the focus setting.

Meteorology

The monitoring of the meteorological conditions on site is important for the Half-arcsecond programme and also, during normal observations, as a help to the telescope operator, who is responsible of telescopes safety too.

3.2 Meteorology investigation

This part of the Half-arcsecond programme is the main topic of this work; in this field some investigation was necessary before taking any actions as not much is known about the influences of meteorological parameters on seeing. It is clear from the literature that these influences strongly depend on the site and general rules are hardly of any use for a specific observatory. It has been observed, for example, that the presence of dust in the atmosphere, or of some particular types of clouds, is frequently associated with good seeing. A better understanding of the relation between similar phenomena and seeing would greatly benefit the whole Half-arcsecond programme.
The phenomena which I dealt with in the present work are:
Wind, which could affect seeing by creating turbulence while passing over peaks, domes or other structures on site.
Temperatures or temperature differences between mirror and dome, air inside and outside the dome, soil or borehole and in the open air; these factors could result in air movement and changes of refractive index of air cells.
Atmospheric pressure could be important for possible changes in the refractive index of air through the atmosphere.
Relative humidity changes also could affect the refractive index of the air, or it could be associated with different air masses which could lead to different seeing conditions.

4 Importance of meteorology

The WHT optics theoretically should give images as good as 0.3 $\widehat{''}$ FWHM as a result of both the diffraction limit and the optical imperfections of the instrument, such as coma (due to misalignment of the mirrors) and other aberrations, especially astigmatism. Experience shows that, most of the time, the image is at least twice as bad. The influence of atmospheric conditions on the image quality is therefore large; typically one half of the image size, even under best observing conditions, is due to atmospheric distortion, which demonstrates the importance of understanding atmospheric behaviour to be able to reduce its effect. The existence of a relation between meteorological parameters and seeing is clear, but to define it and devise actions to improve seeing is another matter. The most significant improvements during the last few years have been achieved using Active and Adaptive Optics Systems, which allow an optical instrument to compensate for some of the image distortions introduced by flexure of the structure or by the atmosphere.
Understanding meteorological influences on seeing can help research in Adaptive Optics techniques, for example, to ascertain whether a faulty system or meteorology is responsible for a change in seeing, or to investigate the time scale of the seeing variations eventually connected with those of some meteorological parameter.
Understanding atmospheric influence on seeing is also important for a more efficient planning of observations. It would be *particularly* valuable to be able to predict seeing at least a few hours in advance, but this kind of research is still at the initial stage.

5 Earlier attempts at seeing investigation

Astronomical observations started on La Palma with a Swedish solar telescope in 1979. Later on, the site was investigated, from the stellar observation point of view, during 1982 and 1983, using a 60 cm telescope of the Swedish Royal Academy. The result of this investigation was that La Palma showed itself to be a most favourable site for astronomical observations. In addition some relationships between seeing and wind direction and speed were pointed out, although not in much detail, in a paper by A. Ardeberg in 1983 (see A. & W. 1984). The main conclusion of that investigation was that there is a pronounced relationship between wind direction and image quality, but no details were reported about the measuring system used, hence the wind height to which Ardeberg refers is unknown. The author mentions another investigation made by Walker in 1974, which showed no relation between wind direction and seeing.
Another interesting paper in the same volume (see A. & W. 1984), concerns the Canada-France-Hawaii telescope on Mauna Kea. The location described in that report matches quite well with ours, since it concerns a high altitude site with other summits around the observatory site, and also Mauna Kea is located in a marine environment, being on a small island. The analysis of wind direction made in a wind-tunnel experiment with a mock-up of the site showed a clear relation between the height of the turbulent layer and wind direction. It was found that the typical turbulence of a surface layer drops consistently above 20 meters from the ground.
A telescope should be placed where turbulence is minimum, therefore quite high above the ground, but this in turn would involve the construction of an expensive structure to support it, therefore a compromise must be accepted and the previous investigation states that an observing floor higher than 20 m above the ground matches well with both requirements.
A layer of this thickness (20 m) plays an important role in another experiment as well, regarding variations of microthermal fluctuations at different heights above the ground. These fluctuations drop dramatically above 20 meters, which supports even more the concept of placing the node of the telescope at some 20 meters above the ground. The Canada-France-Hawaii telescope node was placed at 22 meters above the ground.

6 The structure of this thesis

The first chapter describes the Casella meteorological station and different aspects of the hardware, software and problems related to these. Also the format and collection method of the data used throughout the thesis and some assessment on their quality are reported here. In this chapter I discuss the station in terms of structure, sensors and their characteristics, maintenance and instrument calibration in general. The details of this last topic are explained in Appendix A, while in Appendix B I examine the effect of the environment on the station structure itself. A brief account of the safety limits used at the observatory is also given and the chapter ends with a summary of the programs used for data analysis.
When I first arrived on La Palma, a little over two years ago, the meteorological

station was still in its cases, ready to be mounted, and many problems other than meteorological ones were still to be solved. When I started this research I was aware of the fact that the data I was going to use would not be very reliable for a long time and actually, as a part of my job at the observatory, I was going to deal directly with any problems of the sensors and the equipment in general. It seems reasonable to include in this thesis all the work done on the devices and on the data, including those data collected by other systems. Therefore the second chapter is devoted to the comparisons made with other stations here on site, so as to establish the correct weight to be given to particular features of the weather data from the point of view of the seeing quality. The third chapter can be seen as the heart of the work; here I look for connections between individual meteorological parameters and seeing. Of course, this is only the first step of such an analysis, because I believe the seeing to be related to the whole of the measured meteorological parameters, but such a comprehensive study is well beyond the scope of this work.
The fourth and last chapter includes conclusions made on the basis of the previous chapter results and on the validity and limits of these. Some ideas for carrying on the research are also given here.
Appendix A includes the details of the calculations for the barometric corrections and pressure sensor calibration.
Appendix B gives a description of the severe conditions which can be experienced during the winter months at this site.
Appendix C comprises the source codes of the computer programs used to produce the graphs and data representations.

Chapter 1

INSTRUMENTS AND DATA

1.1 The MET station, general characteristics

The initial function of the meteorological equipment at the observatory was simply to "protect" the telescopes from bad weather and the few sensors and alarms of the old meteorological station (manufactured by the firm Vaisala) could perfectly cover this task. Requirement for meteorological data changed in 1993 because of the start of a new project, called "The Half-arcsecond programme" (See Introduction §3), which involves, amongst other things, a detailed investigation of the meteorology at the observatory site. In the summer of 1994 a new and more advanced meteorological system was purchased and the old Vaisala station now works as a backup system in case of failure of any of the new sensors.
The requirement of the new system was, apart from the usual warnings in the case of bad weather, a computer database to provide more flexible and powerful analysis facilities for the Half-arcsecond programme. The whole station had to be automatic and run all the year round with minimum maintenance to avoid additional work load on the observatory staff.
A system produced by the british manufacturer Casella satisfied these requirements and was selected because of the quality of its devices and the great experience in airport and environmental monitoring provided by this firm.
Climatic conditions at the observatory can be much worse than those at most airports, of course, but the market does not offer devices specifically designed for such a peculiar environment as our mountain top.
A brief description of the observatory site is necessary at this stage to understand the setup of the meteorological station.
As shown in Fig. 1, the smallest of the three anglo-dutch telescopes, the JKT (1 m mirror), is right on the sharp edge of the "Caldera de Taburiente" (the dashed-dotted line), the big crater which extends from the centre of the island down to the west coast. 100 m North of the JKT is found the INT (2.5 m mirror) and finally the WHT (4.2 m mirror) lies some 400 m West of the other two telescopes. The observatory area is thus quite large and one single set of sensors would not give a detailed picture of the meteorology of the site. Hence it was decided to give each telescope an independent station and the JKT station was placed on a mast some 20 m South of the telescope.

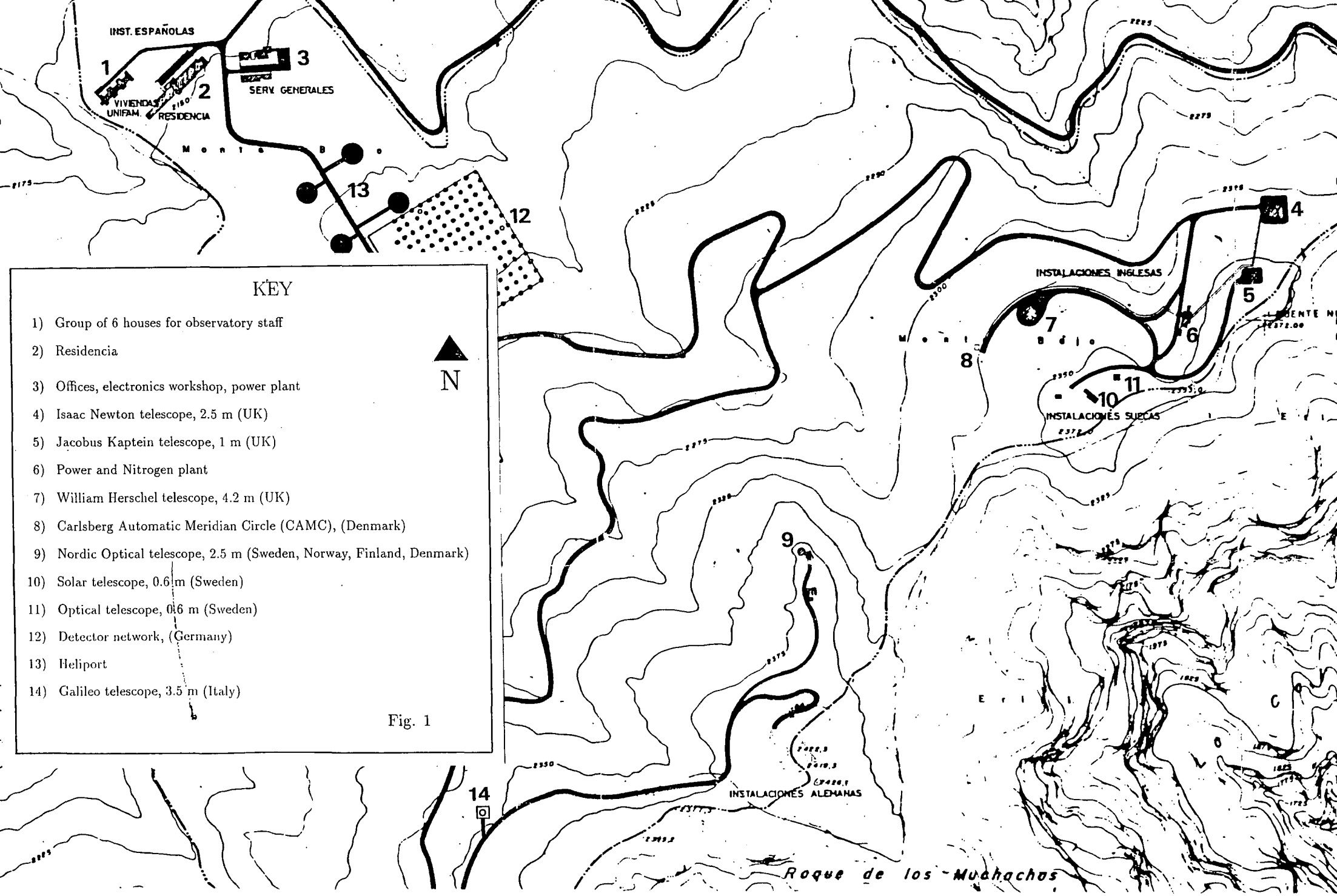

KEY

1) Group of 6 houses for observatory staff
2) Residencia
3) Offices, electronics workshop, power plant
4) Isaac Newton telescope, 2.5 m (UK)
5) Jacobus Kaptein telescope, 1 m (UK)
6) Power and Nitrogen plant
7) William Herschel telescope, 4.2 m (UK)
8) Carlsberg Automatic Meridian Circle (CAMC), (Denmark)
9) Nordic Optical telescope, 2.5 m (Sweden, Norway, Finland, Denmark)
10) Solar telescope, 0.6 m (Sweden)
11) Optical telescope, 0.6 m (Sweden)
12) Detector network, (Germany)
13) Heliport
14) Galileo telescope, 3.5 m (Italy)

N

Fig. 1

By this mean we have at least one set of sensors as far away as possible from obstructions such as telescope buildings, which could alter the natural air flow.
The JKT station was so planned as to be the main one of the three in the sense that it collects all those data for which a single sensor was considered representative of the whole site, such as wind direction, dust, solar radiation, soil and borehole temperature. The INT and WHT station are located on the roof of each respective building. This is a inconvenient place for the local anemometers, of course, because of their proximity to the telescope dome, but because of a financial deadline the alternative was to get no meteorological station at all. It is planned to move the local anemometers to a better location in the future.
Fig. 2, 3 and 4 show the diagrams of the JKT mast and the INT and WHT local stations, their location and size. These diagrams are taken from the documentation of the Casella station.
All the three telescopes have some internal sensors as well, which are located inside the domes. These are important, as it will be seen later, because relative conditions inside and outside the dome may affect image quality. Also, the dewpoint sensor is meant to warn when condensation on the primary mirror is likely, therefore it must be close to the mirror.
Between the stations there is a radio connection and the INT and WHT local stations communicate with each respective control room through fibre optics cables, so as to avoid any copper cables coming into the buildings, which could be dangerous in the case of electric storms.
In each telescope control room there is a PC which records and displays the data. The screens of the INT and WHT PCs show the local data for that telescope plus the JKT mast data, while the JKT PC only shows the JKT mast data.
Each PC updates its local data every 5 seconds; the INT and WHT PCs update the JKT mast data every minute and finally, every 10 minutes, all PCs (independently) store on hard disk all the data they are displaying. In this way the JKT mast data, which are the most comprehensive set, are stored on three different disks as a safety measure against any failures and data losses.
The coordinates and heights of the three stations are as follows:

Site	Height	Latitude	Longitude
WHT	2332 m	28°45′38.1" N	17°52′53.9" W
INT	2336 m	28°45′43.2" N	17°52′39.5" W
JKT	2364 m	28°45′39.9" N	17°52′41.2" W

The instruments of the three stations are distributed as follows:

on the JKT mast

a) The main anemometer with wind speed and direction

b) Hygrometer

J.K.T METEOROLOGICAL MAST

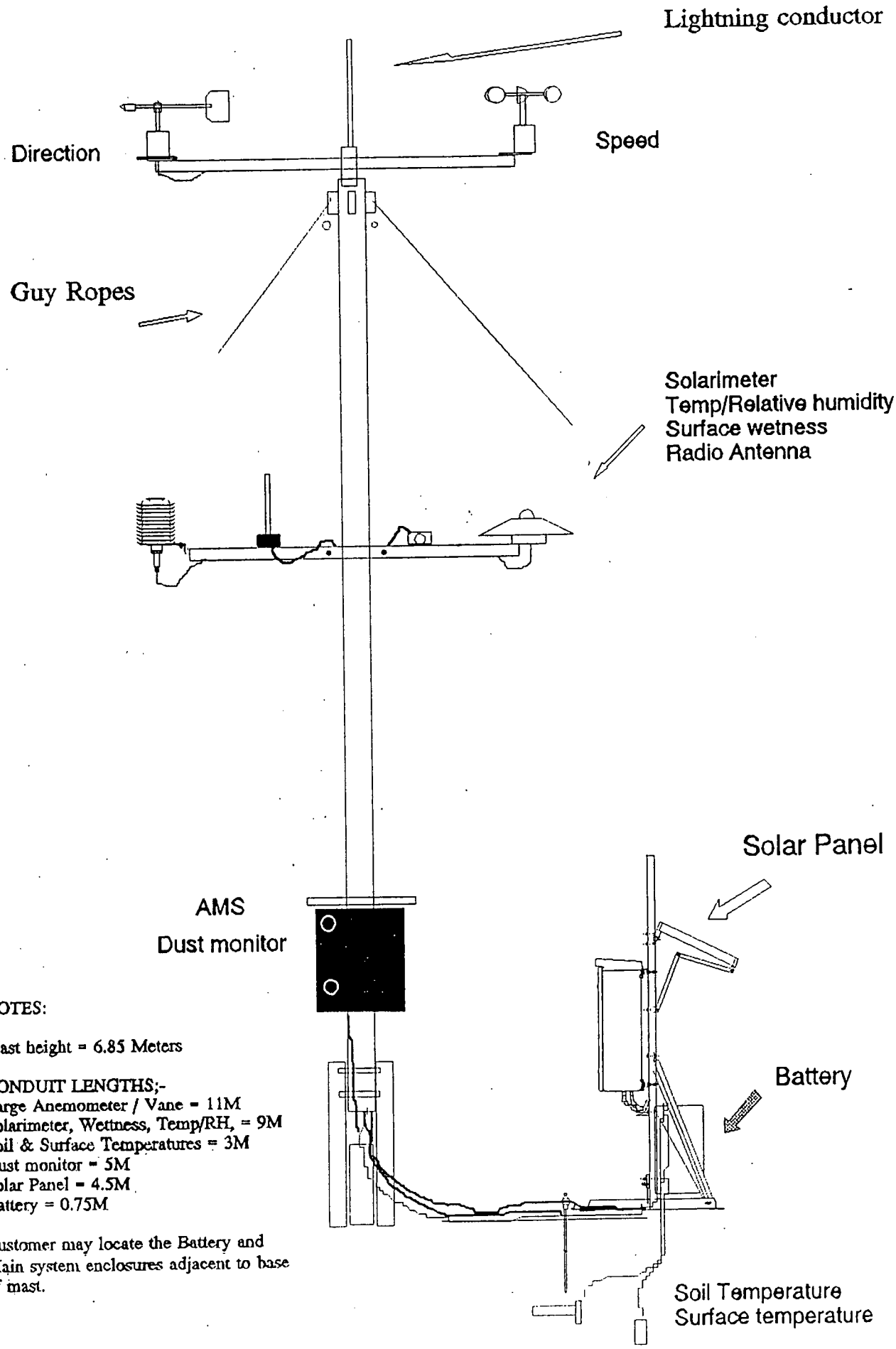

NOTES:

Mast height = 6.85 Meters

CONDUIT LENGTHS;-
Large Anemometer / Vane = 11M
Solarimeter, Wettness, Temp/RH, = 9M
Soil & Surface Temperatures = 3M
Dust monitor = 5M
Solar Panel = 4.5M
Battery = 0.75M

Customer may locate the Battery and Main system enclosures adjacent to base of mast.

ISAAC NEWTON AND WILLIAM HERSCHEL OBSERVATORIES

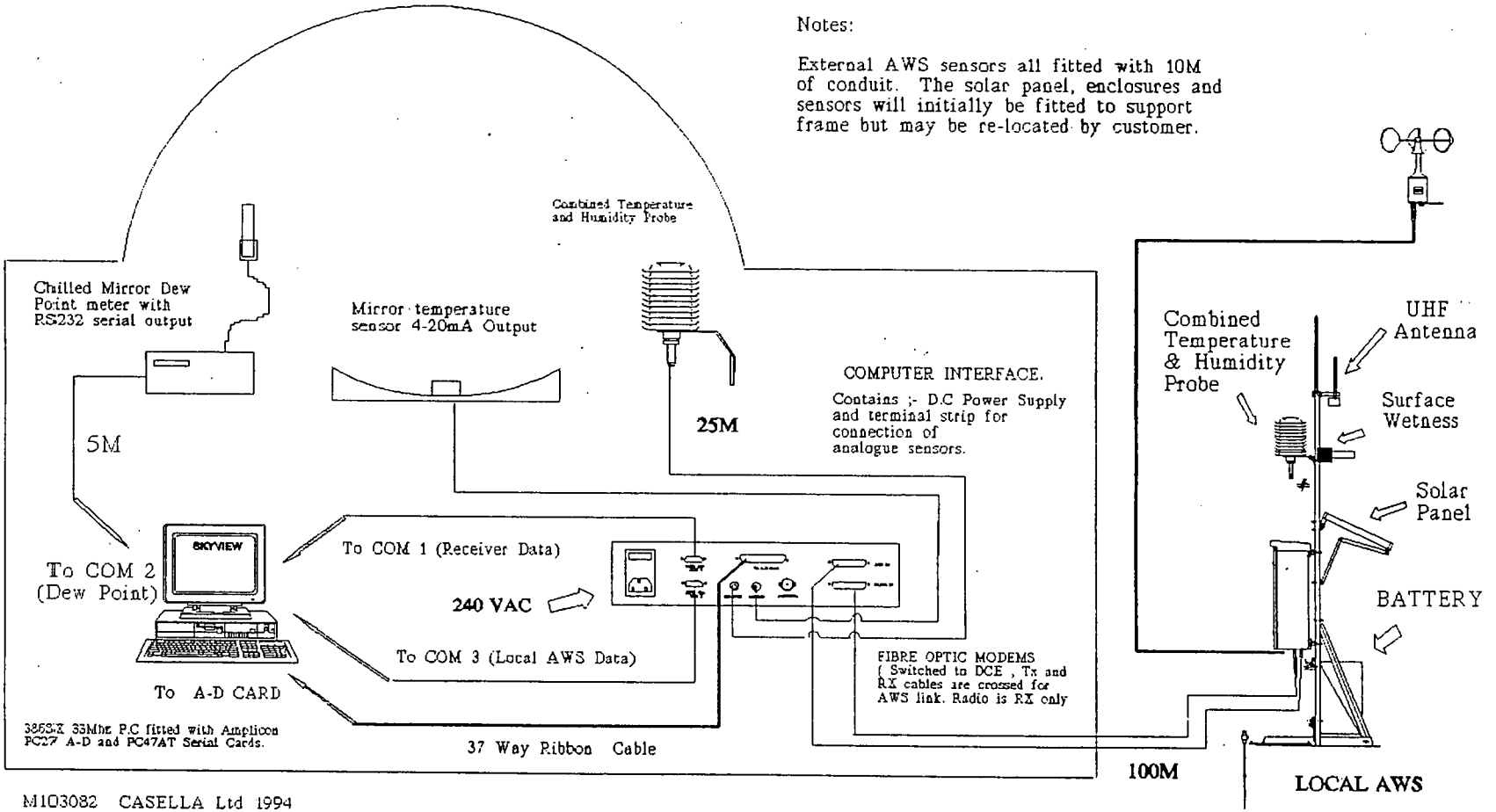

SYSTEM SCHEMATIC LAYOUT.

Environmental monitoring system.
Royal Greenwhich Observatory
Roque de los Muchachos, La Palma.

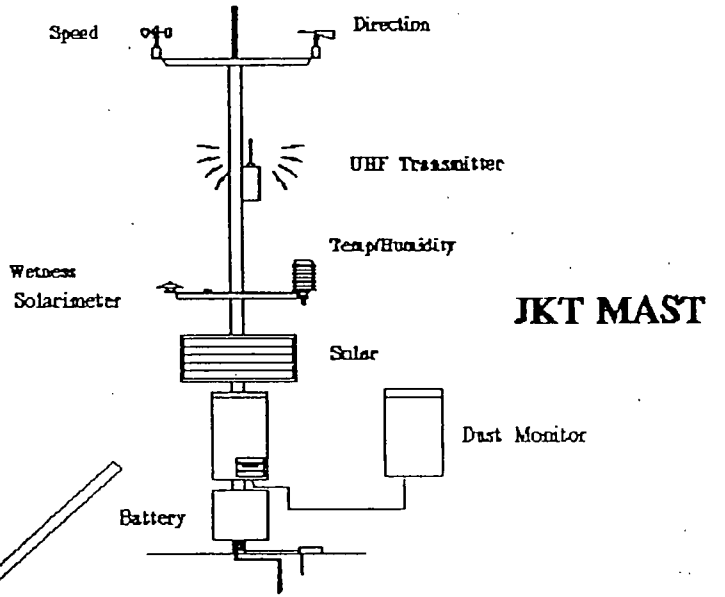

JKT MAST

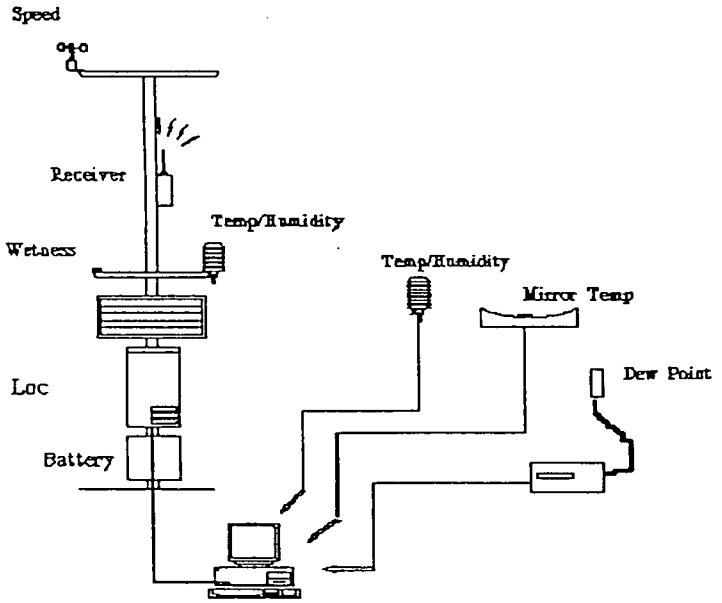

WHT Telescope

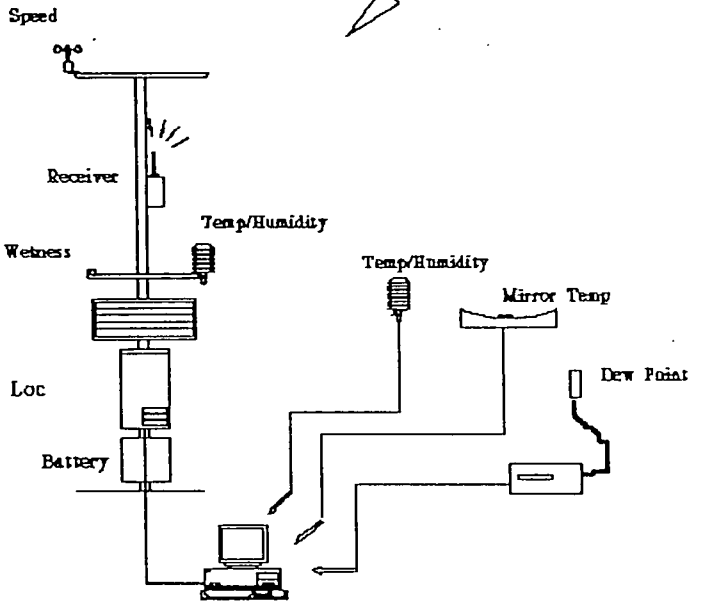

INT Telescope

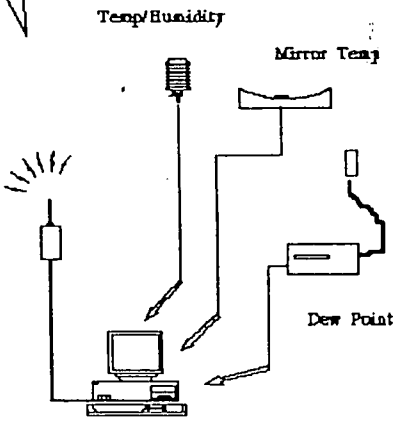

JKT Telescope

c) Thermometer

d) Solarimeter

e) Surface wetness sensor

f) Dust monitor

g) Barometer

Ground and underground level

h) Soil temperature sensor

i) Borehole temperature sensor

on the WHT and INT local stations

a) Local anemometer with speed only

b) Local external hygrometer

c) Local internal hygrometer

d) Local external temperature sensor

e) Local internal temperature sensor

f) Local surface wetness sensor

g) Mirror temperature sensor

h) Dew point sensor

Each group is also provided with:

a) Solar panel

b) Transmitter unit (only JKT mast)

c) 12 V Electrolyte battery

In the control room of each of the telescopes are:

a) Personal computer and display screen

b) Receiver unit

c) Dewpoint meter controller

1.2 Characteristics of the sensors

The characteristics of the sensors are listed here as given by the manufacturer:

1.2.1 Anemometers

JKT main mast Anemometer
Type : Three cup rotor
Range : 0 to 270 Km/h
Accuracy : $\pm 1\%$
Operating temp. : $-40°$ to $+70°$
Location : Top of the JKT main mast
Local Anemometers
Type : Three cup rotor
Range : 7 to 245 Km/h
Accuracy : $\pm 1\%$ over 11 Km/h
Operating temp. : $-40°$ to $70°$
Location : Roof of INT and WHT telescope buildings
Vane
Type : Continuous rotation wire wound potentiometer
Range : 0 - 355 degrees (0=North, 90=East)
Accuracy : ± 5 degrees
Sensitivity : $10°$ offset with 4.5 Km/h of windspeed
Operating Temp. : $-20°$ to $+70°$
Location : Top of the JKT main mast

1.2.2 Hygrometers

Internal and external Hygrometer
Type : Capacitive
Range : 0 - 100 %
Accuracy : $\pm 2\%$ at $+22°$
Operating Temp. : $-40°$ to $+60°$
Location : Inside of each telescope dome, INT and WHT local stations and JKT main mast

1.2.3 Thermometers

Air Temperature thermometers
Type : Platinum resistance
Range : $-25° + 60°$
Accuracy : $\pm 0.35°$ within $-20° + 50°$
Location : All the three stations

Soil and borehole thermometers
Type : Semi conductor current generator type
Range : $-25° + 60°$
Accuracy : $\pm 0.5°$ over $-20° + 50°$
Location : Close to JKT main mast

1.2.4 Solarimeter

Type : Pyranometer of silicon pn junction type
Range : $0 - 1500$ W/m^2
Accuracy : ± 2 W/m^2
Response time : 17 sec. to 66% of final reading
Operating Temp. : $-25°$ to $+70°$
Location : JKT main mast arm

1.2.5 Surface wetness sensor

Type : Three element carbon electrode
Range : Digital signal, $0 - 1$
Accuracy : Not specified
Response time : Not specified
Operating Temp. : $-10°$ to $+55°$
Location : JKT main mast arm and INT and WHT local stations

1.2.6 Dust monitor

Type : Light scattering optical device
Range : 0 mg/m^3 to 2 mg/m^3 (the range 0 mg/m^3 to 200 mg/m^3 is also available)
Sensitivity : ± 10 μg/m^3
Response time : Constant 1 sec or 10 sec
Operating Temp. : $0°$ to $+40°$
Location : JKT main mast electronics box

1.2.7 Barometer

Type : Not specified
Range : $660 - 860$ mbar
Accuracy : ± 0.3 mbar
Operating Temp. : $-20°$ to $+50°$
Location : JKT main mast bottom box

1.2.8 Dewpoint meter

Type : Direct detection of condensation on cooled mirror
Range : From 0° to 40° below ambient temperature
Accuracy : Not specified
Operating Temp. : −40° to +60°
Location : Close to each of the telescope primary mirrors

1.2.9 The Vaisala station

The sensors of the old Vaisala station at the INT and WHT give external and internal (dome) temperature and humidity. There is a rain detector on the roof of the INT which is also part of this system.
There are no sensors at the JKT because all the JKT equipment was struck by lightning in 1992 and the system was so damaged that a decision was taken not to repair it, as it was going to be shortly substituted by the Casella system.
One of the problems of the Vaisala station is that the external hygrometers are located in a wooden screen, which sometimes absorbs humidity and keeps the humidity reading too high. Another problem is that all the Vaisala sensors need frequent calibrations. On the other hand the Vaisala's values are updated on a shorter timescale (a fraction of a second) than those of the Casella system; the humidity warning can be silenced by a physical switch, which avoids continuing annoying noises once the alarm has been recognized. The actual day to day function of the meteorological station is to warn people when weather conditions could be dangerous for the telescopes and for the observatory in general. The old meteorological station only had temperature, humidity, wind speed and direction sensors, plus an aneroid barograph. The new station has improved safety in several ways:
1) It provides a dewpoint meter for each telescope, which is the instrument which really warns about any danger of water condensation on the mirror, which could cause considerable damage to the reflecting surface.
2) The two larger telescopes always have access to the JKT mast data, the highest site and often the first in detecting sudden changes in humidity.
3) WET-DRY alarms at the three sites detect raindrops falling from high and semi-transparent clouds (therefore difficult to detect by eye) over a large area.
4) The graphs on the screens give a good idea about the evolution of parameters such as humidity, wind direction, wind speed and air temperature, and allow simple but quick and effective forecasts.

1.2.10 Alarms

The Casella station provides several prealarms and alarms. A prealarm for a meteorological parameter consists of a beep and the box on the PC screen relative to that parameter turning yellow. The alarm gives a beep and a red box. When the alarm condition finishes the box turns green; an acknowledge key must be pressed to revert it to the original grey colour, or to silence the beep from a red or yellow box.

The Casella station provides prealarms and alarms for local and JKT mast wetness sensors, for windspeeds above 80 Km/h (50 Km/h for the JKT, which has a different dome structure) and when the difference between the dewpoint and the mirror temperature is smaller than 1 degree.
A new humidity alarm has been added by the observatory staff and is presently on test on the new Casella station. It is made the same way as the old Vaisala one, i.e. provided with a switch with three positions: 75% limit, 90% limits and the OFF position to silence the beep. The old Vaisala buzzer, which is actually very good, is still used as it is audible from outside the control room.

1.3 Telescopes safety limits

Basic general limits beyond which domes must be closed are :
Wind: 80 Km/h for INT and WHT, 50 Km/h for JKT
Humidity: 90% for all telescopes
Dust or smoke: dust deposit on horizontal surfaces
Dewpoint: one degree less than mirror temperature
Any precipitation (rain, drizzle, snow, hail)
Danger of falling blocks of ice
Excess of ice causing difficulties in operating domes and shutters
It must be added that whenever observations are impossible (for example due to high clouds) domes should be kept closed even if the conditions listed above are not exceeded.

Wind

Strong wind is not often experienced but it usually comes together with generally bad conditions, so that domes would be shut anyway. Nevertheless it is possible to have clear observing conditions and winds above 90 Km/h. The JKT is the most affected by wind problems; its shutter is made of two wings which move to the side, so that, when open, they offer quite a big surface to the wind and this telescope's safety limit is therefore much lower than that of the other two. A red alarm goes off and a beep sounds in the meteorological PCs when the speed limit appropriate to that telescope is reached.

Humidity

High humidity is possibly the most frequent phenomena which limits the use of the telescopes; it occurs sometimes without clouds, just by orographic lifting and cooling of the air which therefore condenses as fog.
The humidity is detected by the hygrometer and also by the wet-dry sensor (see Precipitation), although this last device only detects water on its surface. Unfortunately there is NO humidity alarm in the new station and we still rely on the old station one. A modification to the system is under investigation to provide this facility.

Dust or smoke

Dust is not checked through the Dust sensor measurements. This is because the instrument is not working properly and the values recorded by the station are not consistent with observed conditions. Severe dust conditions are quite rare and the only one I have

experienced in which domes could not be opened was due to a big forest fire close to the observatory site. Ash and burnt particles fell for several days and at some point the fire was so close that smoke was filling the buildings even when closed.

Dewpoint

This is measured directly by detecting condensation on a small mirror electronically cooled. There is a prealarm at 2 degrees difference between Dewpoint and telescope mirror temperature, then the alarm goes off when the difference gets to one degree or less.

Precipitation

Light precipitation is very difficult to detect. A suitable device is the Wet-Dry state sensor, whose detection system is made of two circuit terminals on a slightly tilted and heated surface. If water bridges the terminals the alarms goes off; if water is not supplied continuously it runs away from the surface, or it evaporates because of the heat of the sensor.

Large droplets and sleet are sometime quite widely separated, so that it might happen that the terminals of the sensor are not short circuited even when precipitation is falling. There is no way other than human check which can be used in such circumstances; experience can tell when conditions are right for such precipitation and periodic inspections outdoor must be made on those occasions by the telescope operator.

Ice falls

Again experience and direct check are the only means of detecting any danger to the telescopes due to ice blocks in particularly dangerous places. Meteorological conditions usually warn clearly for such circumstances: temperature is below zero, moving detectors such as anemometers and wind vanes are frozen, Wet-Dry state is WET and hygrometers read very high.

1.4 Assessment of data quality

This section gives only a general idea of the checks performed. Further details on pressure corrections, as well as numerical values, may be found in Appendix A.

1.4.1 Wind

Comparisons between the JKT anemometer and the one at the Meridian Circle, which has been working on site for over ten years, show good agreement, if one allows for small differences due to the different locations. These differences hide a small shift in the direction indicated by the JKT instrument, which occurred in November 1994. The structure of our device should leave a gap from 356 to 359 (included) degrees. Any value falling within this interval should be set to 0 degrees. This gap was found shifted to the sector 1 to 4 degrees (included). More details are found in § 1.4.11

The wind speed by all the anemometers always look quite consistent with handhold anemometer readings. A difference between the two of (say) 5 Km/h may be accepted as due to the handhold instrument always being lower than the fixed anemometers.

1.4.2 Humidity

Hygrometers, when checked during a stable period, proved to be quite reliable; their error, usually around 2%, gets bigger for either extremely low or high values (up to 15%), but precision at the extremes of the range is not needed for our purpose.

1.4.3 Temperature

Thermometers always showed consistent values with each other, either air or soil ones. The mirror temperature sensors work fine. It should be noted that there is a difference in temperature between the top reflecting surface, which is likely to affect seeing directly, and the under side of the mirror. This is due to the thickness and large mass of the mirror itself.

1.4.4 Solar radiation

We have not checked the solarimeter absolute values; the monthly graphs show a regular and smooth performance. The only error I could detect regards the moment the Sun appears after being obscured by cloud. The instrument cools when the Sun is hidden and gives slightly exaggerated values at the moment the Sun strikes it again. These jumps can be filtered out and are intrinsic of the working principle of the sensor.
The shadow of one of the security ropes holding the mast falls onto the solarimeter for a few minutes around 08:30 UT. This, however, is not detectable on the graphs.

1.4.5 Surface wetness

The surface wetness sensor gives a simple 0 - 1 digital signal and visual checks always confirmed its reading. Only failure of the connection between the sensor and the transmitter and failure of the transmitter itself have caused problems so far.

1.4.6 Dust

The dust monitor has not been taken into account in this thesis because its values are not consistent with visual estimates and the optics of the device have problems due to dust accumulation on the surfaces. Despite frequent calibrations, the performance is very poor and the data unreliable.

1.4.7 Pressure

The Carlsberg Meridian Circle mercury barometer was very useful in detecting quite a large calibration error of the Casella sensor; a new calibration of this sensor is not enough to correct it completely, so the problem is not solved yet, but at least we have a good estimate of the error and some indication of its dependence on temperature and pressure itself. The mean error is estimated to be about 4 mbar, with a maximum error of 8.5 mbar and minimum error of 1.2 mbar. Our sensor is always reading low and the error seems to increase with low external temperature and high pressure.

1.4.8 Dewpoint

The instrument is placed inside the telescope dome, so when the dome is closed (during the day or because of bad weather) it could be very far from the actual atmospheric dewpoint temperature.
The INT dewpoint sensor has occasional problems (see below). Apart from this, the general performance is satisfactory.

1.4.9 Power supplies

The solar panels work very well, the only problem is that the glass covers are quite fragile and during winter they are liable to get broken by ice falling from further up the mast or by water on the panel expanding when it freezes.
Batteries last well enough, if regularly charged during the day; however we have lost some data because the JKT mast battery had not been charged because of failure of the solar panel.

1.4.10 Data transmission

The WHT receiver gave some problems, and still is not completely reliable; the problem is under investigation, but it might be associated with some bad contacts in the internal cards.

1.4.11 Occasional malfunctions

The Casella system has proved to be quite good and most of the instruments have shown no evidence of malfunctions since installation. The instruments which have been tested by analysis of the data are: barometer, hygrometers, anemometers. Visual checks have been performed on the dust monitor, wetness sensor, dewpoint sensor, thermometers, solarimeter.
As mentioned earlier, the INT dewpoint meter has not been as reliable as the other two for reasons which are not so far understood. It is of the same type as the others but sometimes sudden jumps in dewpoint are recorded. These are not seen on the others and they occur in conditions which appear to be quite stable.
Some plots of wind direction for the year 1994 revealed a fault in this data. The plots showed that the gap of 4 degrees, which should be from 356 to 359 degrees (these and intermediate values should be set to zero), moved to 1 - 4 deg. during November 1994. The problem was a small shift of the screw which sets the zero of the variable resistance of the vane. The fault was easily solved.
During the winters of 1994-1995 and 1995-1996 some data were lost due to freezing of sensors and failure of solar panels, mainly during the months of January, February and March.
The three telescopes' sets of data contain the same JKT mast data which can differ from one to the other due to a small difference in the timing of data received, since the three PC clocks may have not been perfectly synchronized.
The best set of JKT mast data is contained in the INT files, in the sense that the

INT receiver has had less problems than the others and less data has been lost. The percentage of data lost until June 1996 is distributed as follows: 1.2% of the INT set, 2.4% of the JKT set and 3.5% of the WHT set. Much of the analysis has therefore been done using the INT set, although the WHT set has also been used when local data were preferable.

1.5 Meteorological data format and storage

As stated in § 1.1, although the data are read and output to the screen more frequently, they are stored on the PC disks only every ten minutes. Three new files (one for each PC) are created every day at 00:00 UT and closed at 24:00 UT. All the files are manually transferred to a database every month.
Figure 5 shows an example of a line of a file, with a header added to clarify which sensors produce the data and their units. The only spacing characters used are a colon (:) between hours, minutes and seconds, the blank space and the symbol #, this last being used when the data are not available. The JKT mast part of the file is common to the three sets of data, and the JKT mast set has no LOCAL part (so # symbols appear in the spaces thus left free).

1.6 The seeing data

1.6.1 The detector system

The seeing measures are performed by a task of the WHT autoguider, which extracts this information from the profile of a guide star image. The software takes a measure of the FWHM of both an X cut and an Y cut of the image, then takes the average of the two values. The result is displayed with a precision of 1/100 of an arcsecond, but several characteristics of the system restrict the useful decimal figures to one only.

1.6.2 Seeing data collection

Until May 1995 the telescope operator had the duty of logging by hand the values as read from the autoguider screen during normal observations and this possibly led to psychological and practical biases. A psychological bias could take place because a good seeing values instinctively looks worth noting, while bad values are easily thought to be as useless as the observation made with such conditions. A practical bias may occur when, during a bad seeing night, the bad weather keeps the telescope operator busy so that he has little time to record seeing values.
After May 1995 the seeing data have been automatically logged by the autoguider software into a daily file; the logging timing is about 10 seconds, but this may vary according to other tasks of the autoguider, such as integration time required for guiding, magnitude of corrections etc.

	JKT MAST											INTERNAL				LOCAL			
Time UT	Wspd Km/h	Wdir Deg	Gust Km/h	airT C	%RH %	Press mbar	Solar W/m^2	Bore C	Soil C	Wet -	Dust mg/m^3	Temp C	%RH %	Mirr C	Dew C	Wspd Km/h	airT C	%RH %	Wet -
11:00:00	28.3	167	32.4	17.7	13	772.2	924	#	#	0	0.5	27.6	31	25.2	#	38.2	18.9	14	0

Fig. 5

1.6.3 Seeing data quality

A few more remarks are necessary to clarify the nature and meaning of the seeing data. First of all the telescope focus directly affects the image size, therefore any defocus slightly exaggerates the seeing estimates with respect to the actual sum of atmospheric, dome and mirror seeing. Then, during observations, the centre of the field usually contains the object to be investigated and the guide stars are intercepted by the autoguider probe off-axis of the telescope. A further deterioration of the image of the guide star is then due to the coma introduced by this misalignment with respect to the optical axis. Finally, seeing values depend on the position on the sky too, because the atmospheric thickness which influences the seeing changes with telescope elevation. It is possible to estimate and correct for off-axis and atmospheric thickness distortions, as the telescope elevation and the autoguider probe position are usually recorded together with the seeing value. The total correction is on average around 0.2 $\widehat{''}$; the corrected values have been used, whenever available, for the present research. These corrections are presently under investigation, so there may be occasions where they either underestimate or overestimate the real seeing value. This is particularly evident with extremely low seeing values, say 0.5 $\widehat{''}$ or 0.4 $\widehat{''}$, for which this kind of correction may give values as little as 0.1 $\widehat{''}$. This explains the extremely low values which appear on some of the graphs of Chapter 3.
The deterioration of seeing caused by incorrect telescope focus is much harder to overcome. The ideal focus of the telescope changes throughout the night because of the thermal expansion of the telescope structure; there is an automatic compensation of this effect, but recent investigations showed that it is not working properly. The telescope focus values are recorded together with seeing values, but the actual *dimensions* of the telescope are not, so there is no mean of checking *later* whether the focus was correct. Only frequent checks of the telescope focus directly on the sky during observations can avoid the problem, but this is not always accepted by the visiting astronomers, who do not wish to lose some of their telescope time.
The conclusion is that most of the seeing values used in this thesis are overestimated because they have an element of defocus included in them. The consequent increment in seeing is around 0.08 $\widehat{''}$.
Another characteristic of the old seeing data is that they were not read at regular intervals, but simply whenever the telescope operator had the time to log them. However, meteorological data are logged every 10 minutes, so we always have meteorological data taken within 5 minutes (in the worst case) from the seeing reading. This limits the present research to phenomena with longer timescale than this, but experience shows that nights with seeing varying significantly on a shorter timescale than 5 minutes are quite rare, and moreover they usually bring bad seeing (2 $\widehat{''}$ or more), so normal conditions are well below this limit and this thesis very probably accounts for them.

1.7 The computer programs used in this work

The programs used throughout this research can be divided into two main groups:
a) Programs for instrument tests.
b) Programs for investigating relationships between seeing and meteorology.
The programming language is Fortran and all the computer codes are collected in Appendix C, so this section gives only a brief description of their function.

1.7.1 Programs for instrument quality control

Barometer checks have been performed using BARO.FOR
The input for this program is a file made up with the data from observations of the CAMC mercury barometer and the Casella barometer. Each single observation forms a row of nine columns, which contains the date and time of the readings, the external temperature at the JKT mast, the mercury temperature, the mercury barometer value (not corrected), the mercury value reduced to 0 degrees at the CAMC height (to be calculated, so left blank at first), the value reduced to 0 degrees (to be calculated) and at the Casella barometer height (2366 meters) (to be calculated); the last two columns are the Casella reading and the difference (mercury reading)−(Casella reading) (this last to be calculated applying the standard corrections for temperature, gravity, height).
The program fills the blanks and produces a file like the input file, but complete (Fig. 6). Corrections for height difference, mercury temperature, gravity acceleration and instrumental errors are described in Appendix A. The program also gives the average error of the Casella sensor and the total number of records.
Wind direction checks have been carried out with the programs WIND.FOR and WMON.FOR, which plot a graph of wind direction against speed, the former on an annual basis and the latter on a monthly basis. Each couple of values recorded for wind speed and direction are simply taken as the coordinates of a point, which is then plotted on a polar graph. These plots allowed the shift in the direction gap to be detected.

1.7.2 Programs for seeing investigation

These can be divided into three groups:
1) Programs which plot separate graphs of seeing and meteorological parameters for a given period of time.
2) Plotting programs which do not involve seeing directly.
3) Programs which plot a meteorological parameter (or combinations of meteorological parameters) against seeing.

Group 1 has been the first attempt to compare seeing with the meteorology of the site; two graphs were plotted: the top graph showing seeing during one month, the bottom graph showing the meteorological parameter during that month. This last graph has a bold line where seeing data overlap with meteorological data, a dotted line elsewhere.

Comparison of barometers CAMC(Hg)/ Casella file ./azzaro/met/baro.
"Hg 0 C" is pressre corrected for temperature and gravity. Year 1995

Date	Time	Test	THg	Hg Read	Hg 0 C	Hg 2366m	Casell	Hg-Cas
03-02	11:00	8.5	7.0	781.4	779.0	775.2	769.0	6.2
10-02	14:00	2.1	3.0	778.8	776.9	773.1	765.0	8.1
24-02	11:50	5.6	7.0	781.7	779.3	775.5	767.0	8.5
18-03	17:20	5.5	7.9	773.4	770.7	766.9	missing	unknown
20-03	18:00	4.0	9.0	771.5	768.9	765.1	761.0	4.1
29-03	09:40	3.3	7.5	770.1	767.7	763.9	760.0	3.9
03-04	17:40	3.0	5.5	771.0	768.8	765.0	758.0	7.0
07-04	18:20	1.4	15.0	772.6	769.2	765.4	759.0	6.4
13-04	11:40	3.5	12.8	772.3	769.2	765.4	759.2	6.2
17-04	15:40	3.5	11.5	772.4	769.5	765.7	759.5	6.2
19-04	17:50	3.5	13.5	773.7	770.5	766.7	760.1	6.6
20-04	17:10	-1.5	13.4	772.4	769.2	765.4	758.0	7.4
21-04	18:10	2.5	13.3	774.2	771.0	767.2	761.1	6.1
08-05	16:40	11.5	9.5	777.8	775.1	771.4	765.7	5.7
09-05	18:00	8.3	10.8	778.4	775.5	771.8	766.3	5.5
10-05	15:40	6.5	9.0	777.7	775.1	771.3	764.7	6.6
11-05	17:20	11.0	10.4	777.3	774.5	770.8	765.1	5.7
15-05	13:40	12.8	10.1	779.3	776.5	772.8	767.8	5.0
21-06	11:50	15.9	12.0	779.8	776.8	773.1	767.9	5.2
26-06	16:00	12.0	10.3	775.2	772.4	768.7	764.8	3.9
27-06	17:20	17.0	12.0	778.3	775.3	771.6	768.2	3.4
28-06	17:00	15.4	12.4	779.1	776.0	772.4	767.7	4.7
29-06	18:10	12.9	13.0	777.9	774.8	771.1	766.6	4.5
30-06	17:20	12.7	12.0	778.1	775.1	771.4	767.2	4.2
06-07	18:40	14.8	14.2	779.9	776.6	772.9	769.5	3.4
07-07	16:40	12.4	12.3	776.5	773.4	769.8	764.8	5.0
08-07	16:30	12.1	11.5	776.6	773.6	770.0	766.4	3.6
09-07	18:00	13.3	12.0	778.6	775.6	771.9	767.8	4.1
10-07	17:40	11.4	12.2	779.5	776.5	772.7	768.2	4.5
20-07	18:30	23.1	19.4	784.0	780.0	776.4	774.9	1.5
21-07	16:30	23.6	19.5	782.6	778.6	775.0	773.3	1.7
22-07	20:10	18.9	19.4	781.5	777.5	773.9	772.2	1.7
23-07	17:40	21.5	19.3	782.0	778.0	774.4	773.2	1.2
17-08	10:50	19.0	12.7	782.2	779.1	775.4	773.9	1.5
25-08	15:30	15.7	13.5	780.9	777.7	774.0	772.4	1.6
26-08	15:40	14.9	13.3	780.7	777.5	773.8	772.0	1.8
27-08	18:00	15.7	13.8	779.7	776.4	772.8	770.9	1.9
28-08	18:00	14.8	16.1	779.0	775.5	771.8	769.6	2.2
09-09	16:50	15.9	14.9	780.9	777.5	773.8	772.2	1.6
18-09	14:30	8.8	11.2	778.5	775.6	771.8	769.3	2.5
03-10	11:00	11.8	9.5	781.2	778.5	774.8	772.3	2.5
16-10	15:00	15.7	11.8	778.6	775.6	771.9	769.5	2.4
26-10	15:20	6.6	10.5	777.4	774.6	770.8	765.9	4.9
27-10	15:30	7.4	9.5	778.4	775.7	771.9	768.1	3.8
02-11	09:50	10.4	9.1	779.3	776.6	772.9	767.8	5.1
07-11	10:45	2.4	9.5	773.5	770.8	767.0	762.2	4.8
23-11	11:10	13.0	8.5	783.3	780.7	777.0	774.8	2.2
27-11	10:35	1.0	7.7	773.4	770.9	767.1	761.3	5.8
04-12	11:15	9.6	6.5	780.9	778.6	774.8	772.0	2.8
13-12	09:30	-0.1	7.0	759.3	757.0	753.2	748.0	5.2

Fig. 6

It is not worth discussing further these programs here because it is clear that a comparison by eye of fragmented and noisy seeing data with the meteorological graph is not scientifically acceptable, so this method has been abandoned.

The second group includes the programs PROWIN.FOR and PROWINN.FOR, with a few variants of these. These programs plot a polar graph of wind direction against wind frequency, either using our data or the NOT meteorological data. The two main programs cover one year, while the variants basically cover shorter periods of time. These plots show an interesting discrepancy between the NOT site and ours, which is discussed in Chapter 2.

The third group is the most important, as nearly all the analysis of Chapters 3 and 4 is based on the plots made by the programs of this set. The basic programs are MMSS.FOR and GRA.FOR, of which many variants have been produced for special cases.
MMSS.FOR matches seeing data with a meteorological parameter selected at input, looking for minimum time difference between the two readings (less than 5 minutes). It writes each couple of coordinates into a file, which GRA.FOR uses to plot the graph of that parameter against seeing. GRA.FOR can also fit a line to the points via a classical Least Squares fit subroutine (See P.F.T.V. 1986).
These two programs can deal with every single meteorological parameter. Modifications to them were necessary to combine different parameters or to set some constraints on other parameters, which is a useful way of defining better a particular meteorological situation. This technique has been used, for example, when plotting seeing against wind direction or seeing against the angle between wind direction and telescope azimuth, in order to select different wind speed ranges and to see how the effect of wind speed changes the patterns of the graphs.
More details on these programs can be found by referring to the source codes in Appendix C.

Chapter 2

COMPARISONS WITH OTHER STATIONS

2.1 Foreword

Since the new meteorological station was first installed on site, several tests on the instruments have been carried out. Some of these tests have been done using the data from our meteorological station only, while others were possible thanks to the availability of data from other meteorological stations on site. In particular, the data from instruments at different locations made it possible to make some interesting comparison of the meteorology and seeing, apart from the instrumental tests. This chapter describes the analysis which involved other sets of data and the meteorological implications of the differences with respect to the Casella set.

2.2 The comparison with the Nordic Optical Telescope data

Thanks to the courtesy of the NOT staff we could access the data collected by their meteorological station from 1990 up till March 1995. This sample is in principle quite a valuable one as it includes several years of observations and seemed a very good base for cross checking instrument performances and comparing typical meteorological conditions on different sites. Unfortunately the overlap with our data is reduced to less than one year.
The NOT data include air and soil temperature, pressure, humidity, wind speed and direction and illumination. The data are not logged at regular intervals nor are logging times taken at the nearest minute. The pressure data have been found to show large intervals of faulty readings, during which the instrument showed a fixed value all the time. However this did not affect the comparison described here which concerns only the wind direction frequency and it is illustrated in two polar graphs, one made from the NOT data and the other from the Casella data.
The wind data from each of the two stations were plotted as points of coordinates ϱ and θ, where θ was the wind direction and ϱ the frequency of that direction over the

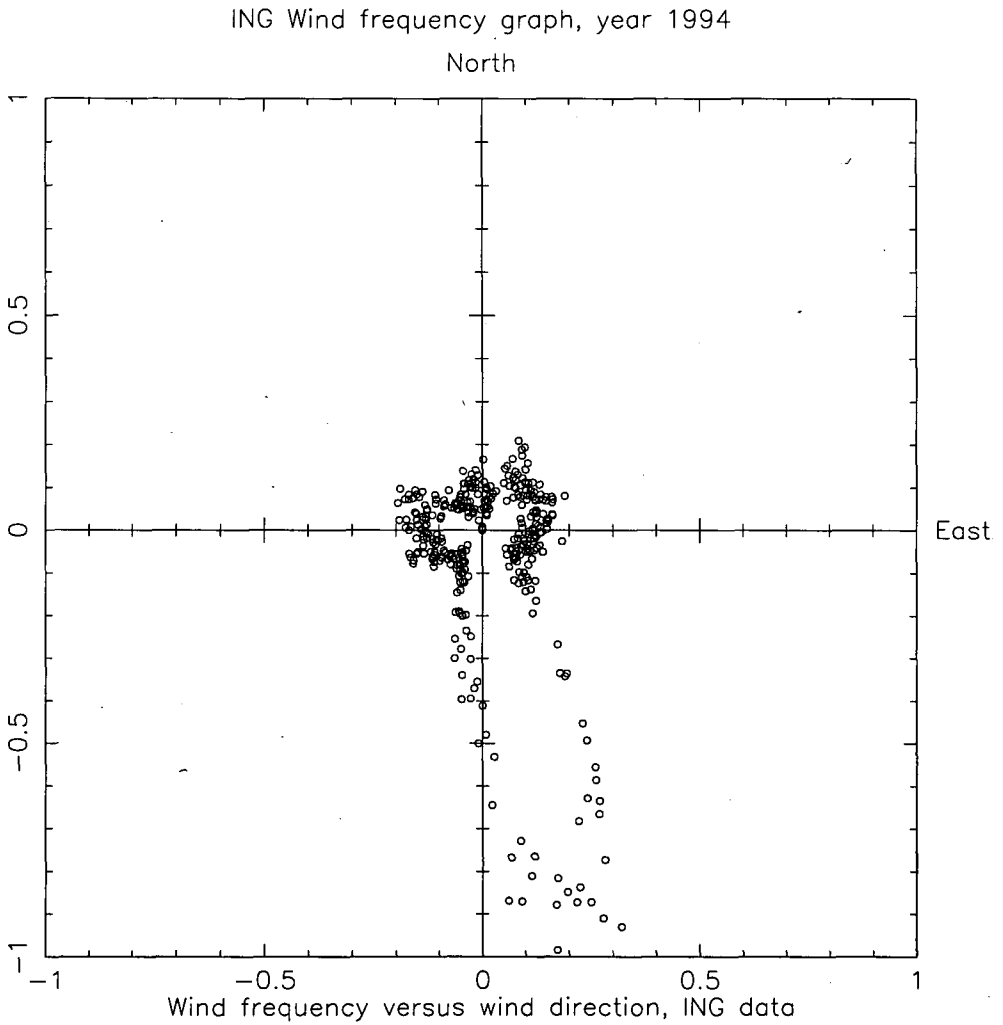
ING Wind frequency graph, year 1994
North
East
1
0.5
0
−0.5
−1
−1
−0.5
0
0.5
1
Wind frequency versus wind direction, ING data

Fig. 1

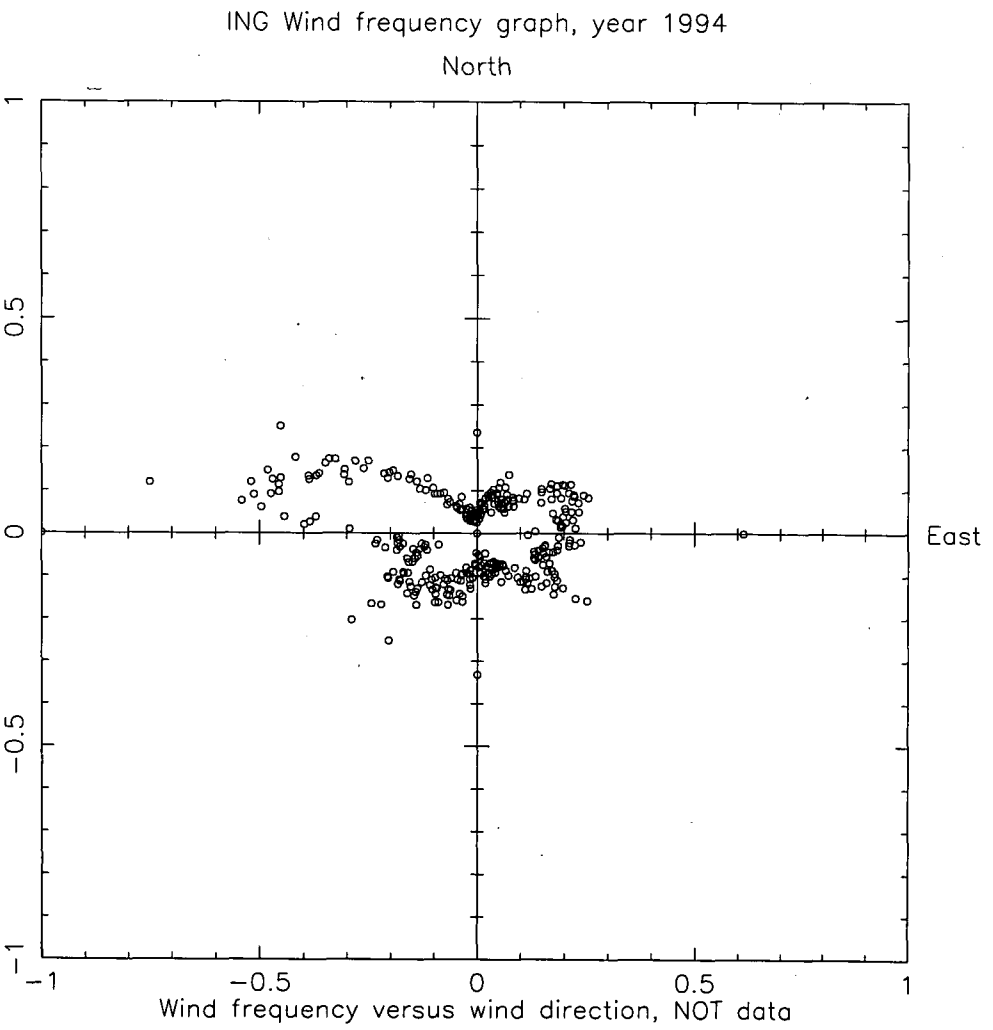
ING Wind frequency graph, year 1994
North
East
1
0.5
0
−0.5
−1
−1
−0.5
0
0.5
1
Wind frequency versus wind direction, NOT data

Fig. 2

whole time interval, usually one year. The frequency was simply computed counting the times each direction appears over the time interval, then normalized taking the maximum frequency as unity. It is important to remember that wind speed is not involved here.
In the case of the NOT data it was possible to make several plots, one for each year from 1990 to 1994, which showed that the same basic pattern occurs every year. The 1995 plot shows that the anemometer had some malfunction, as some directions have a too low frequency with respect to others. This was probably due to the reduced number of data and the fact that these data were taken during the cold part of the winter '94/'95, from January to March. The anemometer was probably frozen for quite a long time, giving faulty readings. In the case of the Casella station, only the 1994 plot was made as it overlaps five months of the NOT record, so the two 1994 plots were chosen for the comparison, and are shown in Figures 1 (Casella data) and 2 (NOT data). At the NOT site the wind seems to come preferably from four directions, ENE, ESE, SW and WNW, and this last direction shows the largest frequency.
At the Casella main mast the situation is surprisingly different. The main directions are WNW, NE and SSE and the last prevails by a large amount.
The meteorological implication of these differences will be discussed in § 2.4. Concerning the technical performance of the two sensors I tested the reliability of the data and I directly checked the two vanes (NOT and Casella) when the wind direction was pretty constant and found them in good agreement. Also the values recorded by each station were consistent with the position of the vanes. A simple transformation is needed because of the different zero point of the NOT vane (for which 0 = South) and this has been taken into account. My conclusion is that both instruments are correct and the differences showed by the graphs are not due to any malfunctions. From the point of view of the quality control of the anemometers the unexpected result of this comparison was quite useful because it forced me to check the two instruments and the plotting programs very carefully, so as to be sure that such differences were not due to any errors or malfunctions.

2.3 The comparison with the Transit Circle data

The Transit Circle instrument (referred to as CAMC) is located in a small building to the West of the WHT, on a side of the hill. The CAMC altitude above sea level is 6 meters less than that of the WHT and 40 meters less than the Casella main mast. The CAMC building is not visible from the WHT as it is hidden by the lee of the hill. The CAMC is provided with a full meteorological station which has been collecting data since 1983. The data used for this comparison concern wind speed and direction and Figures 3, 4 and 5 show the plots for the years 1991, 1992 and part of 1993 respectively. Unfortunately the year 1993 is not complete and no data for 1994 or any successive years were available, so that there is no overlap with the Casella data and the analysis can only be made by eye, extrapolating the CAMC typical pattern from years 1991, 1992 and 1993 and comparing it with the Casella pattern. The CAMC plots show wind direction against speed on a polar graph, where speed is in meters per second,

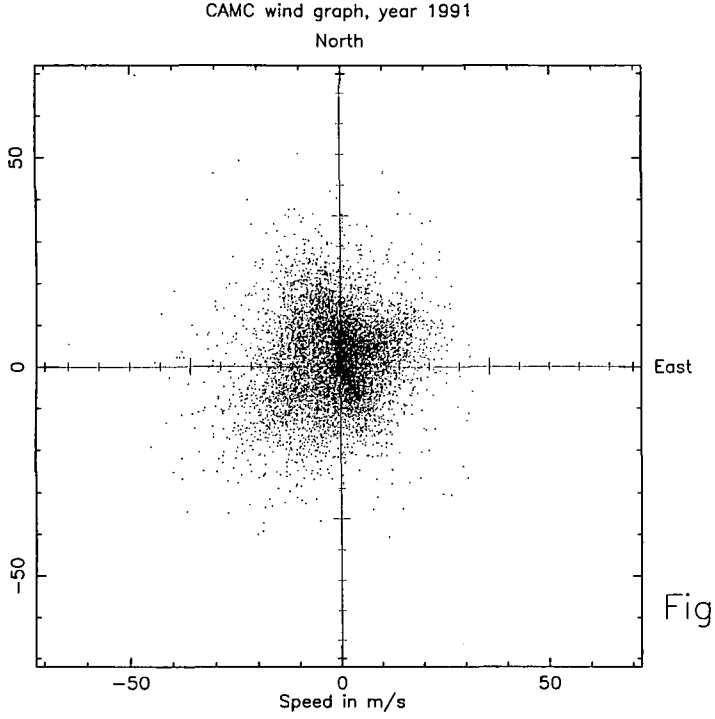

Fig. 3

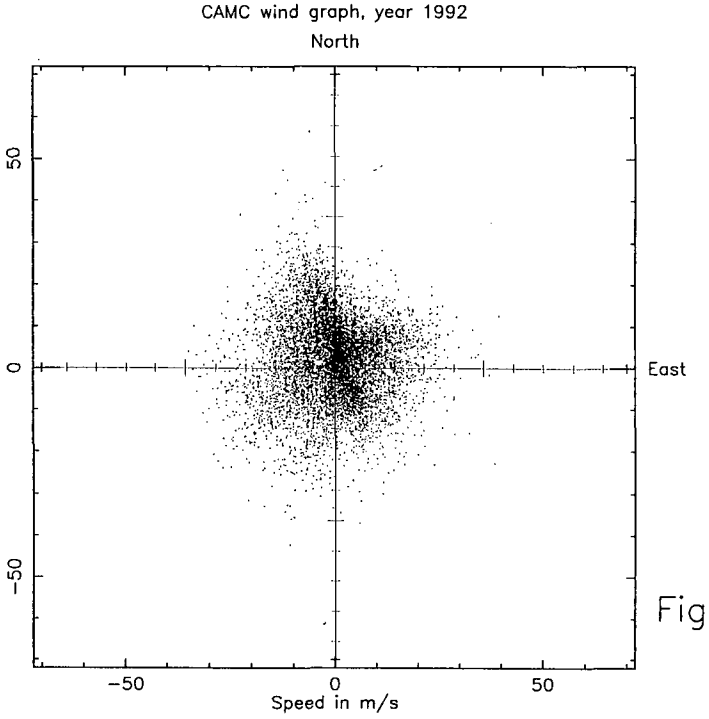

Fig. 4

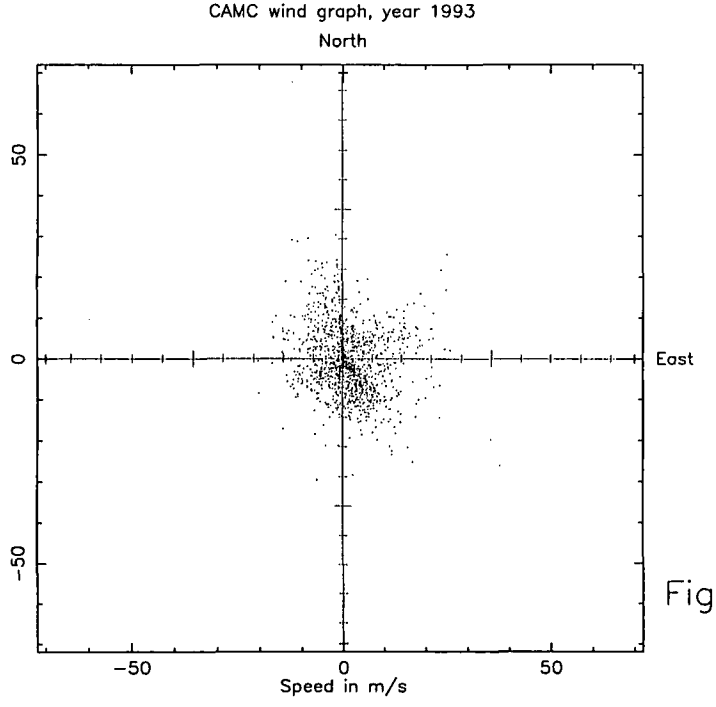

Fig. 5

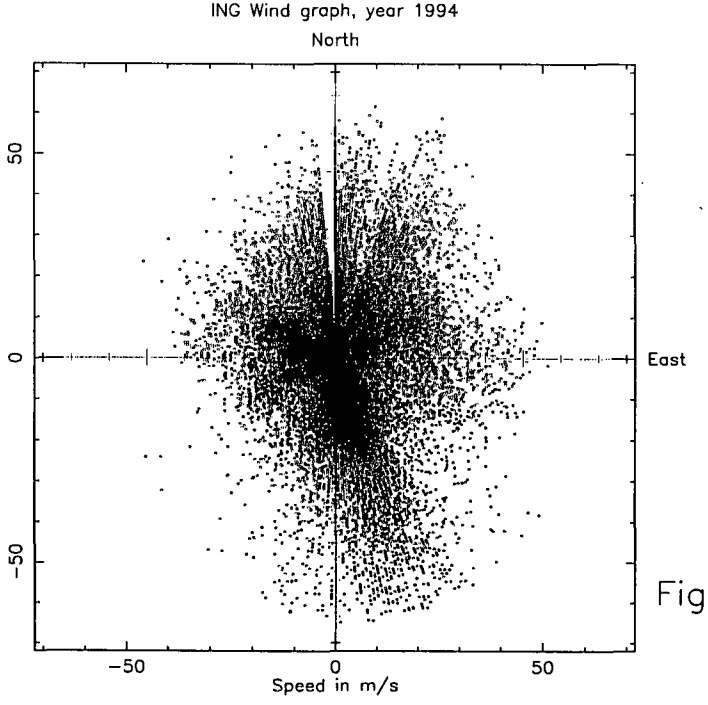

Fig. 6

therefore they can only be compared with graphs of the same type. Fig. 6 shows the corresponding plot of the Casella station for the year 1994. From the three CAMC graphs it seems that the distribution of wind directions is fairly uniform, with a slight preference for an axis along directions SSE - NNW. The Casella graph is less uniform and shows at least three major preferences: SSE, WNW and NE. This is also consistent with the graph of Fig. 1. The small gap (blank sector) from 356 degrees to 359 is due to the structure of the vane (see Chapter 1 § 4.11). Again, the wind distribution is different at the two sites, even if the difference seems less dramatic than with the NOT data. This is strange as, among the three considered, the NOT and the Casella sites seem to be the most similar. Both are well exposed peaks, almost at the same height (2375 m) facing to the caldera southward and with the lee slope of the mountain on the other side. The CAMC site is more hidden and protected from the wind, much lower (2325 m) and far away from the caldera. This is evident also from the lower windspeed which appears on the CAMC plots (the average windspeed at the NOT is not shown here, but it is very similar to the Casella one, sometimes with stronger gusts).
The next section will discuss the possible meteorological implications of these differences.

2.4 Meteorological implications of the differences

We have just seen that every place has its own patterns of wind, which is one of the parameters most likely to affect the seeing. The only possible reason for this is that the anemometers used just measure the local turbulence more than the wind which causes it, because the top of a 6 meters mast is not above the turbulent layer, specially with strong winds. It is not likely that one of the three instruments is the "right" one and gives the true wind direction; more probably each of the three indications of the wind direction has some random error associated with it due to its own particular location with respect to the surrounding peaks. The basic consequence is that the moving direction of the air mass in which the island is imbedded can only be known with some approximation. Any plots involving a relation with wind direction will therefore be affected by a high noise, unless some method is used to extract a better approximation of the *true* wind direction. This is what has been done for the plots of seeing against wind direction of Chapter 3. In this case the option of taking the average wind direction over bins of 4 hours time has been adopted, the reason being that major changes in wind direction always seem to take a few hours (see Chapter 3 § 2.1). The conclusion is that turbulence is present and it is an important phenomena at the observatory site. The data collected by anemometers 6 meters above the ground indicate that the telescopes and domes are imbedded in the turbulent layer, which means that the air turbulence and the wind probably play a very important role in local seeing.
In the next chapter it will be shown that the wind direction is often determinant to the turbulence on site.

Chapter 3

METEOROLOGY AND SEEING

3.1 Foreword

The following analysis was made on the basis of the meteorological data collected by the Casella station over a period of 12 months, from July 1994 to June 1995, and the corresponding seeing data logged by the telescope operators during the same period. After May 1995 a set of seeing data has been recorded by the automatic log of the autoguider and manual logging stopped in June 1995 (see also Chapter 1 § 6.2). The first of these samples, on which is based the analysis of this work, has been used on its own and not in conjunction with the second in order not to mix different peculiarities. For example the lack in regularity of the telescope operator observations surely affects the first set.
The seeing data refer to the WHT only, so the WHT local meteorological data have been used whenever possible, because they represent more directly the conditions of that part of the atmosphere from which originated such seeing values. Unfortunately, parameters like wind direction, atmospheric pressure, soil and borehole temperature are only measured at the main mast (close to the JKT), so the compromise of comparing WHT seeing data with main mast meteorological data has had to be accepted when referring to these parameters. When looking at the main mast data, the INT set turned out to be the best, because it suffered less omissions due to malfunctions (see chapter 1 § 4.11). It is therefore important to note that, whenever the label "INT data" appears on a plot, it does not mean that those data have been collected at the INT site, but it means that the INT set of main mast data has been used to produce the graph. When WHT local data have been used the label "WHT data" appears on the plot. The label "ING graph" refers to the Isaac Newton Group (see Introduction § 1).
Most of the graphs have been plotted according to the following philosophy: the meteorological parameter data have been rounded to the nearest integer and for each of these values the average seeing has been calculated, then the meteorological parameter has been plotted against these average values.
The following comparisons are discussed in this chapter:
1) Wind/seeing, including direction/seeing, speed/seeing, [angle between telescope azimuth and wind direction]/seeing and [gust−windspeed]/seeing.

2) Temperature/seeing, including [air temperature]/seeing, [soil temperature]/seeing and [borehole temperature]/seeing.
3) [Soil temp.−air temp.]/seeing.
4) [Local temp.−internal temp.]/seeing.
5) [Internal temp.−mirror temp.]/seeing.
6) [Atmospheric pressure]/seeing.
7) [Relative humidity]/seeing.

3.2 Wind/seeing

Wind is the meteorological parameter which is most likely to affect the seeing, as turbulence, density and temperature of local air masses are strongly influenced by the wind.
I have used different approaches to the problem, the first of which was to study a possible relation between wind direction and seeing, the second compares seeing with wind speed and the third analyzes the effect of the wind hitting the dome at different angles with respect to the opening.

3.2.1 Wind direction and seeing

The first attempt at finding a relation between wind direction and seeing was made by plotting wind directions against seeing on a polar graph. Each point of the graph of Fig. 1 has coordinates θ and ϱ, where θ = is the wind direction clockwise from 0 = North and ϱ is the average seeing value measured at that wind direction. In other words, for each point, its distance from the centre is proportional to the measured seeing value. The numbers which label the axes refer to the seeing values, from 0 to 4 arcseconds, while wind directions are North = top, East = right.
This graph is not easy to interpret; the number of points at each direction is different and this can bias a visual interpretation of the graph. To avoid this type of bias the graph of Fig. 2 was plotted, this time binning directions by one degree, therefore drawing only one point for each degree. Zones of worse seeing seem to be NW, WSW and SE, although such small deviations from the mean value (1 $\widehat{''}$) could simply be due to statistical fluctuations. However, the clear feature of this graph is the uniformity of the distribution of the points about a circle of radius 1. This would imply that the average seeing is about 1 $\widehat{''}$ and that this value does not depend much on wind direction. This conclusion is not quite satisfactory, as some dependence had been noticed in earlier investigations (See A. & W. 1984) and is also suggested by the dramatic orography of the island, which should cause irregular turbulence along different directions. A further step was therefore made, binning directions by 5 consecutive degrees. The result is shown in Fig. 3 but does not seem to indicate any more than Fig. 2; big values on the SSW and SE quadrants are confirmed, while in NW are not, suggesting that these larger values could actually result from statistical variations due to insufficient data. Still no relation between wind direction and seeing appears, therefore a last and possibly most interesting experiment was made, attempting to filter out local turbulence

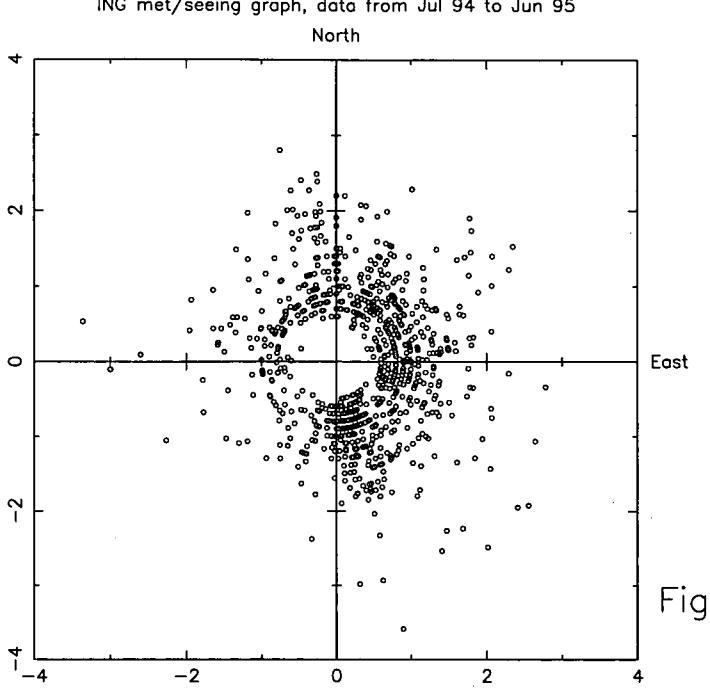

Fig. 1

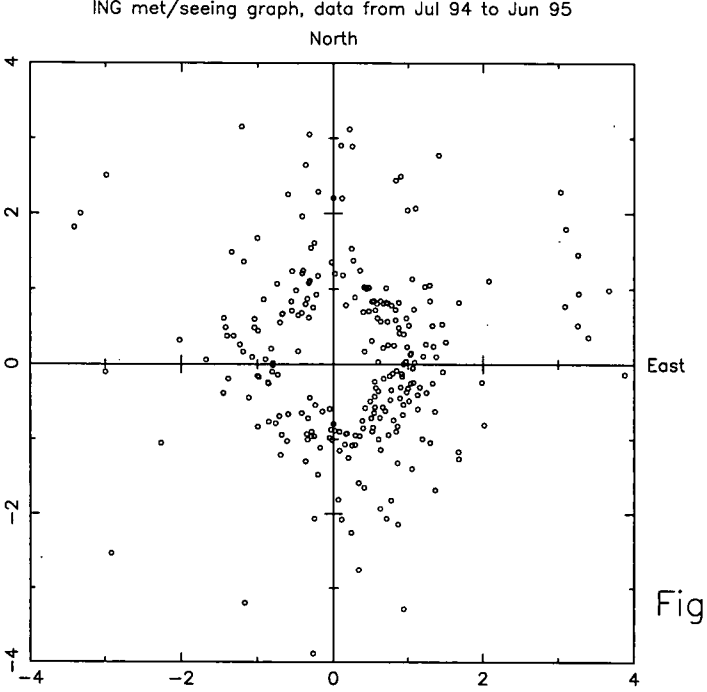

Fig. 2

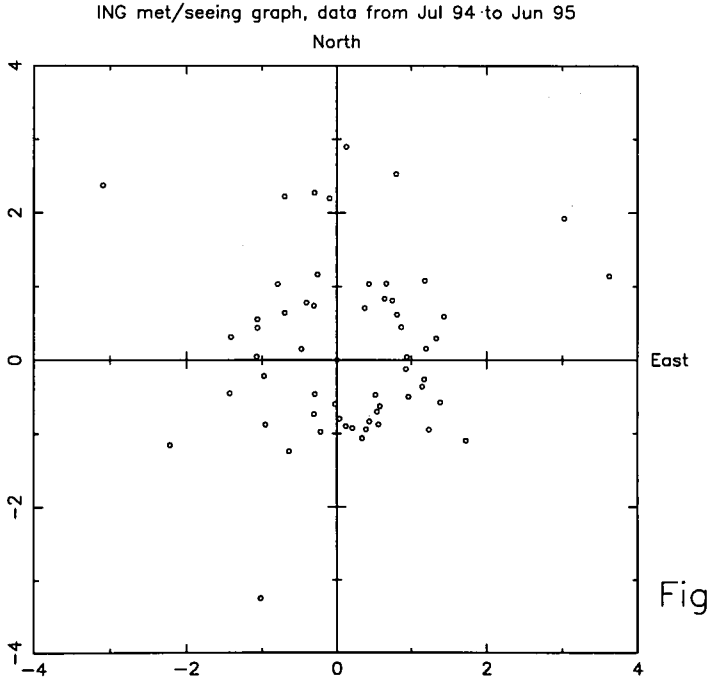

Fig. 3

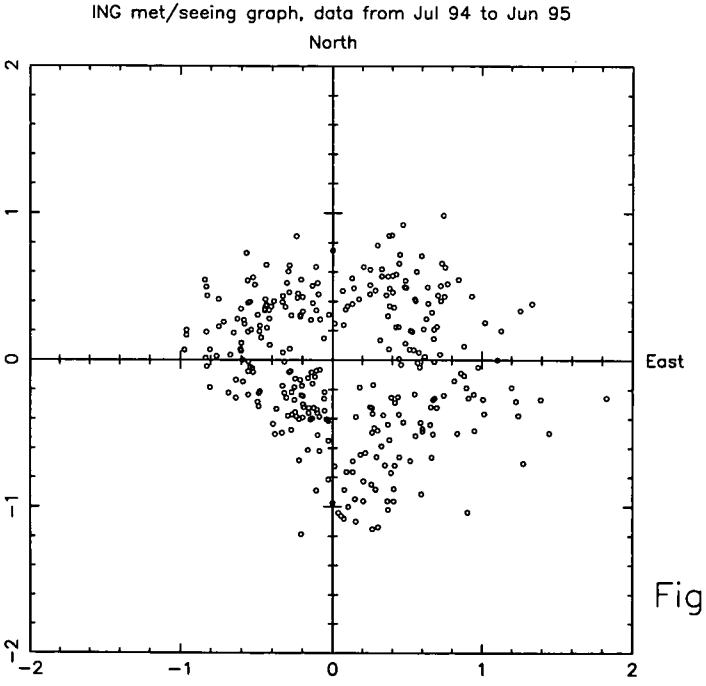

Fig. 4

in the direction of wind (see Chapter 2 § 4).
Wind at a height of, say, 800 m is not affected by the orography of the ground, therefore we could call its direction the *true* wind direction. Down at the ground level, squalls, gusts and whirls due to the irregular surface cause a noise which hides this true direction. The true direction can be extracted from local data as the average direction over a relatively large period of time. Looking at a graph of wind direction against time one can realize that important changes in wind direction always take a few hours, so that over 24 hours just a few changes are possible. The new plot, shown in Fig. 4, was made taking, for each seeing data, the average wind direction over a four hours interval, centered at the time of that seeing observation. The choice of four-hours bins was made estimating the persistence of a wind direction from the graphs given by the Casella station: four hours seemed a good compromise, not too big as to lose major changes but large enough to smooth out temporary orographic variations.
At last some relation appears: the best seeing occurs when the wind comes from the South-West, then it remains fairly good all throughout W, NW, N and NE, with some deterioration around NW and NE. The worst wind direction seems to be the SE, i.e. with wind blowing from across the Caldera. With some imagination this graph has the appearance of the map of the island, with the observatory at point (0,0) (compare it with the map of La Palma before the introduction to this thesis). It is quite conceivable to think that seeing is affected by the history of the airflow, which carries the "signature" of interaction with the ground for a long or short time period, depending on the distance of the observatory from the flat surface of the sea along each direction. Also, the roughness of the side of the mountain exposed to the wind could have some importance; the graph is consistent with this factor as well, as the northern part of the island, although steeper, has corrugations almost set in radial directions, centered at the observatory, while the southern part offers obstructions square to the wind, when it flows towards the observatory. All this will be supported also by the discussion of the next section.
To prove such an hypothesis, however, it would be necessary to carry out a much deeper analysis than can be included in this thesis.

3.2.2 Wind speed and seeing

This comparison was first carried out using two graphs containing a month data in cartesian coordinates, one showing seeing values against time and the other wind speed against time. These were put one above the other, to cross-check the two plots searching for in-phase variations. This method turned out to be not very effective, because it does not allow a detailed analysis of small features; the only conclusion which can be made from it is that the relation between wind speed and seeing, if there is one, is not extremely pronounced.
The next step was to plot windspeed against seeing using data for a whole year. Each point of this graph has windspeed and seeing values as X Y coordinates. One would expect a definite increase in seeing values as windspeed goes up, because higher wind speed probably increases turbulence, specially near the ground, where the air hits the rough surface. Fig. 5 shows this graph, for seeing values up to 2 $\widehat{''}$. The line fitted

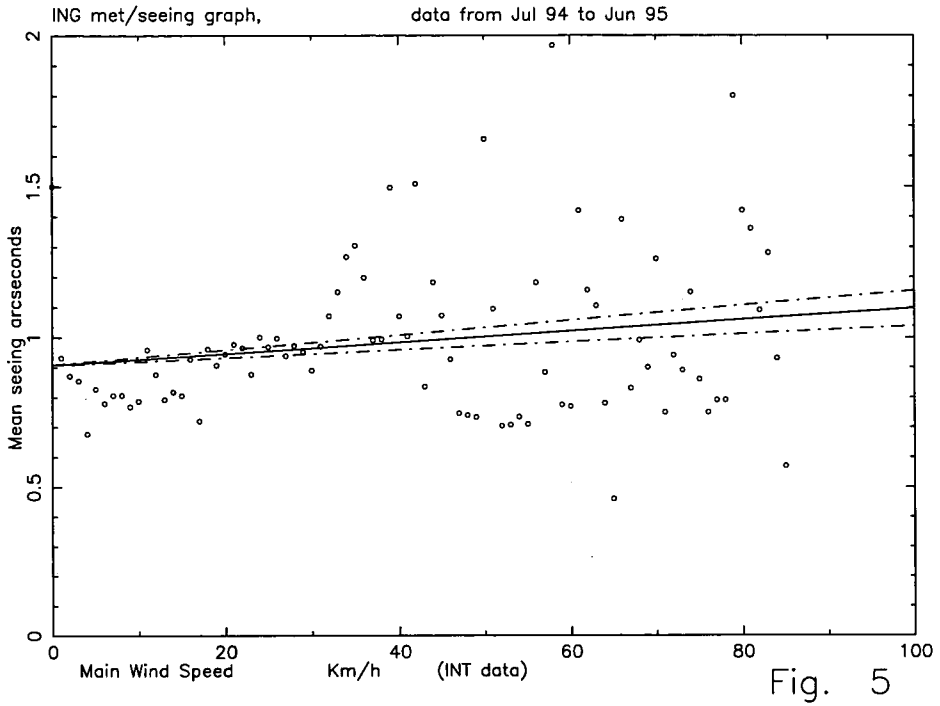

Fig. 5

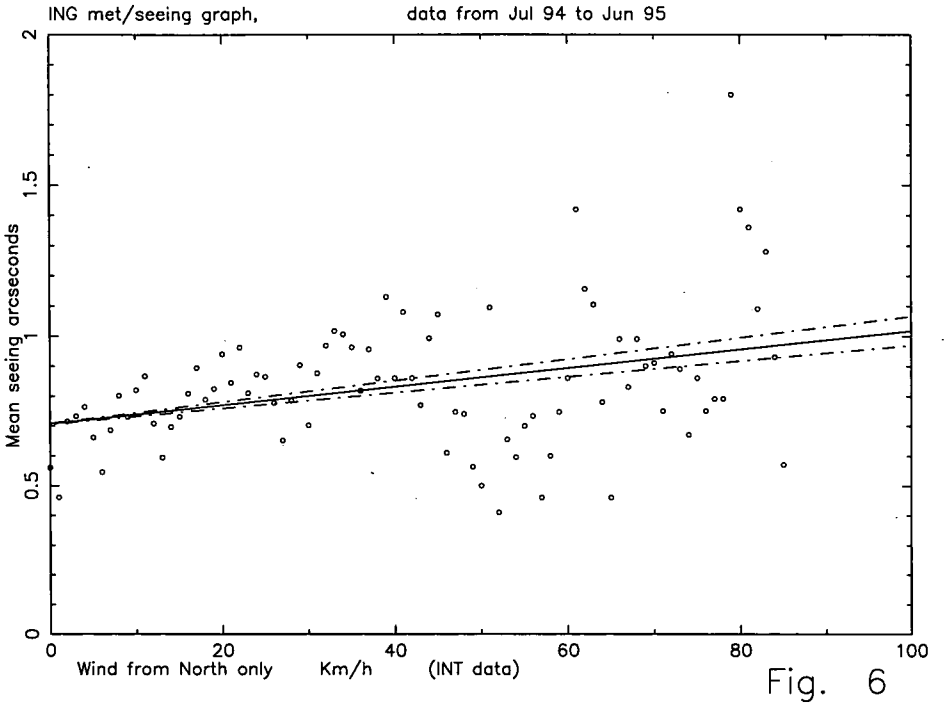

Fig. 6

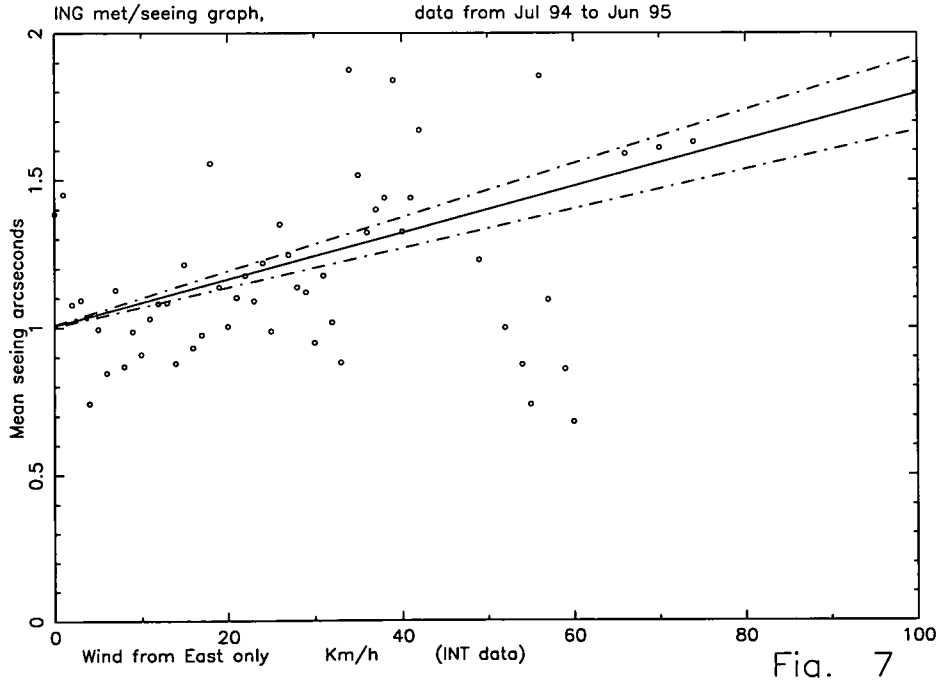

Fig. 7

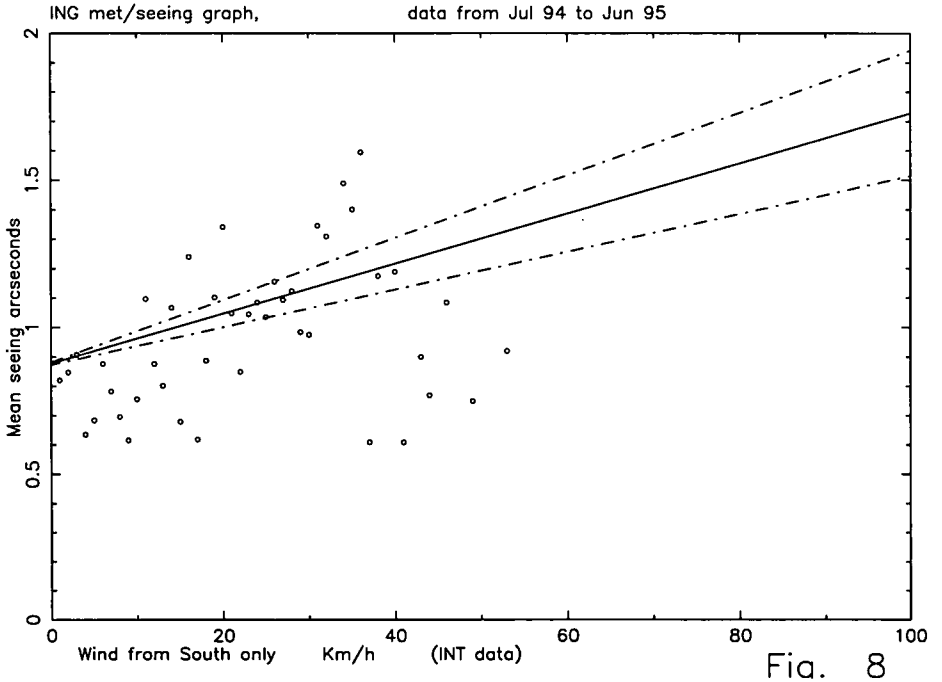

Fig. 8

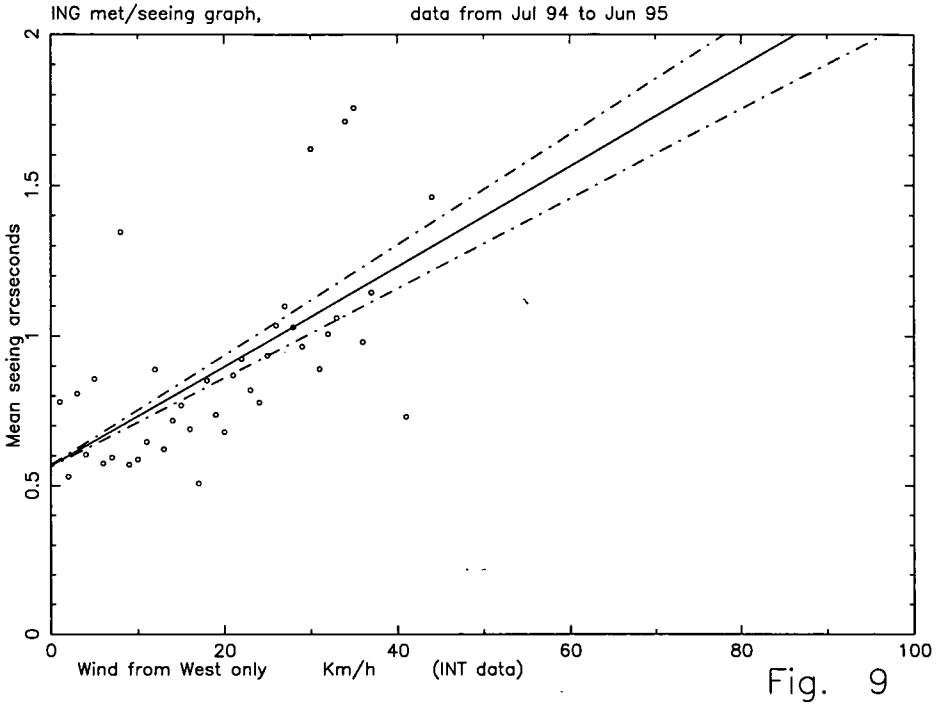

Fig. 9

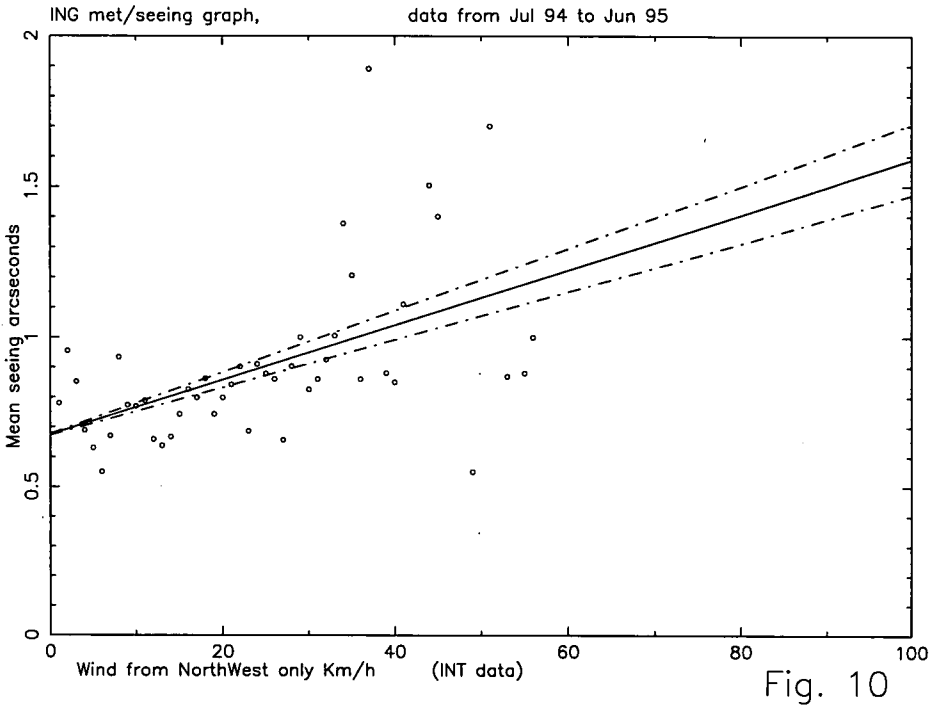

Fig. 10

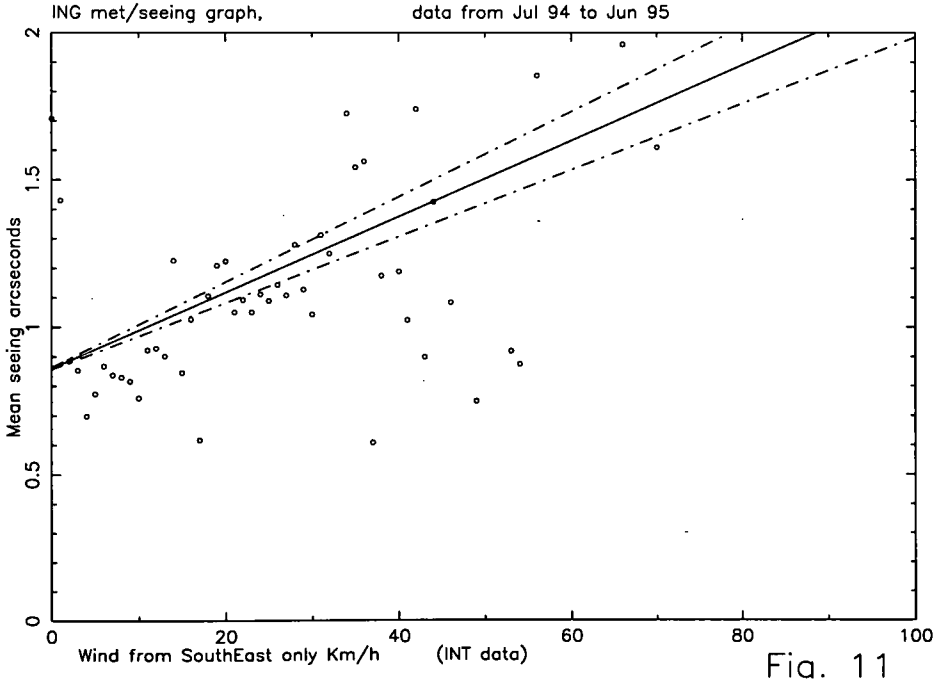

Fig. 11

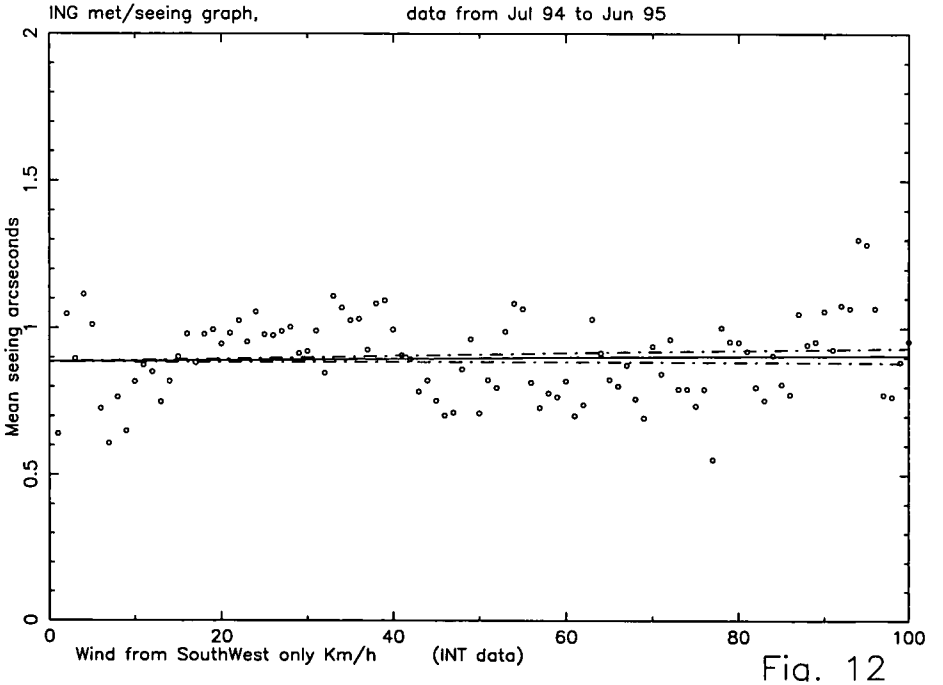

Fig. 12

to the points has a definite increasing slope, as expected, but nevertheless there are still some very good seeing values at speeds as high as 70 Km/h and even more. This suggests that there are circumstances in which high wind speed affects seeing less than in others; the first simple guess is that wind direction could influence the effect of wind speed on seeing, so I have plotted other graphs which are of the same form as the previous one, but with selected wind directions. Figures 6, 7, 8, 9 show the mean seeing as a function of wind speed for wind directions North, East, South, West.
The seeing/speed slope for northern winds is the smallest among these graphs, and the mean seeing is better. Western winds show the strongest slope and finally southern and eastern winds seem to have an intermediate effect. Moreover, western and southern winds appear to be quite light. The last experiment was to look at NorthWestern winds, SouthEastern winds and SouthWestern winds effect separately. From Figures 10, 11 and 12 it is clear that the first two slopes are very similar, but with better seeing with the NW wind, while Fig. 12 clearly shows that with the favourable SouthWesterly winds the wind speed has almost no effect on seeing. Northern and Eastern winds reach very high speeds, in fact the highest which can be seen on these graphs is the closing limit for the telescope at 80 Km/h. The conclusion is that the wind direction affects the seeing significantly and also determines the influence of the wind speed on seeing; winds from SouthWest bring the best seeing and the smallest influence of windspeed on seeing.

3.3 Angle between telescope azimuth and wind direction/seeing

To make the following clearer we will refer to the angle between the telescope azimuth and the wind direction as ϕ. Also the assumption has been made that the dome effect on the wind flow is considered to be symmetric, in the sense that if, for example, the wind is blowing from the North, the two dome positions with the slit facing East and with the slit facing West are assumed to give equivalent seeing conditions. In terms of turbulence caused by the dome and the dome slit, this assumption is quite reasonable as the dome skin is actually symmetric at the sides of the slit, where the turbulence has its greatest effect on seeing. ϕ runs then between 0, when the wind is blowing *into* the dome slit, and 180 degrees, when the wind is blowing towards the dome side opposite to the slit.
The telescope azimuth data have been recorded in the seeing data file by the telescope operator, so, for each seeing datum, the corresponding telescope azimuth is always available.
It is reasonable to suppose that the possible relation between seeing and ϕ could also be influenced by the wind speed, therefore a selection of windspeeds has been adopted. In the first stage the cut was set at 20 Km/h, which is the average wind speed of the site, therefore one graph for windspeed below 20 Km/h and another for windspeed above 20 Km/h have been plotted. Another graph with windspeed above 40 Km/h has also been plotted. All this has been done with wind data from the main mast, as well as with WHT local wind data. Either of these two choices of windspeed data has

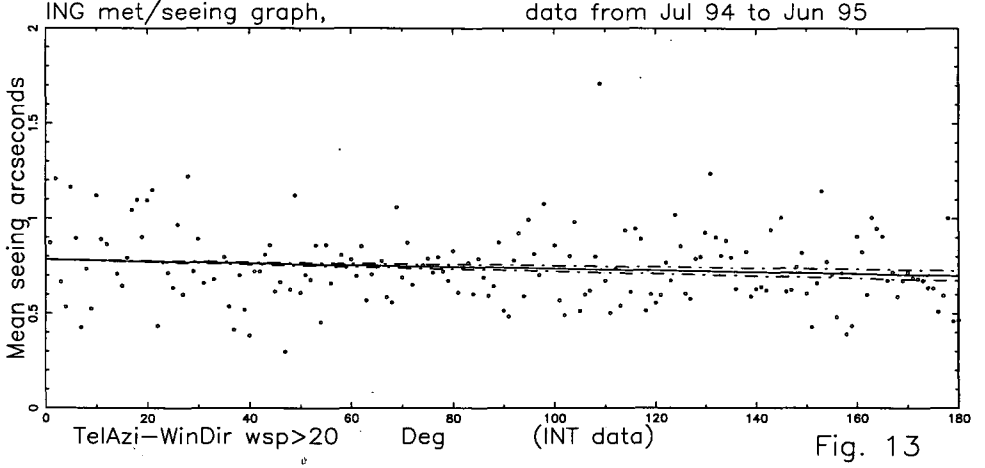

Fig. 13

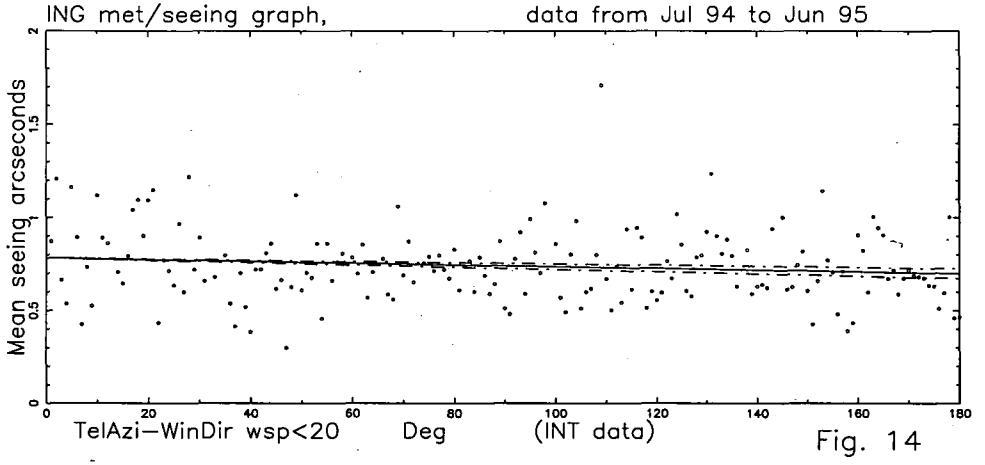

Fig. 14

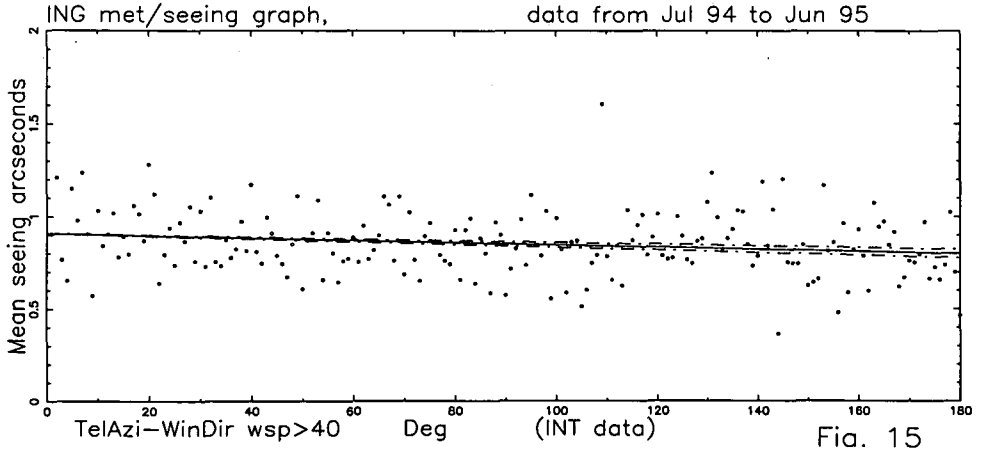

Fig. 15

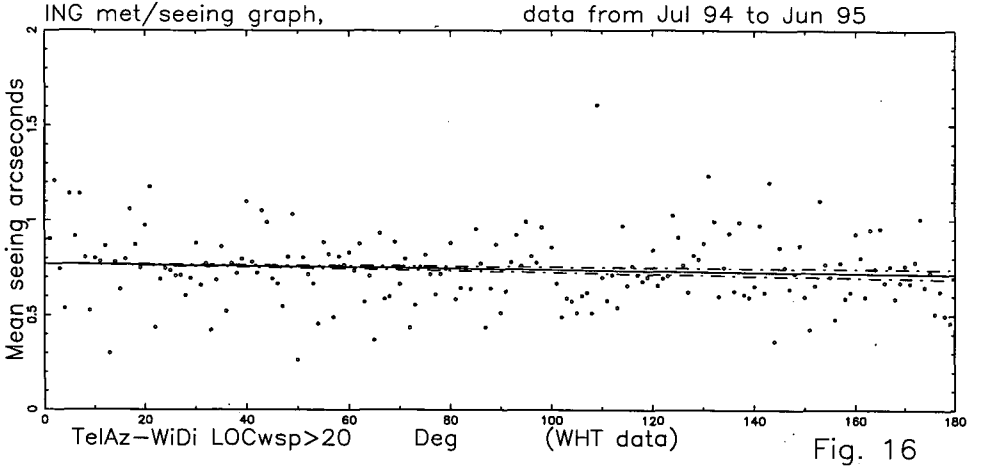

Fig. 16

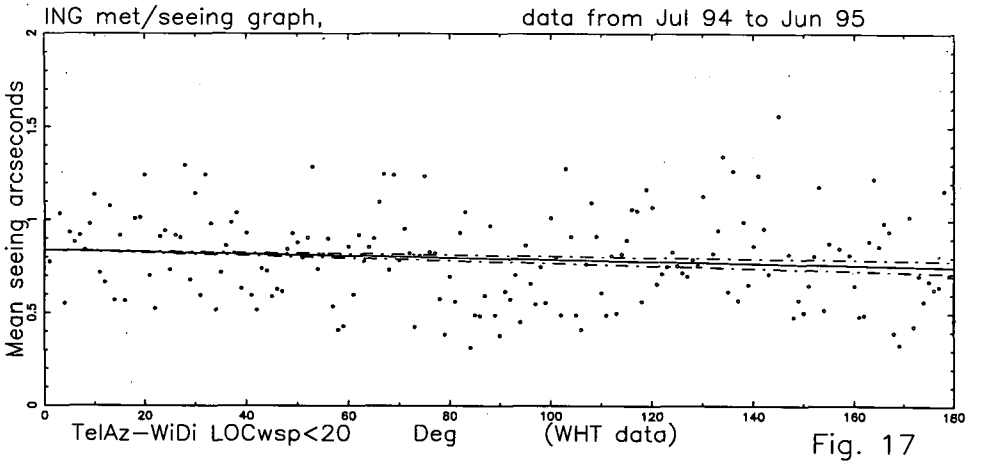

Fig. 17

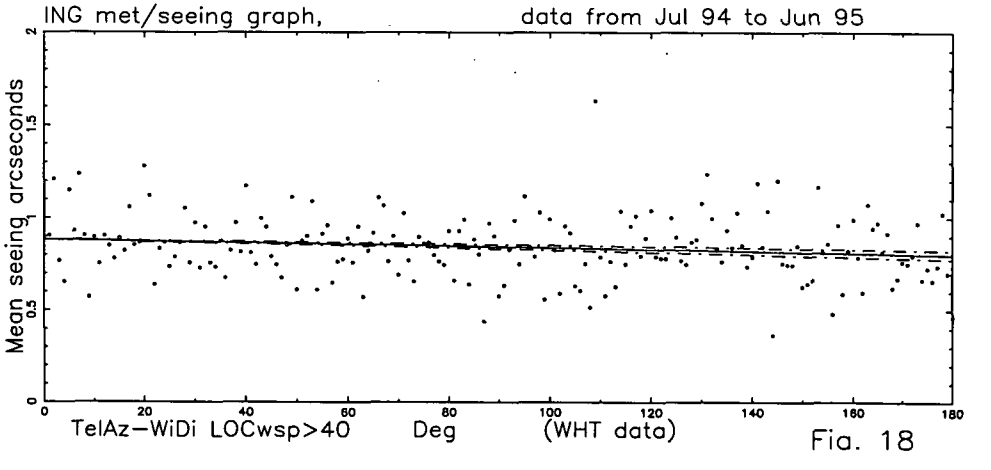

Fig. 18

its advantages and disadvantages: the main mast wind speed data are taken from the same place from where the wind direction is measured, while the WHT local data, of course, are more directly connected with the WHT seeing, but are less reliable due to the very close proximity of the anemometer to the dome.
In total there are six graphs. Figures 13 to 15 show ϕ against seeing for main mast windspeed above 20 Km/h, below 20 Km/h and above 40 Km/h respectively. Figures 16 to 18 are the equivalent with windspeed from the WHT local station.
All the graphs are almost flat, with a slightly negative slope. There seems to be almost no difference between windspeed below or above 20 Km/h, for either set of windspeed data. Above 40 Km/h the slope is still the same but the average seeing is slightly worse. The only difference between the graphs using the main mast windspeed and the ones with WHT local windspeed is a bit more scatter for the latter, specially at low windspeeds. This is probably due to the proximity of the dome to the WHT anemometer. The seeing difference between the two extreme positions ($\phi = 0°$ and $\phi = 180°$) is as little as 0.1 $\widetilde{''}$. The reason for this small difference is not the shake of the telescope caused by the wind blowing into the slit; in fact the same difference is found on the graphs referring to low windspeeds, which surely don't cause any windshake. The most probable reason for this is the turbulence inside the dome, which is likely to be higher when the wind is blowing directly into the slit. The conclusion is that the dome has some effect on seeing, but this varies very little with different dome positions, with slightly better results when the dome slit points away from the wind. No information about the specific dome effect on the WHT seeing can be extracted from the data used, as these always include the "dome seeing".
The bigger scatter on the graphs at low windspeed could be due to a larger uncertainty in wind direction when the wind is light; the wind vane accuracy is better than 10 degrees only with windspeeds above 4 Km/h.

3.4 LocalAir-Soil-Borehole temperature/seeing

These three comparisons have been grouped together because they represent the same phenomenon read at different levels. The WHT local data could be used for the air temperature, while the soil and borehole temperature data come from the main mast because are measured only there. Fig. 19, showing WHT local air temperature against seeing, has a definite negative slope and not much scatter of the points around the fitted line. Fig. 20, showing soil temperature against seeing, also has a clearly negative slope but a somehow bigger scatter, while in Fig. 21, showing borehole temperature against seeing, the fitted line is almost flat and the scatter bigger still. As a general comment, the scatter of the points is quite small in all the three graphs, if compared with graphs of other parameters, and the main feature is that the best seeing is observed when the temperature is high. As the ground depth increases, the slopes of the fitted lines become less pronounced and the scatter of the points increases.
The obvious conclusion is that seeing is better in summer, during which all the temperatures are high, but the effect is less pronounced underground, because of the thermal inertia of the ground and its insulating effect against solar radiation. The scatter vari-

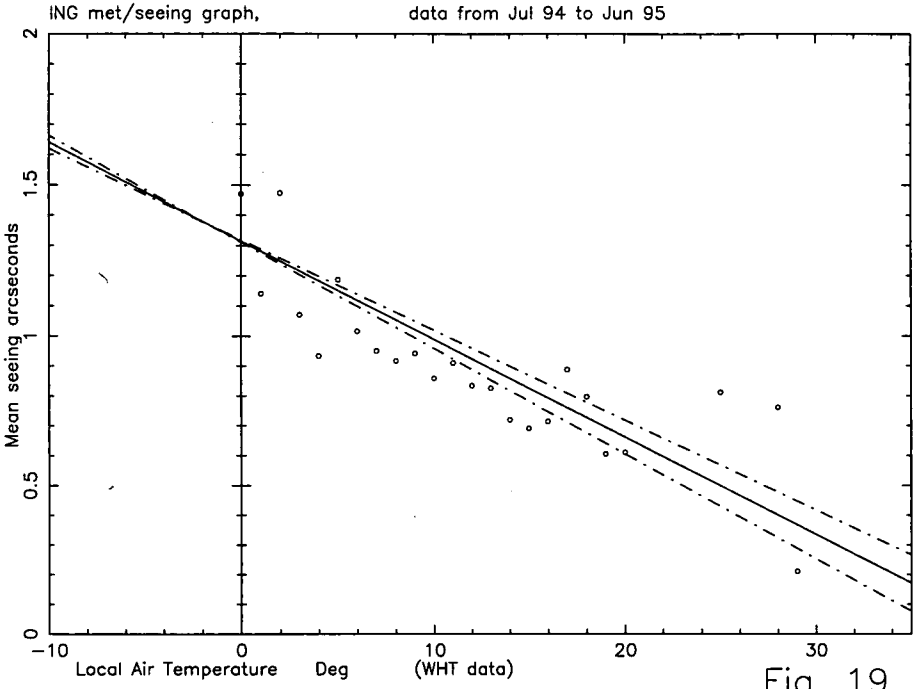

Fig. 19

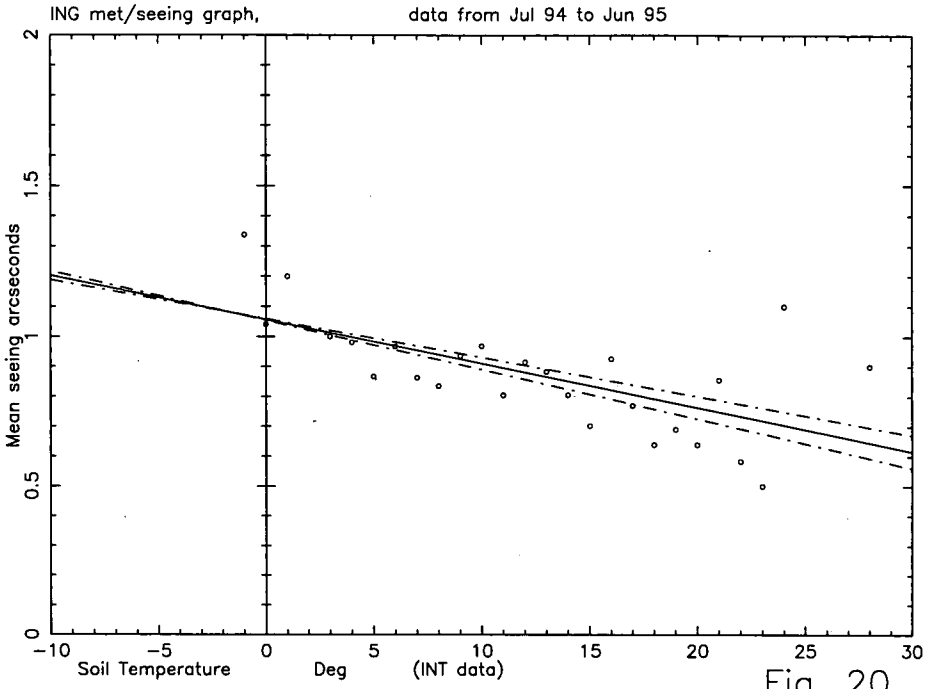

Fig. 20

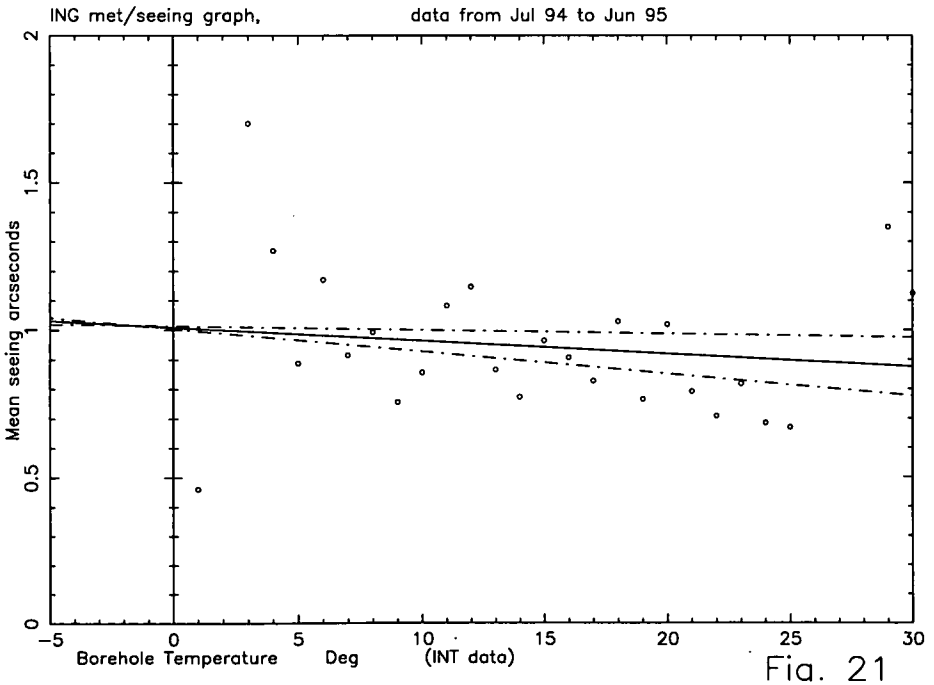

Fig. 21

ation also could be due to the fact that deeper in the ground changes take place more slowly, therefore the connection between the temperature underground and the open air conditions diminishes with depth.
It is worth noting that the lowest temperatures are measured by the soil thermometer; this is what should be expected, because the deep ground is insulated from very low temperatures, the air is warmed by longwave radiation coming from the soil, which therefore loses energy and cools down more than the air above it. This same pattern emerges from the analysis of the next section as well.

3.5 Difference between soil and air temperature/seeing

We will refer to the difference between soil and air temperature as ΔT.
The soil temperature is measured at the main mast, therefore it has been compared with the main mast air temperature. The values of ΔT have been binned to the nearest integer and the data representation has been split to cover three different time intervals. Fig. 22 shows the plot made with data gathered at any time during the night, while Fig. 23 shows data gathered only during the first part of the night and Fig. 24 shows data gathered only during the last part of the night.
Little scatter is observed in the first graph, Fig. 22, which shows a slight negative slope. This would mean that seeing is better when the soil is hotter than the air above it. During the first part of the night, as shown in Fig. 23, the effect seems to be more evident, the slope is a bit more pronounced and the scatter is still quite low. The plot of Fig. 24 has the opposite slope and has more scatter of the points around the fit line. Thus during the last part of the night seeing seems to be better when the soil is colder than the air.
We can conclude that, during a good night, we should expect the ground to be hotter than the air at the beginning, then cooler at the end. These are typical conditions holding during a very clear night, particularly during stable summer weather: the sun heats the ground more during summer, because stable weather brings a good transparent atmosphere and also because the sun is higher in the sky. Then, during the night, the ground loses its heat through long wave radiation, helped by the clear sky, and at the end of the night the situation is reversed, i.e. the ground is cool because of the loss of heat during the whole night, while the air has been kept warm by the ground radiation and therefore its temperature didn't drop much.

3.6 Difference between local temperature and internal temperature/seeing

The data used for this analysis all come from the WHT local set and the values have been binned to the nearest integer. The term "internal temperature" refers to the temperature inside the telescope dome and "local temperature" refers to the temperature outside, but close to the dome. The line fitted to the points shown in Fig. 25 has been added for completeness, but it is clearly not very representative of the graph. The

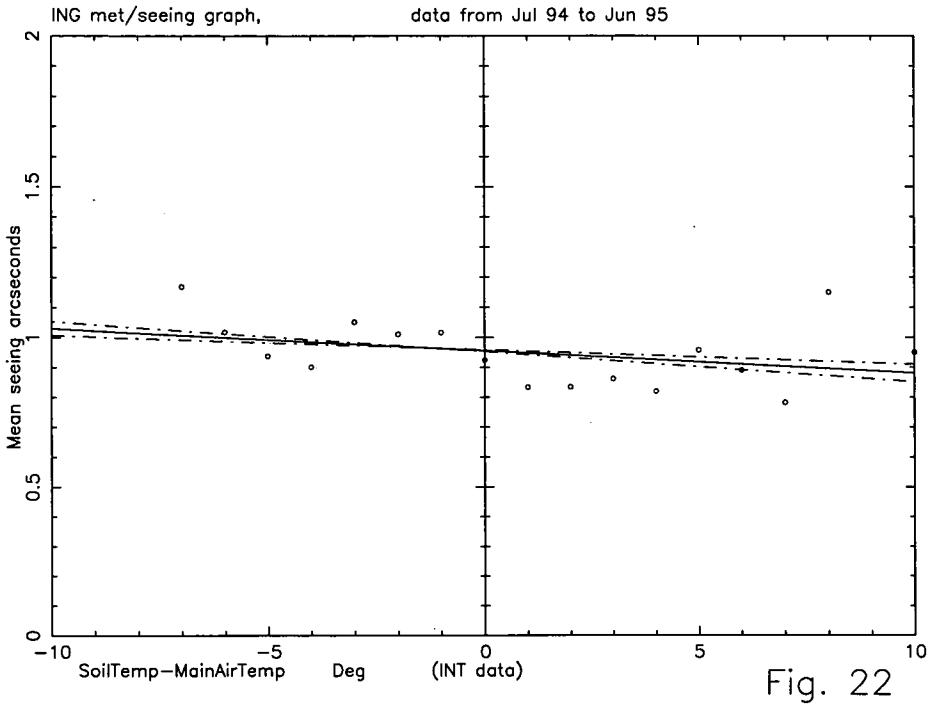

Fig. 22

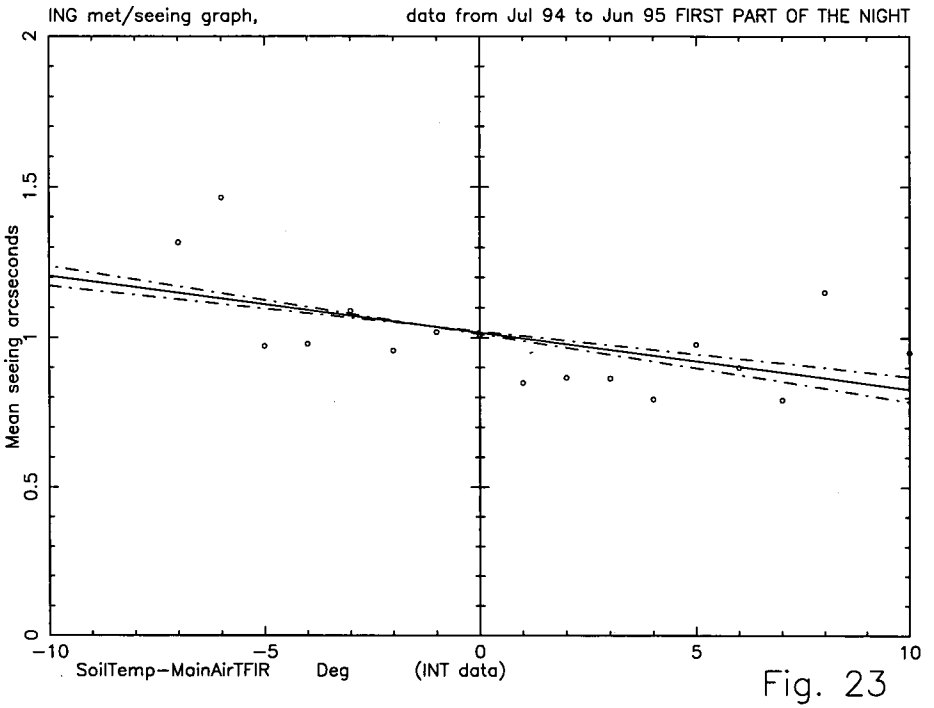

Fig. 23

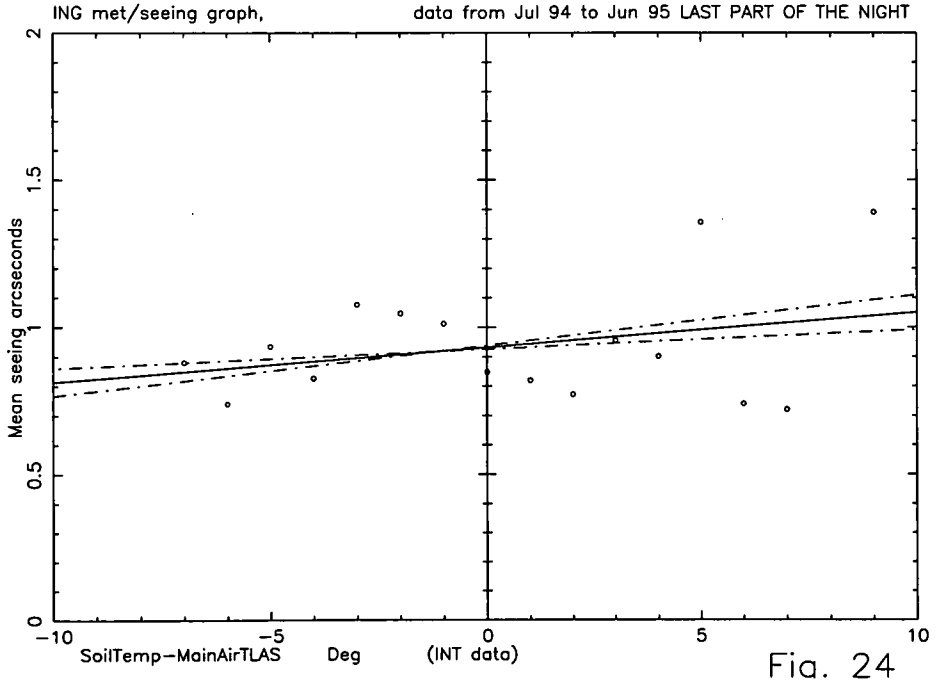

Fig. 24

general tendency is to have better seeing when the dome is cooler than the outside air; there are very high seeing values when the dome is more than 5 degrees hotter than outside air. When the two temperatures are the same the corresponding seeing value is about 0.9 $\widehat{''}$, which can be seen as the average good seeing of this site. Again, the seasonal fluctuation of the temperature is reflected in this graph: in summer the air inside the dome is usually cooler than the outside air, because it has a protection against solar radiation, while in winter the opposite is the case, because the telescope bearing oil and electronics rise the internal temperature even during freezing weather. It is not easy to explain the non-linear pattern of the points; to analyze this in detail it would be necessary to subtract from this curve the seasonal seeing curve in order to filter out the seasonal effects. However this analysis is beyond the scope of this thesis. The conclusion is that dome ventilation, which allows internal and external temperatures to equalate, is very important, but even better seeing would be achieved by cooling the inside of the dome, specially in winter.

3.7 Difference between internal temperature and mirror temperature/seeing

All the data used for this analysis, showed in Fig. 26, come from the WHT local set and the values have been binned to the nearest integer. The points have little scatter around the line fitted, the slope of which is definite and positive. As in the previous graph, when the difference between the two temperatures is small the seeing value approaches the "standard" value of 0.9 $\widehat{''}$, which means that this is the most common situation during observations. Nevertheless the seeing is better when the mirror is cooler than the internal air. It can be added that the seasonal effect should not have great influence on this comparison which concerns a closed environment protected by the dome.
The conclusion is that a cold mirror is an advantage and it seems a good practice to cool the mirror during the day in order to achieve the correct temperature at night.

3.8 Atmospheric pressure/seeing

The data for this graph come from the main mast set, where the only pressure sensor of the station is placed. As usual the values have been binned to the nearest integer. Fig. 27 shows the graph, which presents a definite negative slope and shows very little scattering of the points. Most scatter is found at low pressures, which could be due to the unstable weather that is usually associated with these pressure values. The pattern is "centered" around 0.9 $\widehat{''}$ and 772 mbars, which effectively are close to the average values holding during observing conditions. At low latitudes the seasonal variation of pressure is quite small because, even in winter time, the air temperature drop is not large and it is this which produces the higher average pressure in winter at middle latitudes. Therefore, at subtropical latitudes, the summer simply brings good and stable weather, which, in turn, causes high pressure. Another phenomenon is typical

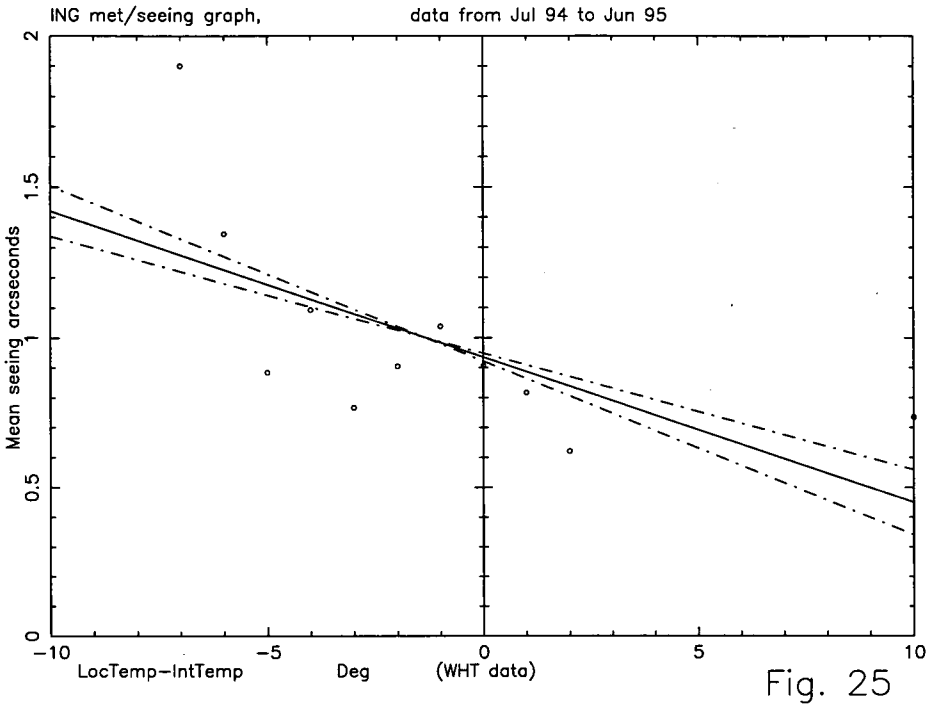

Fig. 25

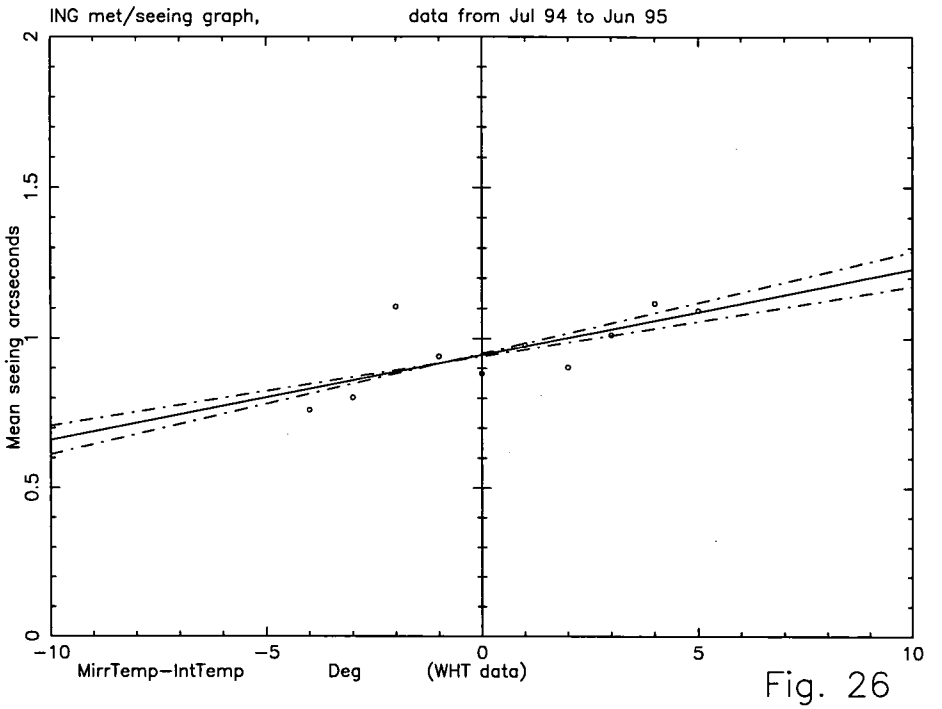

Fig. 26

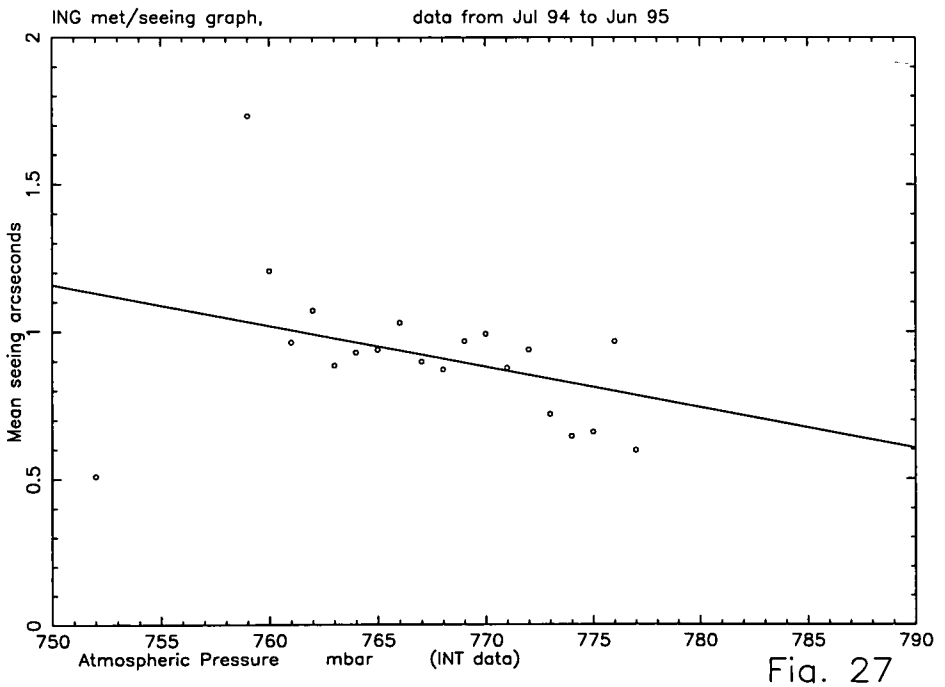

Fig. 27

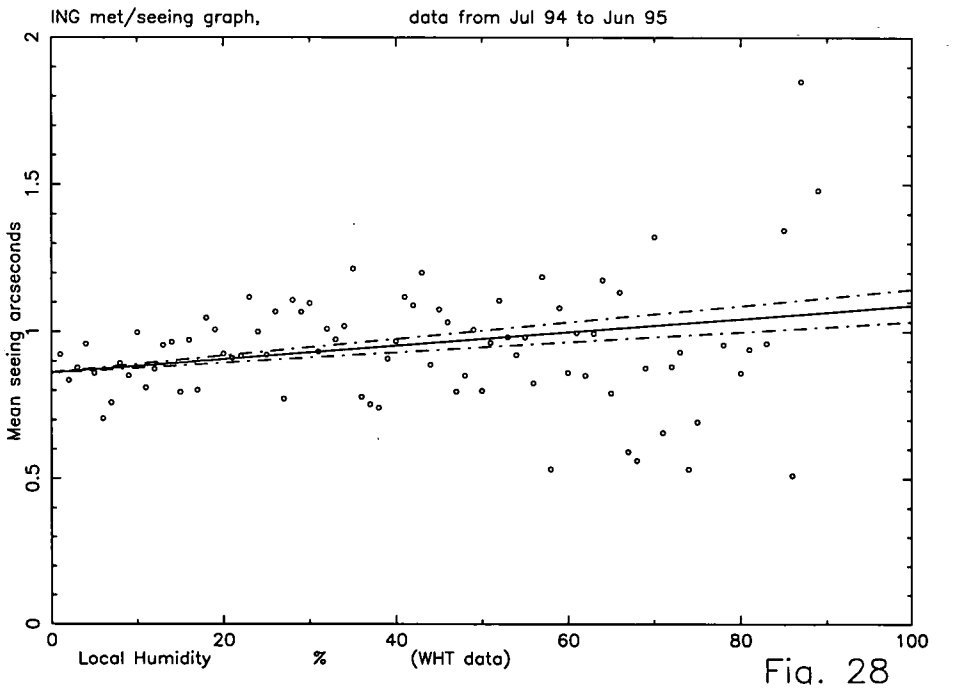

Fig. 28

of low latitudes: it is called "the diurnal variation of pressure", and usually causes pressure oscillations of ± 1 mbars with peaks at midday and midnight and lows in early morning and late afternoon. This effect could contribute to the scatter of the points on this graph (see HMSO 1978).
The simple conclusion is that, at this site, high pressure is associated with stable and good weather. This is typical of summer weather and therefore good seeing conditions occur during that season.

3.9 Humidity/seeing

The humidity data for this graph, shown in Fig. 28, come from the WHT local station. Only integer values are recorded by the meteorological station.
The graph has a large scatter of the points around the line fitted, but, although positive, the slope is quite small and still good seeing values are recorded up to very high humidity. The scatter is nevertheless greater with high humidity. This shows that seeing is more likely to be good with low humidity because the weather and the atmosphere are more stable. However the good seeing values at high humidity suggest that humidity doesn't affect seeing independently. With high humidity others factors may have a greater influence on the seeing values, for example low clouds are usually associated with high humidity and in their proximity the turbulence and temperature differences are increased and the seeing is consequently poorer.
The conclusion is that low humidity is always preferable, but even a considerable percentage of humidity in the air does not affect the seeing if no other factors cause the atmosphere to become unstable, which is nevertheless likely if the humidity is very high.

We have just seen that most atmospheric phenomena have a small effect on seeing, but many of them cannot be controlled and therefore an accurate prediction of seeing is very difficult, if not impossible, with the facilities presently available at the observatory. Nevertheless these results can be useful and the next chapter will discuss and quantify their utility. Also some basic lines for further research on the subject will be given at the end of the next chapter.

Chapter 4

CONCLUSIONS

4.1 Validity of results

The analysis presented in the previous chapter suffers from at least two main limiting factors:
1) The new meteorological station has been working for less than two years at the time the analysis was produced and, in terms of meteorological timescales, this could be a too short period to give a reliable idea of the average weather at this site.
2) The fact that the sample of data used includes values taken during the initial period, when the meteorological station was still under test.
On top of that a further remark must be made, reminding the reader that all the analysis using seeing data refers to weather conditions holding when astronomical observations are possible. This means that no account is made throughout Chapter 3 about all those meteorological data taken during bad weather, as well as the related bad seeing data, which are obviously missing.
The basic consequence of all this is that the results bring some uncertainty and they must not be taken as representative of the general global seeing or weather conditions at the observatory.

4.2 Conclusions

The analysis of the graphs presented in Chapter 3 suggests that there are basically three important factors concerning the lower atmosphere which have an influence on seeing:

1) The wind, its direction and, to some extent, speed.

2) The season of the year.

3) Relative temperatures of the elements of the telescope and its surrounding environment.

4.2.1 Wind effect

From the discussion on the wind effect given in Chapter 3 it is clear that, when the air flow is stable and layers with different temperatures are lying flat one above the other without any mixing, the seeing is at its best, because in this case the whole atmosphere approximates more closely to a single huge "seeing cell", i.e. a region with uniform refractive index. This situation is almost independent of the windspeed, in principle, provided that the surface underneath the wind flow is flat, for example as that of the sea. If the surface is not flat, as is definitely the case for La Palma, the seeing seems to deteriorate as a function of the roughness of the ground, the time the air flow has spent in contact with the rough surface and the speed of the wind flow. These three factors all have the effect of corrugating the layers of air with constant temperature, creating turbulence and mixing between them, or, in other words, producing small "seeing cells". The roughness of the surface is different for different parts of the island, therefore the seeing depends on the direction of the wind. The time the air flow spends in contact with the island's surface also depends on the wind direction, as the distance of the observatory from the flat surface of the sea varies along different directions. Finally, once turbulence is present, i.e. when the wind direction is favourable for turbulence, a higher wind speed will increase the turbulence effect on seeing, therefore the wind speed has a bigger or smaller effect according to the wind direction.
The wind direction seems therefore to be a key parameter. The best seeing is observed when the wind comes from the North or the South-West, for which the averaged seeing values are around 0.6 $\widehat{''}$ or less. The seeing is slightly worse when the wind is coming from the West, North-West and North-East, with seeing values around 1 $\widehat{''}$. Finally, the least favourable wind directions seem to be in the South-East quadrant, with values increasing from the 1.1 $\widehat{''}$ of the South up to the 1.8 $\widehat{''}$ very close to East. As stated before, a high windspeed deteriorates the seeing significantly (up to 0.8 $\widehat{''}$) if the wind direction is unfavourable, but it has a smaller effect (around 0.2 $\widehat{''}$) otherwise. The dome direction relative to the wind is not important, and the effect of the wind shake seems to be quite small, so the WHT dome works as a good shield against wind.

4.2.2 Seasonal effect

When discussing the graphs of Chapter 3 it has been referred several times to a seasonal fluctuation of the seeing, which appears to be better in summer than in winter. When the atmosphere is stable a set of meteorological parameters usually assume values within certain ranges, of which some are related to the season, others are not. When the weather is good, and therefore the atmosphere is stable, the pressure is usually high, humidity is quite low, the wind is light and stable in direction and all the temperatures are relatively high. Amongst these meteorological parameters the external air temperature is the most influenced by the season, because circulation of air in winter always bring colder air masses than in summer. Air pressure is in principle independent of the season, at least at subtropical latitudes, but it has been shown (see Chapter 3 § 8) that the typical summer conditions *cause* the pressure to be higher than in winter, therefore the season has some influence on the seeing/pressure graphs

as well.
It is possible to estimate the seasonal influence on seeing from the graphs of those parameters which are season-dependent: the air temperature is surely the most directly related to the season, but also the soil temperature, the borehole temperature and the air pressure can give some approximate information about the seasonal variation of seeing. The soil temperature could get very high during the day in winter as well, depending on the sunshine, therefore, at least at the beginning of the night, it could be not representative of the season. The borehole temperature is possibly better because of its slow response to sudden external variations, such as diurnal changes in temperature caused by the Sun heat.
The fact that seeing depends on the season means that a seasonal curve is added to all the graphs of Chapter 3, and it should be subtracted if a detailed correlation is needed. An analysis of the air temperature graph of the previous chapter shows that between 0 and 5 degrees the seeing is on average 1.2 $\widehat{''}$, while above 15 degrees the seeing is around 0.7 $\widehat{''}$. This difference of 0.5 $\widehat{''}$, which is very large, is not due to temperature only, but simply the temperature indicates when the general conditions are either favourable to produce a 1.2 $\widehat{''}$ seeing or to produce a 0.7 $\widehat{''}$ seeing. In the case of the soil and borehole temperatures the seeing variation for a 20 degrees difference is reduced to 0.3 $\widehat{''}$ and 0.1 $\widehat{''}$ respectively. The scatter on these graphs is higher than for the air temperature. From the pressure graph the seeing improvement between 760 and 775 mbars is 0.2 $\widehat{''}$, but high pressures are observed in winter as well, so this estimate is probably not as good as the temperatures one. The conclusion is that a reasonable estimate of the seasonal effect on seeing is between 0.2 $\widehat{''}$ and 0.4 $\widehat{''}$. For more precision, as stated earlier, it would be necessary to have more data, because a two years period does not reflect the true average behaviour of seasons.

4.2.3 Internal temperature differences effect

It was showed in the previous chapter that seeing is considerably influenced by the temperature differences between dome air and outside air, or between the mirror and the air. Among the effects caused by the lower part of the atmosphere, these two are the only ones on which some action can be taken. When the air inside and outside the dome has the same temperature the seeing is quite good, but if the inside is cooler than the outside the seeing seems to improve by about 0.3 $\widehat{''}$ for 2 degrees difference. In the case when the mirror is cooler than the surrounding air, the improvement with a 4 degrees difference is about 0.15 $\widehat{''}$. It is possible that a cool mirror is the result of cool air inside the dome, therefore it is probably incorrect to sum the two effects in the case of having both favourable situations (mirror and inside air cool). It is reasonable to assume that the total improvement could be between 0.3 $\widehat{''}$ and 0.4 $\widehat{''}$, which can be subtracted from the average seeing value (0.9 $\widehat{''}$) in the graph, yielding a superb 0.6 $\widehat{''}$ or 0.5 $\widehat{''}$ seeing with the mirror and the dome at the best relative temperatures. These numbers lead to the following conclusion; it is often assumed that the ideal situation for a telescope is the open air and a uniform temperature with the environment, but, if the telescope has to be placed in a protected environment, then this environment and

the telescope itself have to be *cooler* than the open air to give the best result.
In the case of the WHT, a mirror cooling system has recently been put in use, while a bearing oil cooler, which should reduce the internal (dome) temperature, will start working shortly.

4.2.4 General conclusions

The wind and seasonal effects which have just been discussed are not independent variables of the atmospheric conditions. There might appear to be no connection between them at the ground level, but they are surely inter-related, at least in the upper levels of the atmosphere. The differences in internal temperatures also could be related to external conditions such as air temperature, wind, season. Therefore the estimates of all these effects can't be merely added as if they were separate parts of the global observed seeing. For these reasons, a safe estimate of the average local seeing can be around 0.5 $\widehat{''}$, of which possibly 0.3 $\widehat{''}$ are due to the wind and 0.2 $\widehat{''}$ to internal temperature differences. The seasonal fluctuation may make these figures vary by $\pm 0.2\ \widehat{''}$. The differences in internal temperatures, the only ones which can be altered by human action, give an idea of the improvements to be expected from an appropriate thermal control of the structure and buildings. The local seeing contribution to the total seeing is very important when conditions are good, but it must be emphasized that the upper atmosphere can have a far more dramatic effect on seeing as values of 1.5 $\widehat{''}$ or more are not unusual, specially during the unfavourable winter season. Others meteorological parameters such as external temperatures, humidity, atmospheric pressure (taking into account the seasonal curve), usually show graphs with gentle slopes and quite a bit of scatter, therefore they seem to have little influence on seeing and confirm that usually the upper atmosphere conditions should be blamed if the seeing is bad. Concerning the observatory in general, the average seeing of this site is below 1 $\widehat{''}$, the wind direction is frequently favourable and local improvements, such as coolers for dome and mirror, hopefully will improve seeing even further. The WHT dome works as a good shield against wind and the telescope tracking is very good. This is a good system at a good site and both are quite suitable to fully exploit techniques such as Active or Adaptive Optics.

4.3 Possible further investigations

There are obviously many other interesting analyses which could be done with the meteorological data from the Casella station, to take advantage of such a valuable set of data. A few examples are included below.

Seasonal seeing curve

It appears very clearly from the graphs of Chapter 3 that seeing has a marked seasonal variation, therefore it would be very interesting to track these variations on a seasonal seeing curve and then to subtract it from the graphs of the other parameters to isolate their effect.

Seasonal wind directions
It would be interesting to get an idea of the prevailing wind directions according to the season. This, in connection with the seeing/wind direction graphs would allow some sort of prediction about seeing relative to the time of the year.
Solar radiation effect on the dome
The dome absorbs heat from the Sun during the day, and cools down through longwave radiation during the night, mostly at the beginning. This loss of heat should influence the seeing, so it would be interesting to study the relation between the absorbed solar radiation and the observed seeing later during the night.
Combinations of meteorological parameters
In the present work only very simple combinations of meteorological parameter were considered, such as temperature differences or the difference between dome azimuth and wind direction. More complicated combinations would be interesting to study, such as the difference between mean wind speed and gust, or other combinations involving solar radiation, dew point or relating air temperature with humidity, etc.
Selecting data of a parameter according to another parameter
Meteorological parameters influence each other, therefore it would be interesting to select, for example, the effect of humidity on seeing, but only when pressure is high, so as to eliminate the possible effect of clouds. As another example, low temperatures combined with high pressures could have a significant effect on seeing.
Telescope pointing direction with respect to orography
The part of the atmosphere interposed between the object and the telescope is what determines the seeing. When the telescope points, for example, South, it is "looking" through a layer sitting above the caldera, which could be much more turbulent than air in other places. The lower the elevation of the telescope and the closer the light path is to the turbulent layer near the ground, so it would be interesting to plot the seeing as a function of the telescope azimuth and elevation. The situations of wind direction favourable or unfavourable to turbulence should be analyzed separately to eliminate possible biases.
Rate of change of meteorological parameters
Apart from the instantaneous values of a meteorological parameter, its tendency or derivative could give very valuable information about the weather conditions, so a study of changing conditions could lead to the discovery of interesting relations between seeing and meteorology.
Orography and seeing against wind direction
The hypothesis concerning the relation between the shape of the island and the seeing as a function of wind direction should be investigated more deeply, analyzing the same effect on other islands, if possible, or using a larger sample of data.
Turbulence in the atmosphere and seeing
The difference between wind patterns on different locations on site discussed in Chapter 2 could be seen as a "measure" of the turbulence affecting the lower layer of the atmosphere. Many interesting studies could be done using this, here are a few examples: a plot of seeing against difference between wind directions at two different sites, a plot of the difference in wind direction as a function of the wind direction as measured by one of the anemometers, a plot of seeing against wind direction with the constraint

that the two anemometers must indicate the same direction.

Prevailing wind direction and seeing

The graph of wind direction frequency at the ING site of Chapter 2 Fig. 1 shows a pattern similar to the graph of seeing against wind direction in Chapter 3 Fig. 4. A confirmation of such an hypothesis would be important to understand better the wind direction influence on seeing, which appears to be significant.

Meteorology is a complex subject and there is still a lot to be done to understand its influence on astronomical seeing on La Palma.

Appendix A

DETAILS OF THE CALIBRATION OF THE BAROMETER

A.1 Foreword

Due to my personal interests and experience, I gave priority to the pressure measurement problem over the other meterological parameters monitored by the Casella station. This is also justified by the fact that most of the other sensors have not shown major malfunctions, while the barometric error has been considerable.
Thanks to the presence of a good reference instrument on site (and thanks to the courtesy of the CAMC group) the performance of the Casella barometer could be investigated in detail. The importance of having a reference instrument closeby rests on the fact that it is not possible to apply precise pressure corrections for two very different sites, specially when the location of two sites differs not only in height, but also in latitude and longitude; distance causes changes in atmospheric pressure even at the same height above sea level. The different orographic features may also cause pressure shifts beyond any predictable possibility.
To understand better these problems I preferred first to elaborate my own calculations, and then check the results with the help of reference books and known formulas. It should be noted also that such a high altitude environment is quite peculiar so that the known formulas for pressure adjustments might give only a crude approximation of the real values. For this reason, even when using known formulas, I applied corrections to adapt the formulas to this site and therefore improve the result. The calculations involve corrections of the barometer readings for the temperature of the instrument, altitude above sea level and difference of gravity from the standard value. Whenever possible I cross checked the results using two different methods or by comparison with correction tables commonly in use.
The fact of having a formula instead of a table, of course, makes it easier to translate the corrections to a computer program, apart from the fact that greater precision can be obtained.

A.1.1 Temperature barometric error

To ease the following explanation I will refer to a siphon type instrument. This kind of barometer consists essentially of a U-shaped glass tube with the longest arm closed at its end and the shorter arm of greater diameter than the rest, to form a little cistern which ensures that a little displacement of the level in the cistern gives a bigger and more appreciable shift of the long column. The height of this column above the cistern level is proportional to the atmospheric pressure, assuming that there is a vacuum above the mercury in the closed column. The mercury, and therefore the height of the column, expands with temperature and so it is necessary to set a reference temperature to have a standard measure. This temperature is 0 degree Celsius and so a Mercury instrument will overread if the temperature of the mercury is positive and underread otherwise.

The dimensions l_0 and l_1 of a body (with coefficient of expansion k), at the temperatures T_0 and T_1 respectively, are related by the formula

$$l_1 = l_0 \times e^{k\Delta T}$$

(usually the approximate formula $l_1 = l_0(1 + k\Delta T)$ is used)

Now let's suppose pressure to remain constant during the following experiment. We can ideally divide the mercury contained in the U-shaped glass into two main parts: one is the straight column, resting on the ideal surface s, at the same level of the free surface S in the cistern, the other consists of all the remaining mercury. Let's consider the second part of the two, that is, the U-shaped part limited by the cistern surface S and the ideal surface s in the column. The surfaces bear the same pressure, being at the same height, and we supposed this pressure constant while a change (for example positive) in temperature occurs. The U-shaped mercury will expand, but we said that S and s will preserve the same level, this means that both sides will expand by the same amount. The pressure on s is given by the weight of the column, which does not change with temperature, but what does change is its height. Of course the significant part of the column is that above the level of s (same of S) and we can thus think of this part as being displaced, by the expansion of the lower part, by the same amount as the surface S increases its level, so that what really changes the reading of the pressure is only the expansion of the column from s upwards. This means that the height of the column is not influenced by the behaviour of the rest of the mercury, which we can forget in our calculation. We can then use the above formula, taking into account that the glass expands also with temperature, but this only changes the section of the tube, not the length; this will in effect change the coefficient of expansion k of the column, which won't be exactly that of the mercury. Another modification to this coefficient must be introduced because of the brass scale of the instrument, whose length changes with temperature. This will have a first order (linear) influence α. The coefficient of expansion of the glass must have an order 2 influence (two dimensional change in the section of the tube) and that of the mercury an order 3 influence, and having said that, it is known that we can use the linear coefficients to the square and cube power respectively. Let μ be the coefficient of the mercury, λ that of the glass and our ΔT will be the temperature value itself $(T - 0)$ in degrees Celsius.

I used a value of $\mu^3 - \lambda^2 - \alpha = 0.000163$ (the minus signs means that the mercury level reads *less* due to the glass and scale expansion), which takes into account the expansion of the brass scale of the instrument I used. So the relation between the heights H_0 (at 0°) and H_1 (at temperature T) is:

$$H_1 = H_0 e^{(\mu^3 - \lambda^2 - \alpha)T}$$

which gives

$$H_0 = H_1 e^{(\lambda^2 - \mu^3 - \alpha)T}$$

or

$$H_0 = H_1 e^{-0.000163T}$$

This formula gives accurate results and it is obviously independent from the units used to "measure" the height of the column (mm or mbar).
Using the approximate formula (above) for the expansion of a body, we have

$$H_0 = H_1(1 - 0.000163\,T)$$

which could be of more practical use.
The precise temperature correction term k_1 for the CAMC mercury barometer is:

$$k_1 = H_1 \left(1 - e^{-0.000163T}\right)$$

while an approximate correction term is:
$k_1' = 0.000163\,H_1\,T$

A.1.2 Gravity corrections

When measuring the atmospheric pressure with a mercury barometer we are measuring the height of the column of mercury, whose weight will be proportional to the pressure. The same column with different values of the acceleration of gravity will give different pressure readings, so it is necessary to set a standard value of g to which pressure measurements refer. This value is $g = 9.80665\ m/s^2$ (See HMSO 1989)
The difference between the local gravity g_L and g are mostly dependent on the latitude of the site, because the centrifugal force due to Earth rotation is one component of g, but also the altitude of the site and the mean altitude of the surroundings (which will be called "terrain") of the site are of some importance; finally, the irregular shape of the Earth gives small local fluctuations which can only be found experimentally.

A formula to calculate the value of g_L as a function of the latitude and height above sea level of the site is as follows:

$$g_L = g_{45} f(\phi) - 3.08071\,10^{-6} H$$

where:
$f(\phi) = (1 - 0.0026373\cos(2\phi) + 0.0000059\cos^2(2\phi))$

$g_{45} = 9.80616\ m/s^2$, gravity at height 0 and $\phi = 45°$

H is the height of the site in meters and ϕ the latitude. (See HMSO 1956)
The first term concerns the latitude correction, while the second takes into account the altitude above sea level of the site; this latter is a general approximate term, which does not take in to account the "terrain" altitude nor variations of the correction with different pressures, so I prefer to substitute the formula with that given by the maker in the specific instructions of the barometer, who follows the WMO (World Meteorological Organization) standard with greater precision.
I will introduce the new "terrain" and altitude correction after a brief explanation of the latitude correction.

The value of g_L decreases with decreasing latitudes and increasing altitudes. With a lower value of the gravity acceleration the mercury column will weight less for a fixed volume, so the instrument will overread, the column being at a higher level in the tube. The pressure p exerted by the column is

$$p = \frac{\varrho V g}{S}$$

where ϱ is the density of mercury, g the acceleration due to gravity, V the volume and S the cross section of the column. We call then h the height of the column when these conditions hold and substitute V/S with h; then

$$h = \frac{p}{\varrho g}$$

If we now have p constant but a different (local) value of the acceleration of gravity g_L, then the new *observed* height of the mercury column h_L will be

$$h_L = \frac{p}{\varrho g_L}$$

so the ratio h/h_L is equal to g_L/g, therefore

$$h = h_L(g_L/g)$$

So g_L/g is the factor to be applied to the actual reading to find the correct pressure for latitude, or, alternatively, $\frac{g_L - g}{g} h_L$ is the correction to be added to the actual reading. For the Casella sensor this correction (called k_2) is:

$$k_2 = -1.4643603\,10^{-3}\,h_L$$

The altitude and terrain correction k_3 I adopted comes from the formula given by the maker of the instrument:

$$k_3 = -2.007\,10^{-7}\,H\,h_L - 1.140\,10^{-7}\,H'\,h_L$$

Where:
H is the height of the barometer cistern above mean sea level in meters

H' is the mean elevation above mean sea level, of the actual surface of the terrain included within a circle of radius 150 Km and centered at the given point in meters
h_L is the reading of the barometer.
For the CAMC barometer k_3 is:

$$k_3 = -4.757682\,10^{-4}\,h_L$$

The total value of $k_2 + k_3$ for the average pressure of 760 mbar at the Casella sensor site ($H = 2366$ m, $\phi = 28.761$ N) is about -1.47 mbar, of which -0.36 mbar is due to altitude only; the minus sign means that these values must be subtracted from the actual reading. This correction in principle must be applied, together with the temperature correction, when reading the instrument, before the altitude correction is applied; in practice, however, the difference when applying it afterwards is negligibly small, as well as the variation of g_L at the Casella sensor height (40 m higher than the mercury barometer).

A.1.3 Corrections for differences in height

To approach this calculation we must first remember the relation between pressure p, volume V and absolute temperature T of a gas,

$$pV = RT$$

Or in another form

$$\varrho = \frac{p}{RT}$$

as the density ϱ is the inverse of V. R is a constant depending on the gas considered. We can consider the pressure at a point of the free atmosphere as the weight of the column of air of unit-cross section above that point. The difference of pressure $-dp$ (minus means that pressure decreases while height increases) between the level z and $z + dz$ will therefore be given by the weight $g\varrho dz$ (g = acceleration due to gravity) of the layer limited by z and $z + dz$. Then the following holds (See HMSO 1960)

$$g\varrho dz = -dp$$

and substituting ϱ from the first relation

$$dz = -\frac{RT}{gp}dp \qquad (1)$$

So far we have implicitly supposed T constant, which is a good approximation only if we deal with small height differences and therefore small layers of air, which are likely to have a fairly uniform temperature; if we want to find corrections for bigger height differences we must take into account temperature variations; we can then describe T as a linear function of z, such that

$$T(z) = tz + \beta$$

We can then state

$$T(z_0) = T_0 \qquad \text{and} \qquad T(z_1) = T_1$$

and this gives

$$tz_1 + \beta = T_1$$

and

$$tz_0 + \beta = T_0$$

Hence

$$t = \frac{T_1 - T_0}{z_1 - z_0} \tag{2}$$

Then we can integrate both terms of the relation (1) and have

$$\int_{z_0}^{z_1} \frac{dz}{tz + \beta} = -\frac{R}{g} \int_{p_0}^{p_1} \frac{dp}{p}$$

$$\frac{1}{t} \left[\log (tz + \beta)\right]_{[z_1, z_0]} = \frac{R}{g} (\log p_0 - \log p_1)$$

$$\log \left(\frac{tz_1 + \beta}{tz_0 + \beta}\right) = \frac{Rt}{g} \log \left(\frac{p_0}{p_1}\right)$$

$$\frac{T_1}{T_0} = \left(\frac{p_1}{p_0}\right)^{-\frac{Rt}{g}}$$

$$p_0 \left(\frac{T_1}{T_0}\right)^{-\frac{g}{Rt}} = p_1$$

Finally, using relation (2), we have

$$p_1 = p_0 \left(\frac{T_1}{T_0}\right)^{-\frac{g(z_1 - z_0)}{R(T_0 - T_1)}}$$

If for some reason T_0 and T_1 are the same the previous formula becomes

$$p_1 = p_0 e^{\left(-\frac{g\Delta z}{RT_0}\right)}$$

which can also be a useful approximation using the average of the temperatures T_0 and T_1 instead of T_0.

In the case of the Casella barometric sensor, 40 m higher than the CAMC mercury barometer, the correction k_4 is:

$$k_4 = p_0 \left[\left(\frac{T_1}{T_0}\right)^{-\frac{1.367247}{T_0 - T_1}} - 1\right]$$

where temperatures are in Kelvin.
The total correction K to apply to the reading of the mercury barometer is finally:

$$K = k_1 - k_2 - k_3 + k_4$$

A.2 The Transit Circle Mercury barometer

The instrument kept in the CAMC dome is a classic column type mercury barometer, hanging from its upper end to keep it exactly vertical and with an alcohol thermometer applied to the lower part of the structure. The scale is already corrected for the change of level in the cistern and for index errors so that no further adjustment is necessary. The scale is also suitable for high altitude sites and divided in millibars with a vernier which allows readings of tenths of a millibar. The value of g for which it is calibrated is 9.80665 m/s^2 and we already discussed the correction to allow for site variations in the previous section.

A.3 Programs and correction coefficients

The data have been collected from the CAMC barometer and our sensor since January 1995 so that a wide set of pressures, temperatures and atmospheric conditions is covered.
All these data form the input of the Fortran program BARO.FOR, which, using the formulas discussed above, calculates corrections for mercury temperature, difference in height of the two sites and reduces the values to the same standard gravity; index and instrumental errors are also taken into account, according to the manufacturers' instructions.
As a result our instrument is always reading low and the mean difference is 3.5 mbar with a maximum value of 8.5 mbar and a minimum of 0.3 mbar.

Appendix B

INSTRUMENTAL DAMAGE CAUSED BY BAD WEATHER

B.1 Ice accretion

One of the biggest problems during the winter months at the Roque de Los Muchachos is ice accretion. This originates when the site is covered by low clouds, so that the humidity is 100% and the temperature is -2 degrees or less. A strong wind will speed up the process considerably. The icing process can start on flat surfaces, but more likely on vertical surfaces well exposed to the wind. The ice deposit grows leeward up to many centimeters in thickness. This kind of ice is very dangerous because such a block will probably fall down once the temperature rises. The ice grows with the shape of the lateral cross-section of the objects on which it forms and it contains almost no air bubbles, so it is very heavy. Also it can easily form in small spaces or cracks so as to fill them before growing towards the outside of the surface, and this makes it quite difficult to remove it from an irregular surface *without melting* it.
The damages due to ice accretion can be divided into three main types:

Torque due to ice

This kind of problem affects mainly small and moving parts of the station, such as anemometers cups and vane, which sometimes get completely covered and imbedded inside a block. Usually, before the instrument is completely covered, the ice formed on the cups and on the vane weights enough so as to bend the part, or the support. The damage is not only that of some data lost because the instrument has stopped, but also bent or broken parts can result even without strong winds or falling ice blocks.
The ice could also fill the space between two distant part, such as the security rope and the mast itself, so that it increases the surface offered to wind pressure, with greater stress of the whole structure.

Falling ice

Another danger takes place when air temperature rises after blocks of ice have formed on structures located above the meteorological instruments; the ice melts earlier close to the point where it is attached to the structure, because of the great pressure exerted there by its own weight, so the block is likely to fall while still having most of its original bulk.

During 1994/95 winter two heavy blocks hanging from the security ropes, about one metre long and possibly with a 600 cm^2 cross section, fell one onto the delicate Solarimeter and the other on the Dust Monitor box, causing a very considerable damage to both these items.
This icing process has effects on others structures of the telescopes and buildings as well and it represents a very serious danger for safety. Some of the old metal covers on the roof of the INT have been hit by blocks of ice falling from the dome skin onto them; the metal was completely crumpled, suggesting that possibly several hundreds kilos fell on it. There used to be a 40 foot metal container protecting the access to the INT which bore the signs of huge weights of ice falling from the roof above. If the container had not been there, they would have fallen right in front of the main door, in a place where people are likely to be. This entrance is now protected by a concrete structure.

Expansion of freezing water

This is probably the best known effect of icing. After water has filled the space between two rigid parts, its volume increases while icing, and the pressure it can exert is considerable. The two sides of the space originally filled by the water are then pushed apart, and, in situations where they can't move, they bend or break. The forces exerted by this icing process are remarkable. Concerning the meteorological station, the devices most exposed to this danger are the solar panels, which during last winter broke because ice grew between the glass cover and the cell surface underneath. All the other parts of the station, being of metal or plastic, can cope with this kind of ice pressure and just bend, so that it is easy to recover from the damage if indeed there is any.

B.2 Solar panel care

The solar panel, with its glass surface and its low location, is the part most exposed to falling ice. If the panel breaks the battery will discharge and so the transmitter will stop working. The suction pump of the dust monitor also is powered by the battery, and it quickly exhausts a battery not charged for more than 12 hours. This kind of shutdown occurred last winter. The best method for protecting the solar panel against ice falling seems to be a vertical position of the panel itself. In this way the panel offers very little horizontal surface and it is quite unlikely that a block of ice could hit the glass. The aluminium border of the panel would bear a moderate shock and there are no arms protruding from above the solar panel, so that a block falling on the solar panel would come exactly from above and shouldn't hit the glass. Another advantage is that a vertical panel in winter has a higher efficiency because of the lower elevation of the Sun during winter months; the panel gets sunlight more directly if set to an almost vertical position.

B.3 Strong winds

Sometimes quite strong winds are experienced at the site, but so far the instruments of the station withstood this condition. The masts of the local stations have had to be

reinforced, because they were originally weaker than the main mast. Security ropes and rods were fitted and there have been no problems with the strongest winds experienced so far. The dust or small stones which could be lifted by the wind should not affect any of the sensors; only a branch from the codeso stacking one of the anemometer moving part could cause some troubles. Whirls were never experienced close to ING structures.

B.4 Other meteorological factors causing damage

Hail

Hail can be dangerous for any glass component, such as the solar panels, specially during summer, when the panels are set almost horizontal. The small glass dome of the solarimeter is also at risk. Hail damage, however, has never been experienced since the station started its regular service in July 1994.

Dust

The main problem dust can cause to the station is to reduce the efficiency of the solar panels, therefore the panels are cleaned every 7-10 days.

In case of heavy and dusty rain, the dust left on the solarimeter dome could alter its performance to some extent, but this has not been detected so far.

Another action of dust is to increase the wearing of moving parts such as pivots and bearings of the anemometer and to absorb or deteriorate lubricants. However these are long term damages of which we don't yet have any evidence. The steel boxes of the electronics unit are fitted with seals and the Dust monitor is provided with filters which avoid dust contamination of the pump. All the other instruments are not affected by dust.

Lightning

The three stations are earthed and insulated from other electrical networks; the use of the solar panels, the batteries and optics fibres avoids any electrical connection between the stations and the buildings, so as to limit lightning damages to a minimum. Lightning damage was experienced during the winter of 1992, when the JKT was struck and the old Vaisala system at the JKT burnt completely. Other equipment suffered malfunctions for several months but the damage was not detected until burn marks were found on the internal cards of computers and electronic devices.

Snow

Very little snow fell during the 1994/95 winter, while during the 1995/96 winter the snow reached 50 cm in some points. During the past years a snow cover of several centimeters of thickness was fairly common, usually in December, January or February, more rarely in March and just once (since the observatory started its activity) some snow fell as late as May. A thick snow cover usually lasts only a few days, seldom for more than one week; as soon as the strong tropical sun appears again, the snow quickly melts.

Snow is not very heavy, so, even if frozen, it should not cause any of the problems which are associated with ice accretion. It could alter the performance of anemometers, but is unlikely to cause damage. The solarimeter also could be affected and read low for

some time. Snow could cover the Solar panel and stop a considerable part of the light for a few days, rarely more than a week. Again, the vertical position of the panel should minimize the effect and I would not expect any more problems other than an exhausted battery in the worst case.

High humidity

Humidity, when not followed by icing, should in principle not be a factor causing damage, but it has affected some data in the sense that the Dust monitor gave false readings when humidity was high. Probably the moist air sucked in by the instrument was interpreted as dust and the recorded values showed jumps up to the top range of the graph. The device has now been provided of an automatic cut-off when humidity is higher than 80%.

Appendix C

SOURCE CODES FOR DATA REDUCTION PROGRAMMES

C.1 Explanation

Several programs have been written for the present work, but only two are included in this appendix. These two are in fact the most important, as the others were either modifications of these or very simple programs of little interest.
The first program included here has been used to read the data from the meteorological database and produce the graphs required in the form of a file of coordinates; this is called MMSS.FOR. The other program has been used to read the coordinates from the MMSS.FOR files and print the graphs properly grouped and labelled; this is called MULTI.FOR. A simple subroutine is used to fit a line to the data when this is useful to the understanding of the plot (See P.F.T.V. 1986). The PGPLOT package has been used as the graphic tool for these programs.
The Fortran *form* of these programs may not be the best. The expert programmer would surely find better solutions than those used in these programs, but the practical results have been satisfying and, for the purpose of this kind of analysis, more sophisticated routines would have been totally unnecessary.

```
C ****************************************************************
C * Programme to plot annual graphs of Met data versus           *
C * Seeing.                                                      *
C *                                                              *
C * Inputs: SEE.TOT, MYYmmDD.WHT                                 *
C * Output: Screen plot and file with coordinates of plot points *
C ****************************************************************
      program mmss
      implicit none
C type declarations
      integer i,j,dat,day,year,month,numdays(12),
     + unit1,hour,ii,jj,kk,count,hours,mmins,minuti
      integer k,sc,mon,yea,datum,num(100000),high(17),low(17)
      real s(8), x(100000),y(100000),corr,dx(1000),dy(1000)
      real ipsi(100000),a,b,da,db,nday,mm
      character*3 tel
      character*30 infil
      character*10 device
      character*110 row
      character*45 output
      character*22 dataname(17)
      character*9 units(17)
      data numdays /31,28,31,30,31,30,31,31,30,31,30,31/
      common /blk/ infil,unit1
      data high /100,359,100,35,100,790,2000,
     +           30,30,2,30,100,30,8,100,
     +           35,100/
      data low  /0,0,0,-10,0,750,0,-5,-10,
     +           0,-5,0,-5,-8,0,-10,0/
      data device /'xwindows'/
      sc = 1

      data dataname /'Main_Wind_Speed','Main_Wind_Direction',
     + 'Main_Wind_Gust','Main_Air_Temperature',
     + 'Main_Relative_Humidity','Atmospheric_Pressure',
     + 'Solar_Radiation','Borehole_Temperature',
     + 'Soil_Temperature','Dust','Internal_Temperature',
     + 'Internal_Humidity','Mirror_Temperature',
     + 'Dewpoint','Local_Wind_Speed','Local_Air_Temperature',
     + 'Local_Humidity'/

      data units  /'Km/h','Deg','Km/h','Deg','%','Mb',
     +             'W/m\u2\d','Deg','Deg','mg/m\u3\d','Deg',
     +             '%','Deg','Deg','Km/h','Deg','%'/

      write(*,*) '          Choose which datum to plot'
      write(*,*) ' '
      write(*,*) ' ### 1 = Main Wind Speed      ### 10
     + = Dust'
      write(*,*) ' ### 2 = Main Wind Direction  ### 11
     + = Internal Temperature'
      write(*,*) ' ### 3 = Main Wind Gust       ### 12
     + = Internal Humidity'
      write(*,*) ' ### 4 = Main Air Temperature ### 13
     + = Mirror Temperature'
      write(*,*) ' ### 5 = Main Humidity        ### 14
     + = Dewpoint'
      write(*,*) ' ### 6 = Atmospheric Pressure ### 15
     + = Local Wind Speed'
      write(*,*) ' ### 7 = Solar Radiation      ### 16
```

```
     + = Local Air Temperature'
         write(*,*) ' ### 8 = Borehole Temperature ### 17
     + = Local Humidity'
         write(*,*) ' ### 9 = Soil Temperature'
         write(*,*) ' '
         write(*,20)
20          format(' Type an option --> ',$)
         read(*,*) dat

         write(*,*) ' '
         write(*,21)
21       format(' Which telescope ? --> ')
         read(*,'(a)') tel
         call pgbeg(0,device,1,1)
         call pgenv(real(low(dat)),real(high(dat)),0.,2.,0,1)
         call pgmtext('t',2.6,0.,0.0,'ING met/seeing graph,
     +   met data from Jul 94 to Jun 95')
         call pgmtext('l',1.7,0.5,0.5,'Mean seeing arcseconds')
         call pgmtext('b',2.2,0.03,0.0,dataname(dat))
         call pgask(.false.)

         write(output,1112) dataname(dat)
1112        format('[meteodata.for.dat]',a,'.dat')
         do j=1,100000
         ipsi(j) = 0
         num(j) = 0
         enddo
         count = 0
         datum = 1
         if(dat.eq.5.or.dat.eq.12.or.dat.eq.17.and.datum.gt.90) then
         open(unit=3,file='[meteodata.for.dat]hum.dat',status='new')
         endif
c*****************************************************************
C                          READ SEE.TOT
         open(unit=2,file='see.tot',status='old',err=33)
C sdecd.     see      adjs     rs       es       rad       el      az
C s(1)       s(2)     s(3)    s(4)     s(5)      s(6)     s(7)    s(8)
         do 110 while(.true.)
100         read(2,'(a)',end=120) row
         read(row(1:110),*,err=100) s(1),s(2),s(3),
     :   s(4),s(5),s(6),s(7),s(8)
         if(s(1).lt.546) goto 100
         call decdate(s(1),year,month,day,hour,minuti)
         if(s(3).ge.9) goto 100
         sc = sc + 1

C generate input file name
          write(infil,1) tel
 1              format('[meteodata.dat.',a,']M')
          write(infil(21:22),2) year
 2              format(i2)
          if (month.le.9) then
                 write(infil(23:24),3) month
 3               format('0',i1)
          elseif (month.ge.10) then
                 write(infil(23:24),2) month
          end if
          if (day.le.9) then
                 write(infil(25:26),4) day
 4               format('0',i1)
          elseif (day.ge.10) then
                 write(infil(25:26),2) day
          end if
          write(infil(27:30),5) tel
```

```
 5              format('.',a)

C call subroutines to read met data
        call readdata(day,dat,datum,
     +  hour,minuti,hours,mmins)
        write(*,*) datum
        if(dat.eq.5.or.dat.eq.12.or.dat.eq.17.and.datum.gt.90) then
        write(3,*) ' umid., decdate, adjsee ',datum, s(1), s(3)
        write(3,*) infil,' met ore e min. ',hours, mmins
        endif
        datum = datum + abs(low(dat)) + 1
        num(datum) = num(datum) + 1
        ipsi(datum) = ipsi(datum) + s(3)
110        continue
        goto 120
33      write(*,*) ' seeing not read'
        continue
120     write(*,*) ' N. of seeing data =',sc
        close(2)

        open(unit=4,file=output,status='new')
        write(4,*) dataname(dat)
        do j = 1,high(dat)+abs(low(dat))+1,1
        if(ipsi(j).ne.0.) then
        x(j)= j - abs(low(dat)) - 1
        y(j)=ipsi(j)/num(j)
        write(4,*) x(j), y(j)
        call pgpoint(1,x(j),y(j),21)
        count = count + 1
        endif
        enddo
        write(*,*) ' Count = ',count
        call pgend
        close(4)
1000    end

C ***********************************************
C Subroutine to decode date and time
C input:  nday, numdays(12)
C output: year,month,day,hour,minuti
        subroutine decdate(nday,year,month,
     +                           day,hour,minuti)
        implicit none
        integer i,year,month,day,hour,minuti,numdays(12)
        real nday, corr, mm
        data numdays /31,28,31,30,31,30,31,31,30,31,30,31/
        mm = 0
        if(nday.le.365) then
          year = 93
          corr = nday
        elseif(nday.le.730.) then
          year = 94
          corr = nday - 365
        elseif(nday.le.1095) then
          year = 95
          corr = nday - 730
        elseif(nday.le.1461) then
          year = 96
          corr = nday - 1095
        elseif(nday.le.1826) then
          year = 97
          corr = nday - 1461
        endif
```

```
        do 1010 i = 1,12,1
        if(int((real(year))/4.).eq.(real(year))/4.) then
        numdays(2) = 29
        else
        numdays(2) = 28
        endif
        mm = mm + numdays(i)
        if(mm.ge.int(corr)) then
        month = i
        day  = int( numdays(i) - (mm-corr) )
        hour = int(((numdays(i) - (mm-corr)) - day)*24.)
        minuti  = int(((((numdays(i)-(mm-corr))-day)*24.-hour)*60.)
        goto 1111
        endif
1010    continue
1111    return
        end
c****************************************
c* Subroutine to read data for each day *
c****************************************
        subroutine readdata(day,dat,datum,
     +  hour,minuti,hours,mmins)
        implicit none
        character*30  infil
        character*110 row
        character*8 a(20)
        real t(19)
        integer      i,j,ii,jj,kk,extra,day,dat
        integer      hours, mmins, minuti, hour
        integer      high(17),low(17),unit1, datum
        data high /100,359,100,35,100,790,2000,
     +             30,30,2,30,100,30,8,100,
     +             35,100/
        data low  /0,0,0,-10,0,750,0,-5,-10,
     +             0,-5,0,-5,-8,0,-10,0/
        common /blk/ infil, unit1

        open(unit1,file=infil,err=210,status='old')
        write(*,11)infil
 11     format(' from ',a)
109     read(unit1,'(a)',end=210,err=109) row
        read(row(1:2),'(i2)') hours
        read(row(4:5),'(i2)') mmins
        if(abs((hours*60+mmins)-(hour*60+minuti)).
     +                                  gt.5) goto 109
c ***************CHECK IF THERE ARE STRANGE CHARACTERS AMONG DATA
        do 333 jj = 1,110,1
        if(row(jj:jj).eq.'#') then
           do 444 ii = 1,9,1
           if(row(jj-ii:jj-ii).ne.' ') then
                do 555 kk = jj-ii+2,jj,1
                row(kk:kk) = '9'
555             continue
                goto 333
           endif
444        continue
   endif
333        continue
c  1 = Main Wind Speed      10 = Dust
c  2 = Main Wind Direction  11 = Internal Temperature
c  3 = Main Wind Gust       12 = Internal Humidity
c  4 = Main Air Temperature 13 = Mirror Temperature
c  5 = Main Humidity        14 = Dewpoint
c  6 = Atmospheric Pressure 15 = Local Wind Speed
```

```
c  7 = Solar Radiation       16 = Local Air Temperature
c  8 = Borehole Temperature 17 = Local Humidity
c  9 = Soil Temperature
         read(row(9:110),*,end=210) t(1),t(2)
     +  ,t(3),t(4),t(5),t(6),t(7),t(8),t(9),t(19),t(10)
     +  ,t(11),t(12),t(13),t(14),t(15),t(16),t(17),t(18)
         if(t(dat).lt.real(high(dat)).and.t(dat).
     +  gt.real(low(dat))) then
                  if(t(dat)-int(t(dat)).lt.0.5) then
                  datum = int(t(dat))
                  else
                  datum = int(t(dat)) + 1.
                  endif
           endif
         if(datum.lt.755) then
         open(unit=7,file='[meteodata.for.dat]pre.dat',
     +  status='new')
         write(7,*) infil, hours, mmins
         endif
210      close(unit1)
         return
         end
```

```
C ***************************************************************
C * This plots several graphs of seeing against Met parameters
C * Input : Data or combinations, which direct. (dat or data), page n.
C * Output: N graps as required
C ***************************************************************
      program multigraphint
      implicit     none

C Type declarations
      integer pnum,infn(10),high(40),low(40)
      integer ext(10),i,j,t(10),lin(10),fnum(10)
      character*57 infil(40)
      character*3 tel(10)
      character*10 device
      character*26 dataname1(40)
      character*27 dataname2(40)
      character*9 units(40)
      character*3 exte1
      character*4 exte2
      data device /'?'/
      data exte1   /'dat'/
      data exte2   /'data'/
      data high /100,359,100,35,100,790,2000,
     +           30,30,100,100,100,4,2,30,100,30,8,100,
     +           35,100,100,100,100,180,4,180,180,180,
     +           180,180,10,10,10,10,10,90,4,4,2/
      data low  /0,0,0,-10,0,750,0,-5,-10,0,0,0,0,0,-5,
     +           0,-5,-8,0,-10,0,0,0,0,0,0,0,0,0,0,0,
     +           -10,-10,-10,-10,-10,0,0,0,0/
      data dataname1
     +/'main_wind_speed.dat','main_wind_direction.dat',
     + 'main_wind_gust.dat','main_air_temperature.dat',
     + 'main_relative_humidity.dat','atmospheric_pressure.dat',
     + 'solar_radiation.dat','borehole_temperature.dat',
     + 'soil_temperature.dat','east.dat','west.dat','soea.dat',
     + 'seed.dat','dust.dat','internal_temperature.dat',
     + 'internal_humidity.dat','mirror_temperature.dat',
     + 'dewpoint.dat','local_wind_speed.dat',
     + 'local_air_temperature.dat','local_humidity.dat',
     + 'north.dat','south.dat','nowe.dat','azimag20.dat',
     + 'seeda.dat','azimin20.dat','azimag40.dat','azilmag20.dat',
     + 'azilmin20.dat','azilmag40.dat','soiltemp-mainairtemp.dat',
     + 'soiltemp-mainairtfir.dat','soiltemp-mainairtlas.dat',
     + 'loctemp-inttemp.dat','mirtemp-inttemp.dat','gust.dat',
     + 'see5.dat','mwdir.dat','sowe.dat'/
      data dataname2
     +/'Main_Wind_Speed.data','Main_Wind_Direction.data',
     + 'Main_Wind_Gust.data','Main_Air_Temperature.data',
     + 'Main_Relative_Humidity.data','Atmospheric_Pressure.data',
     + 'Solar_Radiation.data','Borehole_Temperature.data',
     + 'Soil_Temperature.data','East.data','West.data','Soea.data',
     + 'Seed.data','Dust.data','Internal_Temperature.data',
     + 'Internal_Humidity.data','Mirror_Temperature.data',
     + 'Dewpoint.data','Local_Wind_Speed.data',
     + 'Local_Air_Temperature.data','Local_Humidity.data',
     + 'North.data','South.data','Nowe.data','azimag20.data',
     + 'azimin20.data','azimag40.data','azilmag20.data',
     + 'seeda.data','azilmin20.data','azilmag40.data',
     + 'soiltemp-mainairtemp.data',
     + 'soiltemp-mainairtfir.data','soiltemp-mainairtlas.data',
     + 'loctemp-inttemp.data','mirtemp-inttemp.data','gust.data',
     + 'see5.data','mwdir.data','sowe.data'/
```

```
      data units  /'Km/h','Deg','Km/h','Deg','%','mbar',
     +      'W/m\u2\d','Deg','Deg','Km/h','Km/h','Km/h','Arcsec',
     +               'mg/m\u3\d','Deg','%','Deg','Deg','Km/h',
     +       'Deg','%','Km/h','Km/h','Km/h','Deg','Arcsec','Deg',
     +               'Deg','Deg','Deg','Deg','Deg','Deg','Deg',
     +               'Deg','Deg','Km/h','Arcsec','Arcsec','Km/h'/
C Initialize infn and pnum
      do j=1,10
      infn(j) = 0
      ext(j) = 0
      enddo
      pnum = 1
C Ask for input
      write(*,*) '                  CHOOSE WHICH DATA TO PLOT'
      write(*,*) ' 1 Main Wind Speed       14
     + Dust                    27 TelAzi wspd<20'
      write(*,*) ' 2 Main Wind Direction   15
     + Internal Temperature    28 Telazi wspd>40'
      write(*,*) ' 3 Main Wind Gust        16
     + Internal Humidity       29 TelAzi Locwspd>20'
      write(*,*) ' 4 Main Air Temperature  17
     + Mirror Temperature      30 TelAzi Locwspd<20'
      write(*,*) ' 5 Main Humidity         18
     + Dewpoint                31 TelAzi Locwspd>40'
      write(*,*) ' 6 Atmospheric Pressure  19
     + Local Wind Speed        32 Soil-MainAirTemp'
      write(*,*) ' 7 Solar Radiation       20
     + Local Air Temperature   33 Soil-MainAirFir'
      write(*,*) ' 8 Borehole Temperature  21
     + Local Humidity          34 Soil-MainAirLas'
      write(*,*) ' 9 Soil Temperature      22
     + North                   35 LocT-IntTemp'
      write(*,*) ' 10 East                 23
     + South                   36 MirrTemp-IntTemp'
      write(*,*) ' 11 West                 24
     + Northwest               37 Gust-WindSpeed'
      write(*,*) ' 12 Southeast            25
     + TelAzi wspd>20          38 SeeDirAve 5 deg'
      write(*,*) ' 13 SeeDir               26
     + SeeDirAverage           39 SeeDirAve 4 h'
      write(*,*) ' 40 Southwest'
10    write(*,*)
     +  ' File, Ext.(1=dat 2=data), Fig.n, Tel(1=INT 2=WHT)'
      write(*,*)
     +  ' lsqfit?(1=Y/2=N), `0 0 0 0 0` to finish (max 6 gr.)'
      read(*,*) infn(pnum),ext(pnum),fnum(pnum),t(pnum),lin(pnum)
      if(infn(pnum).ne.0) then
         if(ext(pnum).eq.1) then
         write(infil(pnum),20) exte1,dataname1(infn(pnum))
         elseif(ext(pnum).eq.2) then
         write(infil(pnum),20) exte2,dataname2(infn(pnum))
      endif
20    format('/home/lpss1/azzaro/ms/t/',a,'/',a)
      write(*,*) ' infil(pnum)=',infil(pnum)
      pnum = pnum + 1
      goto 10
      endif
      pnum = pnum - 1
      write(*,*) 'N. Graphs = ',pnum
      do i = 1,pnum
         if(t(i).eq.1) then
         tel(i) = 'INT'
         else
         tel(i) = 'WHT'
```

```
           endif
         enddo
C Set pgplot environment
         if(pnum.eq.1) then
         call pgbegin(0,device,1,1)
         elseif(pnum.eq.2) then
         call pgbegin(0,device,1,2)
         elseif(pnum.eq.3) then
         call pgbegin(0,device,2,2)
         elseif(pnum.eq.4) then
         call pgbegin(0,device,2,2)
         elseif(pnum.eq.5) then
         call pgbegin(0,device,2,3)
         elseif(pnum.eq.6) then
         call pgbegin(0,device,2,3)
         endif
         call pgask(.false.)
C Loop of the N graphs
         do 300 i = 1,pnum
C Open input data files and plot graphs
         if(infn(i).eq.13.or.infn(i).eq.26.
     +      or.infn(i).eq.38.or.infn(i).eq.39) then
         call polar(device,i,infn,fnum,infil,ext,pnum,tel)
         else
         call readplot(device,
     +                 i,infn,fnum,infil,ext,pnum,tel,lin)
         endif
300         continue
         call pgend
         end
C *************************************************
         subroutine readplot(device,dt,infn,fnum,infil,
     +                       ext,pnum,tel,lin)
         implicit none
C type declarations
         integer i,j,dat,count,sign,start,ext(10)
         integer dt,fnum(6),pnum,infn(10),lin(10)
         real a,b,da,db,xx(10000)
         real high(40),low(40),x(10000),y(10000)
         character*3 tel(10)
         character*57 infil(40)
         character*26 row
         character*10 device
         character*24 dataname(40)
         character*9 units(40)
         character*7 fign
         character*46 title
         data high /100.,359.,100.,35.,100.,790.,2000.,
     +             30.,30.,100.,100.,100.,4.,2.,30.,100.,30.,8.,
     +             100.,35.,100.,100.,100.,100.,180.,4.,180.,180.,
     +             180.,180.,180.,10.,10.,10.,10.,90.,4.,4.,100./
         data low  /0.,0.,0.,-10.,0.,750.,0.,-5.,-10.,
     +             0.,0.,0.,0.,0.,-5.,0.,-5.,-8.,0.,-10.,0.,0.,
     +             0.,0.,0.,0.,0.,0.,0.,0.,0.,-10.,-10.,-10.,-10.,
     +             -10.,0.,0.,0.,0./
         data dataname /'Main Wind Speed','Main Wind Direction',
     + 'Main Wind Gust','Main Air Temperature',
     + 'Main Relative Humidity','Atmospheric Pressure',
     + 'Solar Radiation','Borehole Temperature',
     + 'Soil Temperature','Wind from East only',
     + 'Wind from West only','Wind from SouthEast only','Seedir','Dust',
     + 'Internal Temperature','Internal Humidity','Mirror Temperature',
     + 'Dewpoint','Local Wind Speed','Local Air Temperature',
     + 'Local Humidity','Wind from North only',
```

```
     + 'Wind from South only','Wind from NorthWest only',
     + 'TelAzi-WinDir wsp>20','SeeDirAverage','TelAzi-WinDir wsp<20',
     + 'TelAzi-WinDir wsp>40','TelAz-WiDi LOCwsp>20',
     + 'TelAz-WiDi LOCwsp<20','TelAz-WiDi LOCwsp>40',
     + 'SoilTemp-MainAirTemp','SoilTemp-MainAirTFIR',
     + 'SoilTemp-MainAirTLAS','LocTemp-IntTemp','MirrTemp-IntTemp',
     + 'Gust-WindSpeed','See 5 DegAverage','See 4 hours ave',
     + 'Wind from SouthWest only'/
        data units  /'Km/h','Deg','Km/h','Deg','%','mbar',
     +               'W/m\u2\d','Deg','Deg','Km/h','Km/h','Km/h',
     +         'arcsec','mg/m\u3\d','Deg','%','Deg','Deg','Km/h',
     +       'Deg','%','Km/h','Km/h','Km/h','Deg','arcsec','Deg',
     +               'Deg','Deg','Deg','Deg','Deg','Deg','Deg',
     +               'Deg','Deg','Km/h','arcsec','arcsec','Km/h'/
        dat = infn(dt)
        write(title,1112) dataname(dat),units(dat),tel(dt)
1112       format(a,' ',a,' (',a,' data)')
        write(fign,1113) fnum(dt)
1113       format('Fig. ',i2)
c       if(dat.ge.24) then
c        call pgenv(low(dat),high(dat),0.,4.,0,1)
c       else
         call pgenv(low(dat),high(dat),0.,2.,0,1)
c       endif
C WRITE PROPER TITLES WITH PROPER MAGNIFICATION
        if(pnum.gt.4) then          ! IF LOOP 1
        call pgsch(2.0)

        if(ext(pnum).eq.1) then           ! IF LOOP 2
            if(dat.eq.33) then     ! IF LOOP 3
      call pgmtext('t',0.4,0.,0.0,'ING met/seeing graph,
     + data from Jul 94 to Jun 95 FIRST PART OF THE NIGHT')
      elseif(dat.eq.34) then
       call pgmtext('t',0.4,0.,0.0,'ING met/seeing graph,
     + data from Jul 94 to Jun 95 LAST PART OF THE NIGHT')
            else
      call pgmtext('t',0.4,0.,0.0,'ING met/seeing graph,
     + data from Jul 94 to Jun 95')
            endif                  ! IF LOOP 3
        endif                      ! IF LOOP 2
        if(ext(pnum).eq.2) then           ! IF LOOP 4
            if(dat.eq.33) then     ! IF LOOP 5
      call pgmtext('t',0.4,0.,0.0,'ING met/seeing graph,
     + data from May 95 to Jun 96 FIRST PART OF THE NIGHT')
            elseif(dat.eq.34) then
      call pgmtext('t',0.4,0.,0.0,'ING met/seeing graph,
     + data from May 95 to Jun 96 LAST PART OF THE NIGHT')
            else
      call pgmtext('t',0.4,0.,0.0,'ING met/seeing graph,
     + data from May 95 to Jun 96, AUTOLOG')
            endif                  ! IF LOOP 5
        endif                      ! IF LOOP 4

                           else      ! IF LOOP 1
        if(ext(pnum).eq.1) then
          if(dat.eq.33) then
      call pgmtext('t',0.8,0.,0.0,'ING met/seeing graph,
     + data from Jul 94 to Jun 95 FIRST PART OF THE NIGHT')
       elseif(dat.eq.34) then
      call pgmtext('t',0.8,0.,0.0,'ING met/seeing graph,
     + data from Jul 94 to Jun 95 LAST PART OF THE NIGHT')
            else
      call pgmtext('t',0.8,0.,0.0,'ING met/seeing graph,
     + data from Jul 94 to Jun 95')
```

```
            endif
         endif
         if(ext(pnum).eq.2) then
           if(dat.eq.33) then
       call pgmtext('t',0.8,0.,0.0,'ING met/seeing graph,
     + data from May 95 to Jun 96 FIRST PART OF THE NIGHT')
        elseif(dat.eq.34) then
       call pgmtext('t',0.8,0.,0.0,'ING met/seeing graph,
     + data from May 95 to Jun 96 LAST PART OF THE NIGHT')
            else
       call pgmtext('t',0.8,0.,0.0,'ING met/seeing graph,
     + data from May 95 to Jun 96, AUTOLOG')
            endif
         endif

         endif
            if(pnum.le.4) then
            call pgsch(2.0)
            else
            call pgsch(2.5)
            endif
         call pgmtext('b',1.6,0.9,0.5,fign)
            if(pnum.le.4) then
            call pgsch(1.0)
         call pgmtext('l',1.7,0.5,0.5,'Mean seeing arcseconds')
         call pgmtext('b',2.2,0.03,0.0,title)
            else
            call pgsch(2.0)
         call pgmtext('l',0.89,0.5,0.5,'Mean seeing arcseconds')
         call pgmtext('b',1.5,0.03,0.0,title)
            endif
         call pgsch(1.0)
         count = 0
         i = 1
         write(*,*) 'infil = ',infil(dt)
         open(unit=1,file=infil(dt),status='old',err=1000)
         do 1300 while(.true.)
100         read(1,'(a)',err=100,end=1301) row
         write(*,*) row
         start = 1
         sign = 1
         do j=1,4,1
         if(row(j:j).eq.'-') then
         start = j
         sign = -1
         endif
         enddo
         read(row(start+1:26),*,err=100) x(i),y(i)
         if(x(i).gt.high(dat).or.x(i).lt.low(dat)) goto 100
         xx(i) = sign*x(i)
         write(*,*) xx(i),y(i)
         call pgpoint(1,xx(i),y(i),21)
         count = count + 1
         i = i + 1
1300        continue
1301        close(1)
         write(*,*) ' Count = ',count
         if(lin(dt).eq.2) goto 1001
         call lsqfit(count,xx,y,a,b,da,db)
         write(*,*) ' x1 e y1 = ',low(dat),b + a*low(dat)
         write(*,*) ' x2 e y2 = ',high(dat),b + a*high(dat)
         write(*,*) ' da e db = ',da,db
         write(*,*) ' +dx1 e +dy1 = ',low(dat),b + db/2 +
     +   (a+da/2)*low(dat)
```

```
      write(*,*) ' +dx2 e +dy2 = ',high(dat),b + db/2 +
     +  (a+da/2)*high(dat)
      write(*,*) ' -dx1 e -dy1 = ',low(dat),b - db/2 +
     +  (a-da/2)*low(dat)
      write(*,*) ' -dx2 e -dy2 = ',high(dat),b - db/2 +
     +  (a-da/2)*high(dat)
      call pgmove(low(dat),b + a*low(dat))
      call pgdraw(high(dat),b + a*high(dat))
      call pgsls(3)
      call pgmove(low(dat),b + db/2 + (a+da/2)*low(dat))
      call pgdraw(high(dat),b + db/2 + (a+da/2)*high(dat))
      call pgmove(low(dat),b - db/2 + (a-da/2)*low(dat))
      call pgdraw(high(dat),b - db/2 + (a-da/2)*high(dat))
      call pgsls(1)
c     call pgmove(low(dat),1.)
c     call pgdraw(high(dat),1.)
      goto 1001
1000     write(*,*) '---------> Error'
1001     return
      end
C ***************************************************************************
      subroutine polar(device,dt,infn,fnum,infil,ext,pnum,tel)
C ***************************************************************************
      implicit none
C type declarations
      integer i,dat,count,ext(10)
      integer dt,fnum(6),pnum,infn(10),sc
      real pi,x(10000),y(10000)
      character*3 tel(10)
      character*57 infil(40)
      character*10 device
      character*7 fign
      pi = 4.*atan(1.)
      dat = infn(dt)
      sc = 1
      if(dat.eq.39) then
      call pgenv(-2.,2.,-2.,2.,1,1)
      else
      call pgenv(-4.,4.,-4.,4.,1,1)
      endif
      write(fign,1113) fnum(dt)
1113     format(' Fig.',i2)
      call pgsch(2.0)
      call pgmtext('rv',1.7,0.1,0.5,fign)
      call pgsch(1.0)
      call pgmtext('t',2.6,0.5,0.5,'ING met/seeing graph,
     + data from Jul 94 to Jun 95')
      call pgmtext('t',1.,0.5,0.5,'North')
      call pgmtext('rv',1.7,0.5,0.5,'East')

      if(dat.eq.39) then
      call pgmtext('b',2.2,0.5,0.5,'Mean seeing (arcsec)
     + versus average wind dir. over 4 hours (',tel(dt),' data)')
      elseif(dat.eq.38) then
      call pgmtext('b',2.2,0.5,0.5,'Mean seeing (arcsec)
     + versus average wind dir. binned by 5 deg. (',tel(dt),' data)')
      elseif(dat.eq.26) then
      call pgmtext('b',2.2,0.5,0.5,'Mean seeing (arcsec)
     + versus wind dir. (',tel(dt),' data)')
      elseif(dat.eq.13) then
      call pgmtext('b',2.2,0.5,0.5,'Seeing (arcsec)
     + versus wind dir. (',tel(dt),' data)')
      endif
```

```
        count = 0
        i = 1
        open(unit=1,file=infil(dt),status='old',err=1000)
        write(*,*) ' Reading ',infil
        do 1300 while(.true.)
100        read(1,*,err=100,end=1301) x(i),y(i)
        write(*,*) x(i),y(i)
        if(dat.ne.39) then
        call pgpoint(1,x(i),y(i),21)
        else
        call pgpoint(1,y(i)*sin(x(i)*pi/180.),
     +                 y(i)*cos(x(i)*pi/180.),21)
        endif
        count = count + 1
        i = i + 1
1300       continue
1301       write(*,*) ' Count = ',count
        return
1000       end
C ***************************************************************
        subroutine lsqfit(n,x,y,a,b,da,db)
C       Line : y = A*X + B
C        Calculates slope and abcissa of least-squares-fit straight
C        line to set of < 1000 points with rms errors
C        (weight = 1/error/error; = 0 if error=0)
        implicit none
        integer n,i
        real sumdel,sxx1
        real xmean
        real aest,best
        real x(1000),y(1000),dx(1000),dy(1000)
        real w(1000)
        real a,b,da,db,s,sx,sy,sxy,sxx
C Set weights to 1
        do i = 1, 1000
        dx(i) = 1
        dy(i) = 1
        enddo
C   Unweighted estimates of A and B
        s=0
        sx=0
        sy=0
        sxy=0
        sxx=0
        do i=1,n
        s=s+1
        sx=sx+x(i)
        sy=sy+y(i)
        sxy=sxy+x(i)*y(i)
        sxx=sxx+x(i)*x(i)
        enddo
        aest=(s*sxy-sy*sx)/(s*sxx-sx*sx)
        best=(sy-aest*sx)/s
C   Calculate weights
        do i=1,n
        if(dx(i).eq.0.and.dy(i).eq.0) then
                w(i)=0
        else
                w(i)=dx(i)*dx(i)/aest/aest+dy(i)*dy(i)
                w(i)=1/w(i)
        endif
        enddo
C   Calculate sums
        s=0
```

```
      sx=0
      sy=0
      sxy=0
      sxx=0
      do i=1,n
      s=s+w(i)
      sx=sx+x(i)*w(i)
      sy=sy+y(i)*w(i)
      sxy=sxy+x(i)*y(i)*w(i)
      sxx=sxx+x(i)*x(i)*w(i)
      enddo
C   Calculate A and B
      a=(s*sxy-sy*sx)/(s*sxx-sx*sx)
      b=(sy-a*sx)/s
C   Calculate errors on A and B
      xmean=sx/s
      sxx1=0
      sumdel=0
      do i=1,n
      sxx1=sxx1+w(i)*(x(i)-xmean)**2
      sumdel=sumdel+(a*x(i)+b-y(i))**2*w(i)
      enddo
      sumdel=sumdel/float(n-2)/s
      sxx1=sxx1/s
      da=sumdel/sxx1
      da=sqrt(da)
      db=sumdel*(1/float(n)+xmean*xmean*sumdel*sumdel/sxx1)
      db=sqrt(db)
      return
      end
```

Bibliography

[A. & W. 1984] A. Ardeberg, L. Woltjer
Site Testing for Future Large Telescopes
European Southern Observatory (1984)

[Tyson 1991] R. Tyson
Principles of Adaptive Optics
Academic Press, Inc. (1991)

[Lincoln lab. j. 1992] Various authors
Lincoln Laboratory journal, Spring 1992, vol. 5, n. 1
Massachusetts Institute of Technology (1992)

[HMSO 1978] Meteorological Office
Elementary Meteorology
HMSO (1978)

[HMSO 1960] Air Ministry, Meteorological Office
Handbook of Aviation Meteorology
HMSO (1960)

[HMSO 1956] Meteorological Office
Handbook of meteorological instruments
HMSO (1956)

[HMSO 1989] Meteorological Office
Observer's Handbook
HMSO (1989)

[P.F.T.V. 1986] W.H. Press, B.P. Flannery, S.A.Tekulosky, W.H. Vettering
Numerical Recipes
Cambridge University Press (1986)

List of abbreviations used throughout the text

ING	Isaac Newton Group of telescopes, the Anglo-Dutch part of the Roque de los Muchachos Observatory.
INT	Isaac Newton Telescope, 2.5 m mirror (UK, Holland)
JKT	Jacobus Kapteyn Telescope, 1 m mirror (UK, Holland)
WHT	William Herschel Telescope, 4.2 m mirror (UK, Holland)
NOT	Nordic Optical Telescope, 2.5 m mirror (Sweden, Norway, Finland, Denmark)
CAMC	Carlsberg Automatic Meridian Circle, transit instrument, 18 cm lens, (Denmark, UK, Holland).
DIMM	Differential Image Motion Monitor, seeing measuring instrument (UK, Holland).
WMO	World Meteorological Organization